

PERFORMANCE STUDY OF A GAS TURBINE POWER PLANT USING SECOND LAW ANALYSIS

Handwritten notes in Arabic script, including the word "مراجعة" (Review) and other illegible characters.

Handwritten Arabic characters, possibly initials or a signature.

UNIVERSITY OF JORDAN
FACULTY OF ENGINEERING
DEPARTMENT OF MECHANICAL ENGINEERING
BY
Akram Mahmoud Musa

تعتمد كلية الدراسات العليا
هذه النسخة من الرسالة
التوقيع: *[Signature]* التاريخ: ١٠/٩/٢٠٠٢

رجز الله بكم

Supervisor
Professor Mahmoud Hammad
University of Jordan

Submitted in Partial Fulfillment of the Requirement for the Degree of
Doctor of Philosophy in Mechanical Engineering

Faculty of Graduate Studies
University of Jordan

August 2002

This thesis was successfully defended and approved

on: ..09:01:02.....

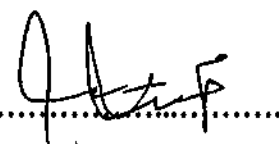
Examination Committee

Signature

**Dr Mahmoud Hammad, Supervisor
Prof of Mechanical Engineering
University of Jordan**

.....

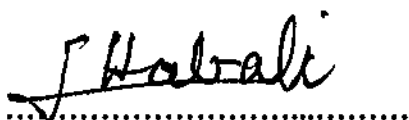

**Dr Mahmoud Alhusein, Member
Prof. of Mechanical Engineering
University of Jordan**

.....


**Dr Taha Alkhamis, Member
Prof. of Chemical Engineering
Mo'ta University**

.....


**Dr Adnan Jaradat, Member
Associate Prof. of Mechanical Engineering
University of Jordan**

.....


DEDICATION

To my father and mother

To my brothers and sisters

To my wife

To my children

ACKNOWLEDGMENT

I am greatly appreciating my supervisor Prof. Mahmoud Hammad for his support and encouragement during this research. Also I would like to extend my thanks to Prof. Mahmoud Alhusein for his assistance and cooperation.

I owe special thanks to Prof. Taha Alkhamis and Dr. Adnan Jaradat for their cooperation and being in the examination committee. I would never forget the cooperation of all members of Mechanical Engineering Department.

Further, to my family and all my friends, goes my eternal gratitude and dedication.

CONTENTES

| | |
|---|------|
| DEDICATION | iii |
| ACKNOWLEDGMENT | iv |
| CONTENTS | v |
| LIST OF FIGURES | viii |
| NOMENCLATURE | xi |
| ABSTRACT | xiv |
| 1. INTRODUCTION | 1 |
| 1.1 Background | 1 |
| 1.2 Brief History of Gas Turbine Development | 1 |
| 1.3 Applications for Gas Turbine Engines | 2 |
| 1.4 Importance of High Speed Gas Turbines | 3 |
| 1.5 An Open Cycle Gas Turbine | 3 |
| 2. LITERATURE REVIEW | 4 |
| 2.1 Introduction | 4 |
| 2.2 Previous Work | 4 |
| 2.2.1 First law analysis | 4 |
| 2.2.2 Second law analysis | 7 |
| 3. THERMODYNAMIC ANALYSIS OF GAS TURBINE POWER PLANT | 15 |
| 3.1 Introduction | 15 |
| 3.2 Open Gas Turbine Cycle | 15 |
| 3.3 First Law Analysis | 17 |
| 3.3.1 Mass rate balance | 17 |
| 3.3.2 Energy rate balance | 17 |
| 3.4 Components of Gas Turbine Cycle | 18 |
| 3.4.1 Compressor | 18 |

| | |
|--|-----------|
| 3.4.2 Combustion chamber | 19 |
| 3.4.3 Turbine | 19 |
| 3.5 Performance Parameters | 20 |
| 3.5.1 Cycle thermal efficiency | 20 |
| 3.5.2 Specific fuel consumption | 21 |
| 3.5.3 Specific work output | 21 |
| 3.6 Second Law Analysis | 21 |
| 3.7 Components Irreversibilities | 23 |
| 3.7.1 Compressor irreversibility | 24 |
| 3.7.2 Combustion chamber irreversibility | 24 |
| 3.7.3 Turbine irreversibility | 25 |
| 3.8 Cycle Second Law Efficiency | 26 |
| 3.9 Check Over-all Energy and Irreversibility. | 26 |
| 4. THEORETICAL ANALYSIS OF GAS TURBINE COMPONENTS | 27 |
| 4.1 Introduction | 27 |
| 4.2 Dimensionless Parameters | 31 |
| 4.3 Radial Turbine Configuration | 30 |
| 4.4 Analysis Procedure | 31 |
| 5. RESULTS AND DISCUSSION | 37 |
| 5.1 First Law Analysis | 37 |
| 5.1.1 Specific fuel consumption | 38 |
| 5.1.2 Specific work output | 39 |
| 5.1.3 Dimensionless mass flow rate | 39 |
| 5.1.4 Cycle thermal efficiency | 40 |
| 5.2 Second Law Analysis | 41 |
| 5.2.1 Irreversibility (exergy destruction) | 41 |
| 5.2.2 Entropy generation | 43 |

| | |
|---|-----------|
| 5.2.3 Availability change | 44 |
| 5.2.4 Second law efficiency | 45 |
| 5.2.5 Effectiveness of components | 47 |
| 6. CONCLUSIONS AND RECOMMENDATIONS | 87 |
| 6.1 Introduction | 87 |
| 6.2 Conclusions | 87 |
| 6.2.1 First law analysis | 87 |
| 6.2.2 Second law analysis | 88 |
| 6.3 Recommendations | 88 |
| 7. REFERENCES | 89 |
| ARABIC ABSTRACT | 93 |

LIST OF FIGURES

| Figure | Description | Page |
|--------|---|------|
| 3.1 | Simple gas turbine cycle | 18 |
| 3.2 | Temperature-Entropy (T-S) diagram of gas turbine cycle | 18 |
| 4.1 | Radial turbine configuration | 34 |
| 4.2 | Velocity triangles of an inward radial turbine | 35 |
| 5.1 | Variation of fuel/air ratio with turbine inlet temperature at 100 kW power output and different compressor pressure ratios | 49 |
| 5.2 | Variation of blade tip velocity at turbine rotor inlet with compressor pressure ratio at 100 kW power out put at different turbine inlet temperatures | 50 |
| 5.3 | Variation of mach numbers at turbine rotor inlet, exducer, mean and hub diameters with compressor pressure ratio at 100 kW power output | 51 |
| 5.4 | Variation of specific fuel consumption with turbine inlet temperature at 100 kW power output and different compressor pressure ratios | 52 |
| 5.5 | Variation of specific fuel consumption with turbine inlet temperature at 100 kW power output and different compressor inlet temperatures | 53 |
| 5.6 | Variation of specific fuel consumption with compressor inlet temperature (ambient) and different turbine inlet temperature at 100 kW power output | 54 |
| 5.7 | Variation of specific fuel consumption with specific work output at $P_{rc}=2$ and different turbine inlet temperatures | 55 |
| 5.8 | Variation of specific fuel consumption with specific work output at $T_{03}=700$ [K] and different compressor pressure ratios | 56 |
| 5.9 | Variation of specific work output with compressor pressure ratio at 100 kW power output and different turbine inlet temperatures | 57 |
| 5.10 | Variation of dimensionless mass flow rate with turbine inlet temperature at 100 kW power output and different compressor pressure ratios | 58 |
| 5.11 | Variation of blade width to rotor tip diameter ratio (b_2/d_2) with turbine inlet temperature at $P_{rc} = 2$ and different power output | 59 |

| | | |
|------|--|----|
| 5.12 | Variation of cycle thermal efficiency with compressor pressure ratio at 100 kW power output and different turbine inlet temperatures | 60 |
| 5.13 | Variation of cycle thermal efficiency with turbine inlet temperature at 100 kW power output and different compressor inlet temperatures | 61 |
| 5.14 | Variation of cycle thermal efficiency with compressor inlet temperature (ambient) and different turbine inlet temperature at 100 kW power output | 62 |
| 5.15 | Variation of cycle thermal efficiency with specific work output at $P_{rc}=2$ and different turbine inlet temperatures | 63 |
| 5.16 | Variation of cycle thermal efficiency with specific work output at $T_{03}=700$ [K] and different compressor pressure ratios | 46 |
| 5.17 | Variation of compressor irreversibility with turbine inlet temperature at different compressor pressure ratios | 65 |
| 5.18 | Variation of combustor irreversibility with compressor pressure ratios at different turbine inlet temperatures | 66 |
| 5.19 | Variation of turbine irreversibility with turbine inlet temperature at different compressor pressure ratios | 67 |
| 5.20 | Variation of turbine, compressor and combustor irreversibilities with turbine inlet temperature at different compressor pressure ratios | 68 |
| 5.21 | Variation of total irreversibility with turbine inlet temperature at different compressor pressure ratios | 69 |
| 5.22 | Variation of compressor entropy generation with compressor pressure ratio | 70 |
| 5.23 | Variation of turbine entropy generation with compressor pressure ratio | 71 |
| 5.24 | Variation of combustor entropy generation with turbine inlet temperature at different compressor pressure ratios | 72 |
| 5.25 | Variation of combustor entropy generation with turbine inlet temperature at different compressor inlet temperatures | 73 |
| 5.26 | Variation of combustor entropy generation with compressor inlet temperature (ambient) at different turbine inlet temperatures | 74 |
| 5.27 | Variation of compressor availability change with compressor pressure ratio at different turbine inlet temperatures | 75 |

| | | |
|------|---|----|
| 5.28 | Variation of combustor availability change with compressor pressure ratio at different turbine inlet temperatures | 76 |
| 5.29 | Variation of turbine availability change with compressor pressure ratio at different turbine inlet temperatures | 77 |
| 5.30 | Variation of compressor, combustor and turbine availability change with turbine inlet temperature at $P_{rc} = 3$ | 78 |
| 5.31 | Variation of second law efficiency with compressor pressure ratio at different turbine inlet temperatures | 79 |
| 5.32 | Variation of second law efficiency and total irreversibility with turbine inlet temperature at $P_{rc} = 5$ | 80 |
| 5.33 | Variation of second Law efficiency with turbine inlet temperature at $P_{rc}=3$ and different compressor inlet temperatures | 81 |
| 5.34 | Variation of second Law efficiency with compressor inlet temperature (ambient) at different turbine inlet temperatures | 82 |
| 5.35 | Comparison of first law and second law efficiencies with turbine inlet temperature at different compressor pressure ratios | 83 |
| 5.36 | Variation of compressor second law efficiency (effectiveness) with compressor pressure ratio | 84 |
| 5.37 | Variation of combustor second law efficiency (effectiveness) with compressor pressure ratio at different turbine inlet temperatures | 85 |
| 5.38 | Variation of turbine second law efficiency (effectiveness) with turbine inlet temperature at different compressor pressure ratios | 86 |

NOMENCLATURE

| | |
|-----------------|---|
| A | Area , m ² |
| a _f | Flow availability , kW |
| b | Blade width , m |
| C | Absolute velocity of gas , m/s |
| C _o | Spouting velocity , m/s |
| C _{pa} | Specific heat at constant pressure for air, kJ/kg K |
| C _{pg} | Specific heat at constant pressure for gas, kJ/kg K |
| d | Diameter, m |
| E | Energy transfer , kJ |
| ex | Exergy, kJ/kg |
| f | Fuel/air ratio |
| g | Acceleration of gravity, m/s ² |
| H | Stagnation enthalpy of the working fluid , kJ/kg |
| h | Static enthalpy of the working fluid , kJ/kg |
| I | Irreversibility, kW |
| LCV | Lower caloric value, kJ/kg K |
| M | Mach number |
| m | Mass, kg |
| N | Rotational speed , r.p.m |
| P | Pressure, kPa |
| P _r | Stagnation pressure ratio |
| P _L | Percent of pressure loss in combustor |
| Q | Heat transfer, kW |
| R | Gas constant, kJ/kg K |
| S | Entropy, kJ/kg K |

561697

| | |
|-------|------------------------------------|
| SFC | Specific fuel consumption, kJ/kW h |
| T | Temperature , K |
| t | Static temperature, K |
| u | Peripheral velocity, m/s |
| v | Relative velocity, m/s |
| W | Work , kJ |
| W_s | Specific work , kJ/kg/s |
| z | Distance from datum, m |

Greek Symbols

| | |
|---------------|--|
| α | Absolute flow angle relative to axial direction, Degree |
| β | Relative flow angle relative to horizontal direction, Degree |
| γ | Ratio of specific heat |
| ε | Effectiveness |
| η | Efficiency |
| ρ | Density the working fluid, kg/m ³ |
| τ | Torque, Nm |
| ω | Angular velocity, rad/s |

Subscripts

| | |
|---------|--|
| o | Stagnation condition |
| 1,2,3,4 | Numbers refers to points of the system |
| a | Air |

| | |
|-----|----------------|
| act | Actual |
| c | Compressor |
| cc | Combustor |
| cv | Control volume |
| e | Exit , exducer |
| g | Gas |
| h | Hub |
| i | Inlet |
| s | Isentropic |
| t | Turbine |
| t-t | Total to total |

Superscripts

| | |
|--------------|---------------------|
| ^o | Time rate of change |
|--------------|---------------------|

PERFORMANCE STUDY OF A GAS TURBINE POWER PLANT USING SECOND LAW ANALYSIS

By

Akram Mahmoud Musa

Supervisor

Professor Mahmoud Hammad

University of Jordan

ABSTRACT

Gas turbine engines are most generally known for their use in aircraft, but recently they received great attention since they are high power output machines with small weight to power units, furthermore they can be easily used for commercial and military applications.

The present work is concerned in the thermodynamic analysis of a gas turbine power plant. The analysis includes both first and second laws of thermodynamics. In order to simulate the gas turbine cycle, a computer program is developed to predict the general performance and to calculate thermodynamic properties of the studied engine.

The effect of design parameters on the turbine performance was studied. In addition the specific fuel consumption, first law efficiency, second law efficiency, components effectiveness and irreversibility losses through each component of the system at different operation conditions are obtained. A first law efficiency of about 24% and second law efficiency of about 36% was found for a turbine inlet temperature of 1200 K and compressor pressure ratio of 5. Also it is found that the combustor is the major source of irreversibility loss, where the losses account for nearly 40-60 % of the cycle losses.

Therefore, the second law analysis of gas turbine may be used as a guide to reduce the sources of irreversibilities when designing the gas turbine components. Furthermore, this analysis enables the location and magnitude of all losses to be identified.

1. INTRODUCTION

1.1 Background

Gas turbine is a heat engine that accepts and rejects heat and produces work. The input heat is usually in the form of fuel that is burned, but may also come from another process via a heat exchanger. The rejected heat is usually in the form of hot engine-exhaust flow released to atmosphere, but may also be rejected to another process via a heat exchanger. The work may be given as an output torque in a rotating shaft.

Gas turbine technology is witnessing continuous advances in its major components. This thesis concern with gas turbine power plant as a source of power that can be used in different applications. This was accomplished by studying the open cycle gas turbine based on the first law of thermodynamics as well as the second law analysis using a computer program to calculate the performance and design parameters at different inlet conditions.

1.2 Brief History of Gas Turbine Development

Gas turbine engine has a long and frustrating history. The use of a turbine driven by the rising flue gases above a fire dates back to Hero of Alexandria in 150 B.C., and the Chinese were operating windmills at about the same period Harman, (1981). It was not until A.D. 1791 that John Barber patented the forerunner of the gas turbine, proposing the use of a reciprocating compressor, a combustion system and an impulse turbine.

After many attempts the first successful dynamic compressor was Rateau's centrifugal type in 1905. Three assemblies of these, with a total of 25 impellers in series giving an over-all pressure ratio of 4, were made by Brown, Boveri and used in the first working gas turbine engine, built by Armengaud and Lemale in the same year. The exhaust gas heated a boiler behind the turbine to generate low-pressure steam,

which was directed through turbines to cool the blades and augment the power. Low component efficiencies and flame temperature (828K) resulted in low work output and an over-all efficiency of 3%. By 1939, the use of industrial gas turbines had become well established. A Hungarian engine with an axial flow compressor and turbine used regeneration to achieve an efficiency of 21%. But this time there was a wide variety of configurations made by numerous British, American and German companies.

While the serious development of the gas turbine began no long before the Second World War with shaft power in mind, but attention was soon transferred to the turbojet engine for aircraft propulsion. The gas turbine began to compete successfully in other fields only in the mid nineteen fifties, Cohen, (1996) however since then a progressively greater impact in an increasing variety of applications, has been made.

1.3 Applications for Gas Turbine Engines

Gas turbine engines are most generally known for their use in aircraft but they are also used in surface transportation and increasingly in stationary applications. The latter field encompasses the greatest variety of configurations and purposes and is still expanding, whereas the aviation field is consolidating. The main applications for gas turbines are summarized as below:

1. Engines for aircraft.
2. Engines for surface transportation.
3. Applications in electricity generation.
4. Oil and gas industry.
5. Combined cycles and cogeneration.
6. Usage or utilization for the exhaust gases.
7. Chemical and process industry Applications.

1.4 Importance of High Speed Gas Turbines

High speed gas turbines produce small units of high output, and they can be easily moved and used for commercial and military applications.

1.5 An Open Cycle Gas Turbine

A gas turbine engine consists of : a compressor, which continuously compresses gas from a low pressure to a higher pressure; a heater or heaters, in which the temperature of the compressed gas is raised; an expander which continuously expands the hot gas to a lower pressure; and a cooler or cooling system, in which the temperature of the gas is reduced to that established for the compressor inlet.

In the open cycle there is no engine cooling. The gas entering the compressor is atmospheric air, and the hot gas leaving the expander or the heat exchanger is discharged to the atmosphere and energy is added by the combustion of fuel in the working fluid itself.

2. LITERATURE REVIEW

2.1 Introduction

Gas turbines have received a great attention by researchers in recent years due to their attractive features and special applications in different industrial applications. Analysis of gas turbine by means of the first law of thermodynamics is a well known topic in the mechanical engineering literature. Analysis might be more effective if a great attention is given to the second law, in which the published literature on this subject is scarce.

This chapter will review some of relevant studies related to gas turbine based on the first law as well as the second law analysis.

2.2 Previous Work

2.2.1 First law analysis

Rice, (1987) analyzed complex open gas turbine cycles by applying the heat balance method. He developed a simple procedure of stream separation to make an easy, simple account for the heat absorbed by evaporative intercoolers, combustion steam injection, or blade stream for cooling, the heat being the difference between entering enthalpy and exiting enthalpy of the separated side stream. It is found that the side stream tool makes it possible to check rather complex cycles and to analyze various modes of operation. Part-load performance can also be readily checked and analyzed by means of a graphic method. Also he presented two examples, the first one is the inter-cooled regenerative cycle and the second is the reheat gas turbine. He concluded that the graphic heat balance solution provides a better understanding of gas turbine cycles and

heat recovery for cogeneration and combined cycles without getting into the mechanical details and component efficiencies of the gas turbine itself.

The thermodynamic performance of a gas turbine cogeneration system was predicted using a computer model by Baughn and Kerwin, (1987). The predicted performance is compared to the actual performance, determined by measurements, in terms of various thermodynamic performance parameters such as the electric power output, fuel flow rate, steam production, electrical efficiency, steam efficiency, and total plant efficiency. Also they derived other parameters that influence the performance such as net heat rate, and the fuel saving rate. They described the cogeneration plant, the computer model and the measurement techniques used to determine each of the necessary measurements. They concluded that the predicted and the measured electric power compare well, while the predicted fuel flow and steam production are less than measured. Their results demonstrate that this type of comparison is needed if computer models are to be used successfully in the design and selection of cogeneration systems.

Sokolov and Martyor, (1994) developed formulas for calculating the main output characteristics of gas turbine cogeneration installations. The problem of choosing the optimal parameters of the working fluid at the inlet and the outlet of the gas turbine was discussed. They concluded that it would be best to use gas turbine cogeneration installations in the field of low pressure ratios for the compressor and the turbine because in this case the internal losses due to nonisentropicity of the compression and expansion processes are small. Also it is found that the application of gas turbine cogeneration installations to residential heating networks makes sense economically if the design levels of temperature differences in the circuit water are much greater than the levels for steam turbine installations, because the former enables heat to be

withdrawn from the gas turbine exhaust at a higher temperature without extra losses in the output, and in some cases even with a gain in the output. This provides the opportunity to both cut down initial expenditures for the construction of heating networks and reduce the electricity required pumping the heating agent.

Sokolov and Martynov, (1996) presented a method for calculating the output parameters of combined-cycle (steam-gas), and gas turbine installations is described. This method is based on the thermodynamic characteristics of heat-power cycles and their dependence on the mean temperatures at which heat is supplied and removed. The dependences of the main output characteristics of these installations on the mean temperatures, at which heat is supplied and removed, enable the selection of thermal parameters of the working media and the relationships between the electrical capacities of the gas and steam cycles when designing cogeneration gas turbine and combined cycle installations.

Allen and Kovacic, (1984) discussed the principles and practice of gas turbine cogeneration system, which were installed in various industries, including chemical, petroleum refining, pulp and paper, and metals. They reviewed some of the technical considerations in the application of gas turbine cogeneration technology. The flexibility of these systems in meeting the varied industrial energy demands were also discussed. They concluded that the gas turbine cogeneration is not an economic option for all industrials. Site-specific evaluations based on plant thermal demands, available fuels and their costs and the value of power are required to define whether this technology can be justified.

2.2.2 Second law analysis

Tsatsaronis and Pisa, (1994) developed a simple cogeneration system consisting of a regenerative gas turbine system and a heat recovery steam generator that serves as an example to illustrate the application of exergy economic methods for evaluating and optimizing complex energy systems. Furthermore, they discussed various exergy costing approaches, the exergy economic variables, and the procedures used in evaluating and optimizing energy systems. It was concluded that the exergy economic techniques provide a powerful and systematic tool for identifying all cost sources and for optimizing or improving the design of complex energy systems. From this promising result, applications of this method to other energy systems are required before final conclusions, with respect to its effectiveness, can be drawn.

Bisio, (1998) examined a coupled arrangement in which turbine waste gas is used as the oxygen carrier for combustion of the fuel gas in hot blast stoves and preheaters of a blast furnace. The blast furnace gas and the turbine waste gas are preheated by the combustion of blast furnace gas, in order to achieve the necessary combustion temperatures. The arrangement makes provision also for utilization of external thermal energy. He also compared the coupled process with a hot blast stove system and a gas turbine plant without thermal waste energy recovery, which operates separately. The main result of this study using the usable exergy gives more meaningful results but does not reverse the conclusions obtained by means of only the first law of thermodynamics. The savings obtained by means of the coupling of a gas turbine with a hot blast stove are similar to those of the best steam gas combined cycle plants.

Exergy analysis of semi-closed gas turbine combined cycle (SCGT/CC) has been presented by Fiaschi and Manfrida, (1998). Exergy destruction has been analyzed

at the component level in order to identify the critical plant devices, considering several operating conditions. The power - plant configuration was designed to allow the possibility of total or partial water injection in the combustion chamber at peak load conditions. It was found that combustion, heat recovery system generator, water injection, mixing and water recovery system are the main sources of losses, representing globally more than 80% of the overall exergy destruction. The second law efficiency ranges between 49% and 53% moving from fully injected to the not injected condition. Furthermore, these values are close to those of standard open cycles, which means a good potential for the SCGT/CC, which has several advantages from the point of view of containment of emissions and capability of peakload shaving.

Habib, (1992) presented an analysis of two different cogeneration schemes. Also he compared them with a conventional plant of separate units for producing process heat and power. In the cogeneration schemes, the required process heat is obtained either from a boiler and a back pressure turbine or from a combined-cycle gas turbine. He also investigated the effects of the process pressure and heat to power ratio on performance using the first and second law efficiencies, cogeneration efficiency and irreversibility rates for the different components in each plant. The main results obtained from this study were:

- As the process pressure increases the first law efficiency decreases.
- The cogeneration combined cycle gas turbine presents the best efficiency at all pressures, which are in the range of 0.1 to 0.5 for the ratio of process to boiler pressure.
- The gas turbine provides the lowest irreversibility rates for a fixed power output.

- The second law efficiency increases as the ratio of process to boiler pressure increases for the conventional and back pressure turbine plants.
- The irreversible losses occur mostly in the boiler and combustion chamber and are greatly reduced in a gas turbine cogeneration unit.

Guarinello *et al.*, (2000) studied the thermodynamic concepts of a projected steam injected gas turbine (STIG) cogeneration system. They evaluated the power plant on the basis of the first and second laws of thermodynamics. A thermoeconomic analysis using the theory of exergetic cost was performed in order to determine the production costs of electricity and steam. They analyzed the assumed gas turbine by means of energetic, exergetic and thermoeconomic methodologies. All of those methodologies point to the same basic conclusion: The operation of the turbine in the STIG cycle in a system that requires supplementary burning in basic operation leads to lower thermal efficiencies. Also they mentioned that the thermoeconomic analysis could be improved with more improved methodologies.

Lee and Wagner, (1994) presented the exergy analysis to determine the second law efficiency for a modified GM 510K gas turbine engine operating on a Cheng cycle. The study showed that the Cheng cycle can be operated in a wide range of power and processing steam cogeneration and the first law efficiency was found to range between 30% to 39%, while the second law efficiency was between 49% and 63% when the power delivery varied between 26% and 100%.

A first and second law analysis of a single diesel engine and a single gas turbine in combined cycle with supplemental firing in a burner is presented by Ferrari and Bianco, (1997). They studied the effects of steam pressure and temperature on system performance, as are the effects of changing the pinch point and stack temperatures. The

agreement with the reported data. It is shown that by changing various relevant parameters, parametric studies can be carried out to determine thermodynamic and engineering parameters as well as suitable operational conditions.

Hisazumi, (1999) evaluates three types of energy systems including electricity from a power company together with a boiler system, a gas engine cogeneration system and a gas turbine cogeneration system, using exergy analysis in relation to customer energy usage. So the presented gas turbine power generation efficiency, which is 33% for 6000 kW class system, is low. Based on this analysis, he proposed a new gas turbine cogeneration system, which achieves higher generation efficiency by using two-stage combustion and steam injection.

Kam, (1992) presents the methodology of the cogeneration study and its application to the gas turbine-based cogeneration system. He includes the first law as well as the second law analysis. The study indicates that the system generation efficiency and its heat power ratio are two important design variables. These two design variables will affect the cogeneration system performance, which are expressed in terms of energy utilization factor and the fuel energy saving ratio. In addition to the cogeneration system, various equations have also been developed to show the effect of these two variables on the performance of the overall and combined generation system, which is defined as the cogeneration unit plus existing boilers and simplified utility Network. The second law analysis of gas turbine cogeneration system has also been presented. It is found that the fuel availability saving ratio has similar functional relationship as the fuel energy saving ratio. The availability utilization factor has been formulated. By nature, this parameter is much better than the energy utilization factor, which is based

on the concept of energy. The availability parameter would reflect more realistically and accurately the picture of the cogeneration system performance.

The thermodynamic performance of selected combustion gas turbine cogeneration system has been studied based on first law as well as second law analysis by Huang, (1990). The effects of the pinch point used in the design of the heat recovery steam generator, and pressure of process steam on fuel utilization efficiency, power-to-heat ratio, and second law efficiency, were examined. Results for three systems using state-of-the-art industrial gas turbines show clearly that performance evaluation based on first law efficiency alone is inadequate.

The second law of thermodynamics, applied in the form of entropy and availability balances for components and processes, can locate and quantify the irreversibilities, which cause loss of work and efficiency. Perhaps one reason that such analysis has not gained widespread engineering use may be due to the additional complication of having to deal with the combustion irreversibility, which introduce an-added dimension to the analysis. A method of cycle analysis, believed to overcome this added difficulty for combustion cycles is proposed by El-Masri, (1985) and applied to complex combined cycles with intercooling and reheats. The fuel is treated as a source of heat, which supplies potentially available work to the cycle depending on the peak temperature constraint on work extraction. Linkage with the traditional first law efficiency is thus preserved, while establishing the location, cause, and magnitude of losses.

El-Masri, (1987) developed a theme to include actual chemical and thermodynamic properties as well as relevant practical design details reflecting current engineering practice. The second law model is applied to calculate and provide a detailed breakdown

of the sources of inefficiency of a combined cycle. Stage-by-stage turbine cooling flow and loss analysis calculations were performed using computer program.

It is shown that the dominant interaction governing the variation of cycle efficiency with turbine inlet temperature is that between combustion irreversibility and turbine cooling losses. Compressor and pressure drop losses are shown to be relatively small. Also he found that the simplified model for combustion irreversibility, based on the Carnot efficiency at the logarithmic mean combustion temperature, is in good agreement with the detailed calculation.

Chin and El-Masri, (1987) presented a study for selecting the optimum parameters of a dual-pressure bottoming cycle as a function of the gas turbine exhaust temperature. Exergy analysis is applied to quantify all loss sources in each cycle. Compared to a single pressure at typical exhaust gas temperatures the optimized dual-pressure configuration is found to increase steam cycle work output on the order of 3 percent, principally through the reduction of heat transfer irreversibility from about 15 to 8 percent of the exhaust gas energy. Measures to further reduce of the heat transfer irreversibility such as three-pressure systems or use of multi component mixtures can therefore only result in modest additional gains.

It can be concluded that the energy balance approach to cycle analysis makes no distinction between heat and work and thus does not quantify the quality of the heat. Therefore, this method of analysis does not show which system components of the cycle losses should be attributed to. The exergy balance method of analysis enables all loss sources to be quantified.

All previous studies and researches were only concerned with combined cycles and cogeneration systems of gas turbine. It is noted that the published literature on small

unit with high speed gas turbines according to second law method of analysis is scarce. Therefore, the present study is going to investigate the whole gas turbine unit in the form of entropy generation, exergy and availability balances for all components of the gas turbine system to locate and quantify the second law efficiency and compare results with those obtained from first law analysis.

3. THERMODYNAMIC ANALYSIS OF GAS TURBINE POWER PLANT

3.1 Introduction

Gas turbines are used for many applications in military and household at different ranges of power output, mass flow rates, and rotational speeds. For small power output most gas turbines work on the open cycle (Wilson, 1998) in which ambient air enters the compressor, fuel is burned in the air and the products of combustion emerge from the engine exhaust at above atmospheric temperature. In contrast to steam turbines and spark- ignition engines, gas turbines can operate on a wide variety of different cycles. So the cycle to be used for a gas turbine engine must be chosen before any component design can be started. The thermodynamic analysis of the cycle will yield the potential efficiency, power output and approximate size of the engine (Burghardt, 1978).

3.2 Open Gas Turbine Cycle

Figure (3.1) illustrates the configuration of an open simple gas turbine cycle and figure(3.2) shows the T-S diagram representation of this cycle. The gas turbine thermodynamic analysis can be simplified by making the following assumptions :

- 1- The change of kinetic energy of the working fluid between inlet and outlet of each component is negligible
- 2- The air used by the gas turbine as well as the products of the combustion are satisfying the perfect gas laws or equation of state.
- 3- The specific heat capacities are constants through the process and represented at the average temperature of that process .
4. The loss of stagnation pressures in the combustion chamber is constant fraction of the inlet pressure.

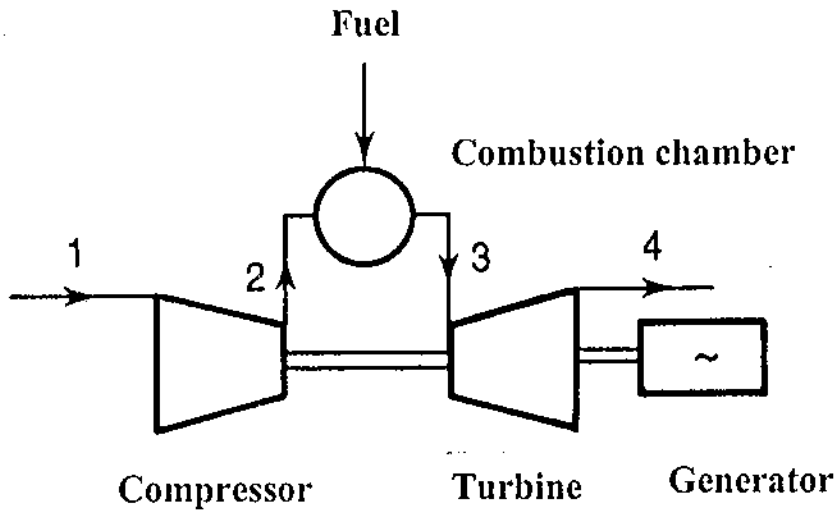


Figure 3.1 Simple gas turbine cycle

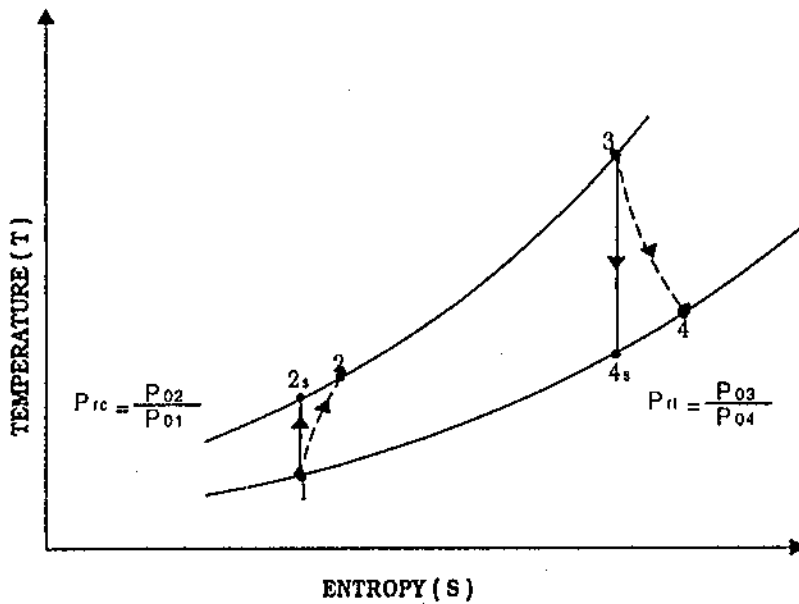


Figure 3.2 Temperature-entropy (T-S) diagram of gas turbine cycle

3.3 First Law Analysis

3.3.1 Mass rate balance

The mass rate balance for control volume is given by :

$$\frac{dm_{cv}}{dt} = \sum_i \dot{m}_i - \sum_e \dot{m}_e \dots\dots\dots(3.1)$$

where \dot{m}_i and \dot{m}_e denote, respectively, the amount of mass that enters at i and exits at e during the time interval.

For a control volume at steady state with single inlet and exit equation (3.1) reduces to:

$$\dot{m}_i = \dot{m}_e \dots\dots\dots(3.2)$$

That is, the total incoming and outgoing rates of mass flow are equal.

3.3.2 Energy rate balance

The energy rate balance for control volume is given by:

$$\frac{dE_{cv}}{dt} = \dot{Q}_{cv} - \dot{W}_{cv} + \sum_i \dot{m}_i \left(h_i + \frac{V_i^2}{2} + gz_i \right) - \sum_e \dot{m}_e \left(h_e + \frac{V_e^2}{2} + gz_e \right) \dots\dots\dots(3.3)$$

For steady state operation with single inlet and with single inlet and exit equation (3-3) reduces to:

$$0 = \dot{Q}_{cv} - \dot{W}_{cv} + \dot{m}_i \left(h_i + \frac{V_i^2}{2} + gz_i \right) - \dot{m}_e \left(h_e + \frac{V_e^2}{2} + gz_e \right) \dots\dots\dots(3.4)$$

Using equation (3.2) above and assumption (1) , then equation (3.4) becomes:

$$\frac{\dot{Q}_{cv}}{\dot{m}} - \frac{\dot{W}_{cv}}{\dot{m}} + (h_i - h_e) = 0 \dots\dots\dots(3.5)$$

This equation is applied to each component of the gas turbine cycle.

3.4 Components of Gas Turbine Cycle

3.4.1 Compressor

$$W_c = \dot{m}_a (h_1 - h_2) \dots \dots \dots (3.6)$$

$$W_c = \dot{m}_a C_{pa} (T_{o1} - T_{o2}) \dots \dots \dots (3.7)$$

Making use of the isentropic P-T relation, we have:

$$\frac{T_{o2}}{T_{o1}} = (P_{rc})^{\frac{\gamma_a - 1}{\gamma_a}} \dots \dots \dots (3.8)$$

Then

$$W_c = \dot{m}_a C_{pa} \frac{T_{o1}}{\eta_c} \left[(P_{rc})^{\frac{\gamma_a - 1}{\gamma_a}} - 1 \right] \dots \dots \dots (3.9)$$

Where P_{rc} is the compressor pressure ratio and is given by :

$$P_{rc} = \frac{P_{o2}}{P_{o1}} \dots \dots \dots (3.10)$$

From the definition of the compressor isentropic efficiency (Burghardt, 1978)

$$\eta_c = \frac{T_{o2s} - T_{o1}}{T_{o2} - T_{o1}} \dots \dots \dots (3.11)$$

The outlet temperature of the compressor T_{o2} is given by :

$$T_{o2} = T_{o1} + \frac{T_{o1}}{\eta_c} \left[(P_{rc})^{\frac{\gamma_a - 1}{\gamma_a}} - 1 \right] \dots \dots \dots (3.12)$$

3.4.2 Combustion chamber

From mass balance equation (3.2)

$$\overset{\circ}{m}_a + \overset{\circ}{m}_f = \overset{\circ}{m}_g \dots\dots\dots(3.13)$$

Define fuel/air ratio f as:

$$f = \frac{\overset{\circ}{m}_f}{\overset{\circ}{m}_a} \dots\dots\dots(3.14)$$

The energy balance of the combustion chamber using equation (3.5) can be expressed as:

$$\eta_{cc} f(\text{LCV}) = (1 + f)C_{pg}(T_{o3} - T_{o2}) \dots\dots\dots(3.15)$$

Solving equation (3.15) for fuel/air ratio f to have

$$f = \frac{C_{pg}(T_{o3} - T_{o2})}{\eta_{cc}(\text{LCV}) - C_{pg}(T_{o3} - T_{o2})} \dots\dots\dots(3.16)$$

Using assumption four the pressure loss across the combustion chamber is a constant percent of the inlet pressure

$$P_{o3} = (1 - P_L)P_{o2} \dots\dots\dots(3.17)$$

Where P_L is the percent of pressure loss across the combustion chamber.

3.4.3 Turbine

Using equation (3.5) the work output of the turbine is given by:

$$W_t = \overset{\circ}{m}_g C_{pg}(h_{o3} - h_{o4}) \dots\dots\dots(3.18)$$

$$W_t = \overset{\circ}{m}_g C_{pg}(T_{o3} - T_{o4}) \dots\dots\dots(3.19)$$

Making use of the isentropic P-T relation, we have

$$\frac{T_{o3}}{T_{o4}} = \left(\frac{P_{o3}}{P_{o4}} \right)^{\frac{\gamma_g - 1}{\gamma_g}} \dots\dots\dots(3.20)$$

Then

$$W_t = (1 + f) m_a C_{pg} \eta_t T_{o3} \left[1 - \left(\frac{1}{P_{rt}} \right)^{\frac{\gamma_g - 1}{\gamma_g}} \right] \dots\dots\dots(3.21)$$

Where P_{rt} is the turbine pressure ratio and given by

$$P_{rt} = \frac{P_{o3}}{P_{o4}} \dots\dots\dots(3.22)$$

From the definition of the turbine isentropic efficiency (Bughardt, 1978)

$$\eta_t = \frac{T_{o3} - T_{o4}}{T_{o3} - T_{o4s}} \dots\dots\dots(3.23)$$

The outlet temperature of the turbine T_{o4} is given by:

$$T_{o4} = T_{o3} - \eta_t T_{o3} \left[1 - \left(\frac{1}{P_{rt}} \right)^{\frac{\gamma_g - 1}{\gamma_g}} \right] \dots\dots\dots(3.24)$$

3.5 Performance Parameters

3.5.1 Cycle thermal efficiency

If the amount of fuel added to the cycle. \dot{m}_f is evaluated, then the thermal efficiency is evaluated as :

$$\eta_{\text{cycle}} = \frac{W_{\text{net}}}{\dot{m}_f \text{LVC}} \dots\dots\dots(3.25)$$

where

$$W_{net} = W_t - W_c$$

Where \dot{m}_f is the mass flow of fuel required at the lower caloric value of the fuel reevaluated at a reference temperature and pressure of 288 K and one atmosphere respectively (Wilson, 1998).

3.5.2 Specific fuel consumption

Once the fuel/air ratio is known, the fuel consumption \dot{m}_f is simply $f \times \dot{m}_a$ where \dot{m}_a is the air mass flow, and the specific fuel consumption can be found directly from.

$$SFC = \frac{f}{W_{net}} \dots \dots \dots (3.26)$$

Since the fuel consumption is normally measured in kg/h, while W_{net} is in kW per kg/s of air flow, the SFC in kg/kWh is given by the following numerical equation:

$$SFC = \frac{3600f}{W_{net}} \dots \dots \dots (3.27)$$

3.5.3 Specific work output

The specific work output of the cycle is given by:

$$W_s = \frac{W_t - W_c}{\dot{m}_a} \dots \dots \dots (3.28)$$

3.6 Second Law Analysis

The availability rate balance equation for a control volume is given by:

$$\frac{dA_{cv}}{dt} = \sum_j \left(1 - \frac{T_o}{T_j} \right) \dot{Q}_j - \left(\dot{W}_{cv} - p_o \frac{dV_{cv}}{dt} \right) + \sum_i \dot{m}_i a_{fi} - \sum_e \dot{m}_e a_{fe} - \dot{I}_{cv} \dots \dots \dots (3.29)$$

where

The term $\frac{dA_{cv}}{dt}$ represents the time rate of change of availability (exergy) of the control volume.

The term \dot{Q}_j represents the time rate of heat transfer at the location on the boundary where the instantaneous temperature is T_j .

The term $\left(1 - \frac{T_o}{T_j}\right) \dot{Q}_j$ represents the accompanying availability transfer.

The term \dot{W}_{cv} represents the time rate of energy transfer by work other than flow work.

The terms $\dot{m}_i a_{fi}$ and $\dot{m}_e a_{fe}$ operating in these expressions are evaluated from the following equation:

$$a_f = (h - h_o) - T_o(s - s_o) + \frac{V^2}{2} + gz \dots \dots \dots (3.30)$$

The term \dot{I}_{cv} accounts for the time rate of availability destruction due to irreversibilities within the control volume.

At steady state, $\frac{dA_{cv}}{dt} = \frac{dV_{cv}}{dt} = 0$, so equation (3.29) reduces to:

$$\dot{I}_{cv} = \sum_j \left(1 - \frac{T_o}{T_j}\right) \dot{Q}_j - \dot{W}_{cv} + \sum_i \dot{m}_i a_{fi} - \sum_e \dot{m}_e a_{fe} \dots \dots \dots (3.31)$$

The rate at which availability is transferred into the control volume must exceed the rate at which availability is transferred out, and the difference being the rate at which availability is destroyed within the control volume due to irreversibilities.

For single inlet and single exit, then equation (3.31) becomes.

$$\dot{I}_{cv} = \sum_j \left(1 - \frac{T_o}{T_j}\right) \dot{Q}_j - \dot{W}_{cv} + \dot{m}(\Delta a_f) \dots \dots \dots (3.32)$$

where Δa_f will be evaluated using equation (3.30) as:

$$\Delta a_f = \Delta h - T_o \Delta s + \Delta(\text{K.E.}) + \Delta(\text{P.E.}) \dots \dots \dots (3.33)$$

Substituting equation (3.33) back into equation (3.32) gives:

$$\dot{I}_{cv} = \sum_j \left(1 - \frac{T_o}{T_j}\right) \dot{Q}_j - \dot{W}_{cv} + \dot{m}(\Delta h - T_o \Delta s + \Delta(\text{K.E.}) + \Delta(\text{P.E.})) \dots \dots \dots (3.34)$$

Where K.E. and P.E are the kinetic and potential energies respectively.

Neglecting the changes in kinetic and potential energy, the above equation reduced to:

$$\dot{I}_{cv} = \sum_j \left(1 - \frac{T_o}{T_j}\right) \dot{Q}_j - \dot{W}_{cv} + \dot{m}(a_{fi} - a_{fe}) \dots \dots \dots (3.35)$$

This equation is used to calculate the irreversibility to each component in the gas turbine cycle.

3.7 Components Irreversibilities

The enthalpy, entropy and exergy may be found using the perfect gas equation of state. The exergy requires that the reference state be the temperature and pressure of the environment. It is convenient to use this as the reference state for enthalpy and entropy as well. The properties are calculated from the following relations for a perfect gas:

$$h = C_p (T - T_{o1}) \dots \dots \dots (3.36)$$

$$s = C_p \left[\ln \frac{T}{T_{o1}} - \left(\frac{\gamma - 1}{\gamma} \right) \ln \frac{P}{P_{o1}} \right] \dots \dots \dots (3.37)$$

$$ex = h - T_{01}S \dots\dots\dots(3.38)$$

$$a_f = m \overset{\circ}{ex} \dots\dots\dots(3.39)$$

3.7.1 Compressor irreversibility

Using equation (3.35) and assume that there is no heat transfer with surroundings, the irreversibility of the compressor is given by:

$$\overset{\circ}{I}_c = -\overset{\circ}{W}_c + m(a_{f1} - a_{f2}) \dots\dots\dots(3.40)$$

This equation can be rearranged to

$$\left(\frac{-\overset{\circ}{W}_c}{m} \right) = (a_{f2} - a_{f1}) + \frac{\overset{\circ}{I}_c}{m} \dots\dots\dots(3.41)$$

Thus, the availability input to the compressor, $\frac{-\overset{\circ}{W}_c}{m}$ is accounted for either as an increase in the flow availability between inlet and exit or as availability destroyed.

The second law efficiency (effectiveness) of the conversion from work input to flow availability increase is given by (Moran, 1989):

$$\epsilon_c = \frac{a_{f2} - a_{f1}}{\left(-\overset{\circ}{W}_{cv} / m \right)} \dots\dots\dots(3.42)$$

3.7.2 Combustion chamber irreversibility

Using equation (3.35) the irreversibility of the combustion chamber is given by:

$$\overset{\circ}{I}_{cc} = \left(1 - \frac{T_{01}}{T_m} \right) Q_{cc} + m(a_{f2} - a_{f3}) \dots\dots\dots(3.43)$$

where

T_m is the mean temperature of the combustion chamber and Q_{cc} is the heat rate added to the combustion chamber, which is given by:

$$Q_{cc} = \dot{m}(h_3 - h_2) \dots \dots \dots (3.44)$$

The second law efficiency (effectiveness) of the combustion chamber is:

$$\epsilon_{cc} = \frac{a_{f2} - a_{f3}}{\left(1 - \frac{T_{o1}}{T_m}\right) Q_{cc}} \dots \dots \dots (3.45)$$

3.7.3 Turbine irreversibility

Using equation (3.35) and the assumption that there is no heat transfer with surroundings, the irreversibility of the turbine is given by:

$$\dot{I}_t = -\dot{W}_t + \dot{m}(a_{f3} - a_{f4}) \dots \dots \dots (3.46)$$

This equation can be rearranged to

$$a_{f3} - a_{f4} = \frac{\dot{W}_t}{\dot{m}} + \frac{\dot{I}_t}{\dot{m}} \dots \dots \dots (3.47)$$

The term on the left hand side of equation (3.47) is the decrease in flow availability from turbine inlet to exit.

Also the above equation shows that the flow availability decreases because the turbine develops work, \dot{W}_t/\dot{m} , and availability is destroyed, \dot{I}_t/\dot{m} .

The second law efficiency (effectiveness) of the flow availability decrease is converted to the desired product is

$$\epsilon_t = \frac{\dot{W}_t/\dot{m}}{a_{f3} - a_{f4}} \dots \dots \dots (3.48)$$

3.8 Cycle Second Law Efficiency

The second law efficiency of the gas turbine cycle is defined as the ratio of the availability rate desired to the availability rate consumed. In this gas turbine engine, the availability rate desired is the net power output and the availability rate consumed is the availability rate associated with the heat rate to the combustion chamber.

The second law efficiency is given by:

$$\eta_2 = \frac{W_{net}^o}{\left(1 - \frac{T_{ol}}{T_m}\right) Q_{cc}^o} \dots\dots\dots(3.49)$$

3.9 Check Over-all Energy and Irreversibility

An over-all energy balance of the cycle gives the following:

$$Q_{cc} - W_{net} = \dot{m}(h_4 - h_1) \dots\dots\dots(3.50)$$

Which gives a consistency check of the individual component results, relative to the energy balances.

An overall irreversibility rate of the cycle gives:

$$\dot{I}_{tot} = a_{f1} - a_{f4} + a_{qc} + W_c - W_t \dots\dots\dots(3.51)$$

where

$$a_{qc} = \left(1 - \frac{T_{ol}}{T_m}\right) Q_{cc} \dots\dots\dots(3.52)$$

Which checks with the sum of the irreversibility rates of the components. This is a consistency check of the use of the availability rates in the component analysis.

4. THEORETICAL ANALYSIS OF GAS TURBINE COMPONENTS

4.1 Introduction

The analysis of a real flow in a turbomachinery is extremely a complex process, due to the effects of viscosity, compressibility, heat transfer and three-dimensional flow. Thus a one-dimensional flow, based on Euler's equation, will be used in the following analysis of gas turbine components.

There are many control, design and performance variables that affect the gas turbine cycle. Therefore, the dimensionless parameters will reduce the number of variables and simplify the presentation of gas turbines performance results.

In this chapter the selection and performance of gas turbine components based on literature are introduced.

4.2 Dimensionless Parameters

The widest comprehension of the general behavior of all turbomachines is, without doubt, obtained from dimensional analysis. This is the formal procedure whereby the group of variables representing some physical situation is reduced into a smaller number of dimensionless groups Dixon, (1978).

Dimensional analysis applied to turbomachines has two important uses:

- 1- Prediction of a prototype's performance from tests conducted on a scale model (similitude).
- 2- Determination of the most suitable type of machine, on the basis of maximum efficiency, for a specified range of head, speed, and flow rate.

The actual work produced by the turbine is given by:

$$W_{act} = \dot{m} C_p \eta_{t-t} T_i \left[1 - \left(\frac{p_i}{p_c} \right)^{\frac{\gamma-1}{\gamma}} \right] \dots\dots\dots(4.1)$$

where η_{i-t} is the total to total isentropic efficiency. Also, the actual work produced may be written as:

$$W_{act} = \tau\omega = \tau 2\pi N / 60 \dots \dots \dots (4.2)$$

Equating equations (4.1) and (4.2), then dividing by $d_2^3 P_i$, the result is given by:

$$\frac{\tau}{d_2^3 P_i} = \left(\frac{\eta_{i-t}}{2\pi} \right) \left(\frac{\dot{m} \sqrt{C_p T_i}}{d_2^2 P_i} \right) \left(\frac{d_2 N}{\sqrt{C_p T_i}} \right)^{-1} \left[1 - \left(\frac{P_e}{P_i} \right)^{\frac{\gamma-1}{\gamma}} \right] \dots \dots \dots (4.3)$$

or

$$\frac{\tau}{d_2^3 \dot{m} \sqrt{C_p T_i}} = \frac{\left[\frac{\eta_{i-t}}{2\pi} \right]}{\left[\frac{d_2 N}{\sqrt{C_p T_i}} \right]} \left[1 - \left(\frac{P_e}{P_i} \right)^{\frac{\gamma-1}{\gamma}} \right] \dots \dots \dots (4.4)$$

Defining the spouting velocity as that velocity which has an associated kinetic energy equal to isentropic enthalpy drop from turbine inlet stagnation pressure to the final exhaust pressure. The exhaust pressure can have several interpretations depending upon whether total or static conditions are used in the related efficiency definition and upon whether or not a diffuser is included with the turbine. Thus, when no diffuser is used the spouting velocity can be expressed as, (Dixon, 1978):

$$\frac{1}{2} C_o^2 = (h_{oi} - h_{oe})_s \dots \dots \dots (4.5)$$

If the working fluid is a perfect gas, equation (4.5) can be expressed as:

$$C_o = \sqrt{2C_p (T_i - T_e)_s}$$

$$C_o = \sqrt{2C_p T_i \left(1 - \left(\frac{P_e}{P_i} \right)^{\frac{\gamma-1}{\gamma}} \right)} \dots \dots \dots (4.6)$$

Also the blade tip speed u_2 can be written as:

$$u_2 = \pi d_2 N / 60 \dots \dots \dots (4.7)$$

Using equations (4.6) and (4.7), an expression for the velocity ratio is given by:

$$\frac{u_2}{C_o} = \frac{\pi}{\sqrt{2}} \left[\frac{\frac{d_2 N}{\sqrt{2 C_p T_i}}}{\sqrt{1 - \left(\frac{p_e}{p_i}\right)^{\frac{\gamma-1}{\gamma}}}} \right] \dots \dots \dots (4.8)$$

By substituting equation (4.8) in equation (4.4), the following expression for specific torque is obtained:

$$\frac{\tau}{d_2 m \sqrt{C_p T_i}} = \frac{1}{2\sqrt{2}} \left[\frac{\eta_{t-t}}{\left(\frac{u_2}{C_o}\right)} \right] \left[1 - \left(\frac{p_e}{p_i}\right)^{\frac{\gamma-1}{\gamma}} \right]^{\frac{1}{2}} \dots \dots \dots (4.9)$$

where

$$\frac{\tau}{d_2 m \sqrt{C_p T_i}} = \text{Specific torque parameter}$$

$$\frac{m \sqrt{C_p T_i}}{d_2 p_i} = \text{Mass flow parameter}$$

$$\frac{d_2 N}{\sqrt{C_p T_i}} = \text{Speed parameter}$$

$$\frac{u_2}{C_o} = \text{Velocity ratio}$$

4.4 Radial Turbine Configuration

In the radial turbine flow is changed from a radially inwards to axial direction. This allows a far greater area ratio and hence expansion ratio than may be achieved by only changing gas angles and the annulus lines for an axial flow stage.

Figure 4.1 shows the configuration of a radial turbine. The velocity triangles are shown in figure 4.2. From these triangles the following relation can be obtained:

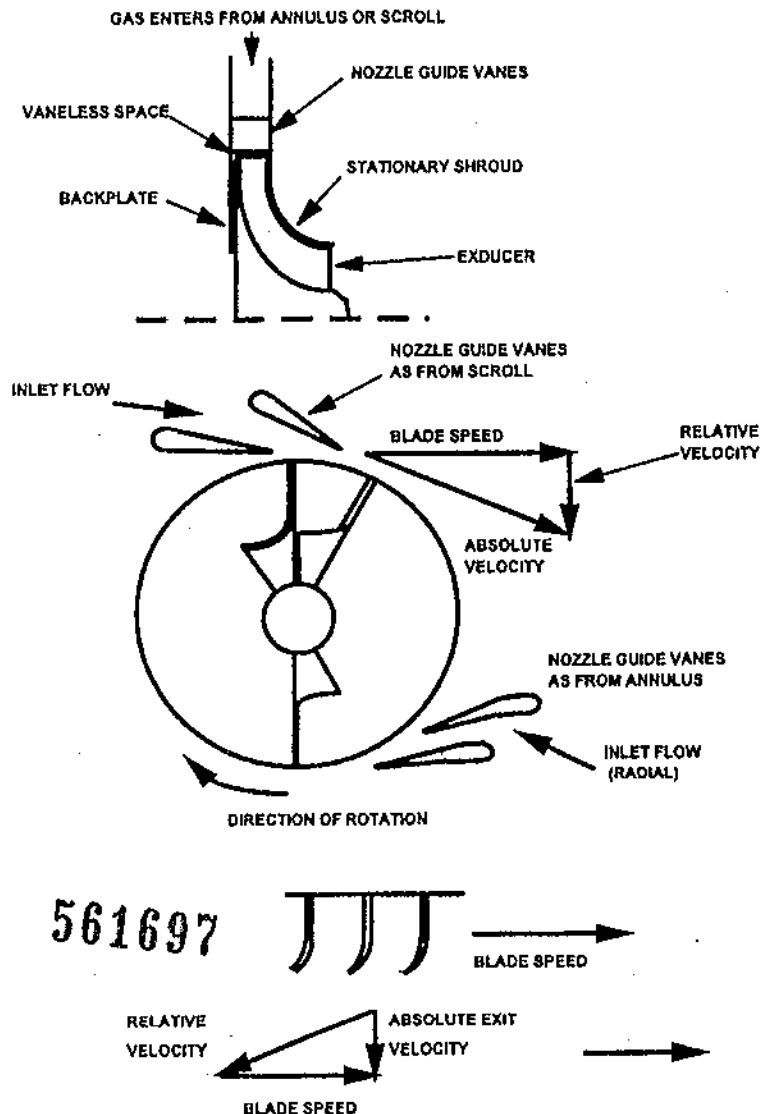


Figure 4.1 : Radial turbine configuration

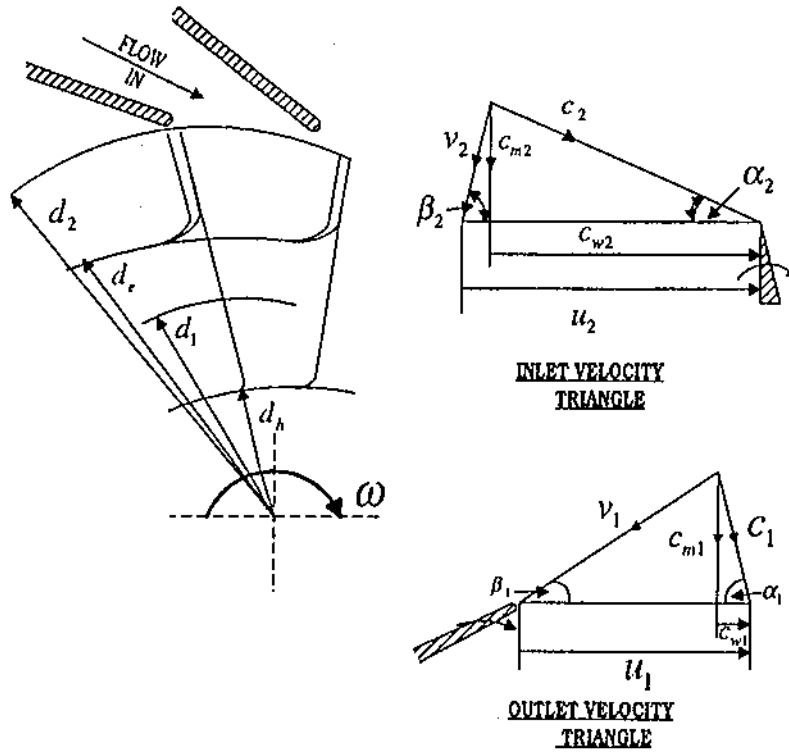


Figure 4.2: Velocity triangles of an inward radial turbine.

$$C_2 = u_2 \left[\frac{\sin \beta_2}{\sin(\alpha_2 + \beta_2)} \right] \dots \dots \dots (4.10)$$

$$C_{w2} = u_2 \left[\frac{\sin \beta_2 \cos \alpha_2}{\sin(\alpha_2 + \beta_2)} \right] \dots \dots \dots (4.11)$$

$$C_1 = u_1 \left[\frac{\sin \beta_1}{\sin(\alpha_1 + \beta_1)} \right] \dots \dots \dots (4.12)$$

$$C_{w1} = u_1 \left[\frac{\sin \beta_1 \cos \alpha_1}{\sin(\alpha_1 + \beta_1)} \right] \dots \dots \dots (4.13)$$

The total to total efficiency in equation (4.9) can be written as:

$$\eta_{t-t} = \frac{\Delta H_{act}}{\Delta H_s} = \frac{u_2 C_{w2} - u_1 C_{w1}}{\frac{1}{2} C_o^2} \dots \dots \dots (4.14)$$

Substituting for C_{w2} and C_{w1} from equation (4.11) and (4.13) then equation (4.14) becomes.

$$\eta_{t-t} = \frac{2}{C_o^2} \left[u_2^2 \left(\frac{\sin \beta_2 \cos \alpha_2}{\sin(\alpha_2 + \beta_2)} \right) - u_1^2 \left(\frac{\sin \beta_1 \cos \alpha_1}{\sin(\alpha_1 + \beta_1)} \right) \right] \dots \dots \dots (4.15)$$

Substituting for $\frac{u_2}{C_o}$ from equation (4.8) in equation (4.15) gives

$$\eta_{t-t} = \pi^2 \left[\frac{\left(\frac{d_2 N}{\sqrt{C_p T_i}} \right)^2}{1 - \left(\frac{p_e}{p_1} \right)^{\frac{\gamma-1}{\gamma}}} \right] \left[\left(\frac{\sin \beta_2 \cos \alpha_2}{\sin(\alpha_2 + \beta_2)} \right) - \left(\frac{d_1}{d_2} \right)^2 \left(\frac{\sin \beta_1 \cos \alpha_1}{\sin(\alpha_1 + \beta_1)} \right) \right] \dots \dots \dots (4.16)$$

Substituting for η_{t-t} from equation (4.16) in equation (4.4), the specific torque is given by:

$$\frac{\tau}{d_2 m \sqrt{C_p T_i}} = \frac{\pi}{2} \left[\frac{d_2 N}{\sqrt{C_p T_i}} \right] \left[\left(\frac{\sin \beta_2 \cos \alpha_2}{\sin(\alpha_2 + \beta_2)} \right) - \left(\frac{d_1}{d_2} \right)^2 \left(\frac{\sin \beta_1 \cos \alpha_1}{\sin(\alpha_1 + \beta_1)} \right) \right] \dots \dots \dots (4.17)$$

The blade tip velocity at rotor inlet, u_2 can be determined from the spouting velocity definition as:

$$u_2 = \left(\frac{u_2}{C_o} \right) C_o \dots \dots \dots (4.18)$$

Substitute equation (4.6) for C_o gives

$$u_2 = \left(\frac{u_2}{C_o} \right) C_o \sqrt{2 C_p T_i \left(1 - \left(\frac{p_e}{p_1} \right)^{\frac{\gamma-1}{\gamma}} \right)} \dots \dots \dots (4.19)$$

The absolute Mach number at rotor inlet is given by:

$$M_2 = \frac{C_2}{\sqrt{\gamma_g R t_2}} \dots\dots\dots(4.20)$$

and t_2 given by

$$t_2 = T_{o3} - \frac{C_2^2}{2C_p} \dots\dots\dots(4.21)$$

substituting equation (4.21) into equation (4.20) gives

$$M_2 = \frac{C_2}{\left[C_{pg} (\gamma_g - 1) \left(T_{o3} - \frac{C_2^2}{2C_{pg}} \right) \right]^{\frac{1}{2}}} \dots\dots\dots(4.22)$$

The mass flow rate at inlet to rotor is given by:

$$\dot{m} = \rho_2 A_2 C_{m2}$$

$$\dot{m} = \left(\frac{p_2}{R t_2} \right) (\pi d_2 b_2) (C_2 \sin \alpha_2) \dots\dots\dots(4.23)$$

where

$$p_2 = p_{o2} \left(\frac{t_2}{T_{o2}} \right)^{\frac{\gamma-1}{\gamma}}$$

$$t_2 = T_{o2} \left(1 - \frac{C_2^2}{2C_p T_{o2}} \right)$$

$$C_2 = u_2 \frac{\sin \beta_2}{\sin(\alpha_2 + \beta_2)}$$

Substituting for p_2, t_2 and C_2 in equation (4.23) gives

$$m = \frac{P_{o2}}{RT_{o2}} \left(1 - \frac{C_2^2}{2C_p T_{o2}} \right)^{\frac{1}{\gamma-1}} \left(\pi d_2^2 \frac{b_2}{d_2} \right) \left[u_2 \frac{\sin(\alpha_2 + \beta_2)}{\sin \alpha_2 \sin \beta_2} \right] \dots \dots \dots (4.24)$$

After substituting for u_2 , C_2 and rearranging equation (4.24) an expression for the blade width to rotor tip diameter ratio, $\frac{b_2}{d_2}$, is given by:

$$\frac{b_2}{d_2} = \frac{\left[\frac{\gamma-1}{\frac{\gamma}{2} P_L} \right] \left[\frac{m \sqrt{C_p T_i}}{d_2^2 P_i} \right] \left[\frac{\sin(\alpha_2 + \beta_2)}{\sin(\alpha_2 + \beta_2)} \right]}{\left(\frac{d_2 N}{\sqrt{C_p T_i}} \right) \left[1 - \frac{\pi^2}{2} \left[\left(\frac{d_2 N}{\sqrt{C_p T_i}} \right) \left(\frac{\sin \beta_2}{\sin(\alpha_2 + \beta_2)} \right) \right]^2 \right]^{\frac{1}{\gamma-1}}} \dots \dots \dots (4.25)$$

4.5 Analysis Procedure

In the preceding two chapters the simple gas turbine cycle equations based on first and second laws of thermodynamic were derived. In this section the method of analysis and the case study will be introduced.

The required equations for the gas turbine cycle were solved using a computer program written in C++ language, the flow chart for this program is shown in figure 4.3, which also list the number of equations to be solved. The input variables and constant values were used in this program as shown below:

- Input variables
- power output, $W_{net} = 50,75$ and 100 kW
- Rotational speed, $N = 50,000$, 70000 and 90000 r.p.m.
- Compressor inlet stagnation (ambient) temperature, $T_{o1} = 288,293$ and 298 K.
- Mass flow rate of air, $m_a = 0.5$, 0.75 and 1.0 kg/s

- Velocity ratio, $u_2/C_0 = 0.67$
- Constant values
 - Ratio of specific heat of air, $\gamma_a = 1.4$
 - Ratio of specific heat of gas, $\gamma_g = 1.33$
 - Specific heat at constant pressure for air, $C_{pa} = 1.005 \text{ kJ/kg K}$
 - Specific heat at constant pressure for gas, $C_{pg} = 1.155 \text{ kJ/kg K}$
 - Compressor isentropic efficiency, $\eta_c = 0.85$
 - Combustion isentropic efficiency, $\eta_{cc} = 0.95$
 - Turbine isentropic efficiency, $\eta_t = 0.87$
 - Relative flow angle at rotor inlet, $\beta_2 = 85 \text{ degree}$
 - Absolute flow angle at rotor inlet, $\alpha_2 = 17 \text{ degree}$
 - Lower caloric value, $\text{LCV} = 43100 \text{ kJ/kg K}$
 - Fraction of pressure loss in combustor, $P_l = 0.02 \%$
 - Gas constant, $R = 287 \text{ J/kg K}$.

5. RESULTS AND DISCUSSION

5.1 First Law Analysis

All the previous relations for gas turbine cycle based on first law as well as second law of thermodynamics were solved using a computer program and the results are illustrated in the following figures.

Figure 5.1 shows the variation of fuel to air ratio (f) with turbine inlet temperature at 100 kW power output and different compressor pressure ratios. It is clearly shown that the relation is a linear increasing one, as the turbine inlet temperature increased as the fuel to air ratio increased. Where f is in the range of 0.005 to 0.025 for turbine inlet temperatures of 700 to 1200 K. Also it is clear that the effect of compressor pressure ratio is inversely proportional to fuel to air ratio, the fuel to air ratio decreased about 36% as the pressure ratio increased from 2 to 5. The increase in fuel flow leads to an increase in compressor speed and gas turbine inlet temperature.

Figure 5.2 shows the variation of tip blade speed u_2 at turbine rotor inlet with compressor pressure ratio at different turbine inlet temperatures. It is clear that the turbine tip blade speed increased with both increase of turbine inlet temperature and compressor pressure ratio. The maximum speed is about 638 m/s. Both figures 5.1 and 5.2 limited by material stresses on the blade tip.

The variation of Mach numbers at turbine rotor inlet M_2 , exducer M_e , mean diameter M_1 and hub diameter M_h with compressor pressure ratio is shown in figure 5.3. It is clear that $M_2 > M_e > M_1 > M_h$ and all Mach numbers increased slightly with the increase of compressor pressure ratio. It is clear from the definition of Mach number M_2 , which is given by equation 4.20, that the increase of Mach number is due to the

increase of the blade tip velocity u_2 ; therefore, Mach number is controlled mainly by the blade tip velocity. Also, it is noted from this figure that the increase of P_{rc} above 4.5 produce a super sonic flow in the stator part o the turbine high excessive losses.

5.1.1 Specific fuel consumption

The cycle performance can be expressed in terms of fuel consumption per unit network output, i.e. in terms of the specific fuel consumption rather than efficiency, not only because its definition is unambiguous, but also because it provides both a direct indication of fuel consumption and a measure of cycle efficiency to which it is inversely proportional.

Figure 5.4 shows the variation of specific fuel consumption with turbine inlet temperature at 100 kW power output and different compressor pressure ratios. It is clear that the SFC decrease with the increase of turbine inlet temperature and most of the decrease occurs in the range of 700-900 K. And then the curves are slowly decreased in the range 900 – 1200 K. While the effect of compressor pressure ratio is inversely proportional to the SFC. It is clear that about 66% of SFC reduction occurs by increasing P_{rc} from 2 to 3, 22.5% by increasing P_{rc} from 3 to 4 and 11.5% by increasing P_{rc} from 4 to 5. Therefore the increasing of P_{rc} above 5 will not effectively improve the SFC ratio.

The effect of ambient temperature (inlet compressor temperature) on SFC is shown in figures 5.5 and 5.6. It is clear that the SFC is affected strongly by the decrease of ambient temperature to 288 K, while the increase of ambient temperature from 293K to 298K does not affect the SFC and the two curves are nearly the same for most of the turbine inlet temperature range. This decrease of SFC is due to the decrease of compressor work as ambient temperature decreased.

Figure 5.7 shows the variation of specific fuel consumption with specific work output at $P_{rc} = 2$ and different turbine inlet temperatures. The SFC is inversely proportional to specific work output, as the specific work output increased the SFC decreased. Also from this figure it is noticed that as the turbine inlet temperature increased the SFC increased. Figure 5.8 shows the effect of varying the P_{rc} on the SFC with specific work output at $T_{03} = 700$ K. The main result from this figure is that as the pressure ratio increased the SFC decreased especially for specific work output below 100 kW/kg.

The specific fuel consumption is increased as the power output is reduced because the reduction in fuel flow leads to a reduction in compressor speed and gas turbine inlet temperature. It is well known that the efficiency of a real cycle falls as the turbine inlet temperature is reduced. This poor part-load economy is a major disadvantage of the simple gas turbine.

5.1.2 Specific work output

The variations of specific work output with both turbine inlet temperature and compressor pressure ratio are shown in figure 5.9. It is obvious from this figure that the specific work output (W_s) is increased as the turbine inlet temperature increased and as the P_{rc} increased the W_s increased also. The maximum W_s obtained at $P_{rc} = 5$ and $T_{03} = 1200$ K.

5.1.3 Dimensionless mass flow rate

Figure 5.10 shows the variation of dimensionless mass flow rate (MFR) with compressor pressure ratio at 100kW power output and different turbine inlet temperatures. From the figure, It is clear that MFR decreases with increasing of turbine

inlet temperature and most of the decrease occurs in the range of T_{03} from 700 to 900 K. It can be concluded that a recommended turbine inlet temperature not to be below 900K. The effect of pressure ratio is clearly observed that as the P_{rc} increased the MFR decreased with large decrease in the range of P_{rc} from 2 to 3. So it can be concluded that a recommended compressor pressure ratio not to be below 3.

Figure 5.11 shows the variation of blade width to rotor tip diameter ratio b_2/d_2 with turbine inlet temperature at $P_{rc} = 2$ and different power output. It is obvious from this figure that the b_2/d_2 ratio decreased at T_{03} increased. Also the b_2/d_2 ratio decreased by decreasing the power output. It is clear that the effect of turbine inlet temperature on b_2/d_2 ratio is large at low values of turbine inlet temperature and become less effective at higher values.

5.1.4 Cycle thermal efficiency

The main performance parameter to be analyzed in the first law is the cycle thermal efficiency. Figure 5.12 shows the variation of cycle thermal efficiency with P_{rc} at different T_{03} . From this figure it can be shown that the cycle thermal efficiency is strongly affected by both P_{rc} and T_{03} . Also it is noted that most of the increase occurs for P_{rc} from 2 to 3 and T_{03} from 700 – 900 K as previously discussed in mass flow rate, it is better to use P_{rc} above 3 and T_{03} above 900 K. Also it is clear that the efficiency curve increased to reach an optimum point and then decreased as P_{rc} increased, this trend is clearly shown for $T_{03} = 700$ K, while for other values of T_{03} the same behavior may be obtained if we extend the range of operating P_{rc} , which mean that there is an optimum value of maximum efficiency for each turbine inlet temperature. The advantage of using as high value of T_{03} as possible, and the need to use a higher P_{rc} to take advantage of a higher permissible temperature, is evident from this figure. The

efficiency increases with T_{03} because the component losses become relatively less important as the ratio of positive turbine work to negative compressor work increases.

The remaining parameter of importance is the ambient temperature, to which the performance of gas turbine is particularly sensitive. Figures 5.13 and 5.14 show the variation of cycle thermal efficiency with turbine inlet temperature and different compressor inlet temperatures (ambient temperatures). It is clear that as the ambient temperature reduced the cycle thermal efficiency increased especially when T_{01} is reduced to 288 K. the increase in thermal efficiency is due to the decrease of compressor work as T_{01} decreased.

Figure 5.15 shows the variation of cycle thermal efficiency with specific work output at $P_{rc} = 2$ and different turbine inlet temperatures. It is clear from this figure that the relation between η_{cycle} and W_s is a linear proportional one, as W_s increased η_{cycle} increased. But it is noted that as turbine inlet temperature increased the thermal efficiency decreased. So it is a design point to choose a maximum efficiency or a maximum specific work output. The effect of P_{rc} on the variation of cycle thermal efficiency with specific work output at $T_{03} = 700$ K is shown in figure 5.16. From this figure, it is clear that as P_{rc} increased η_{cycle} decreased.

5.2 Second Law Analysis

5.2.1 Irreversibility (exergy destruction)

Figure 5.17 shows the variation of compressor irreversibility (exergy destruction) with turbine inlet temperature at different P_{rc} . It is clear from this figure that compressor irreversibility decrease with increasing turbine inlet temperature from about 55 kW at $T_{03} = 700$ K to about 10 kW at $T_{03} = 1200$ K. Also it is noted that the curves of

irreversibility drop more steeply in the range of T_{03} from 700 – 900 K and then they become nearly flat in the remaining range to 1200 K. It is obvious from this figure that the irreversibility increases with increasing P_{rc} . This is attributed to the increased of heat-power ratio as the pressure increases. Also this increase is more rapidly for T_{03} of 700 and 800 K, while it is nearly flat for T_{03} from 900 to 1200 K.

Figure 5.18 shows the variation of combustor irreversibility (exergy destruction) with compressor pressure ratio for different turbine inlet temperatures. It is clear from this figure that the combustor irreversibility decreased with increasing of P_{rc} to reach a minimum value, as shown fro $T_{03} = 700$ and 800 K, and then increased. The same trend for other values of T_{03} may be obtained if the range of operating P_{rc} is extended. It is clear that the optimum conditions of combustor irreversibility at $P_{rc} = 3$ and 4 for $T_{03} = 700$ and 800 K respectively. Also it is noted that the effect of turbine inlet temperature on combustor irreversibility is small since the curves approach each other especially for P_{rc} below 3.

Figure 5.19 shows the variation of turbine irreversibility (exergy destruction) with turbine inlet temperature at different P_{rc} . It is clear from this figure that the turbine irreversibility decrease with increasing turbine inlet temperature from 63 kW at $T_{03} = 700$ K to about 10 kW at $T_{03} = 1200$ K. Also a steep decrease is noted in the range of $T_{03} = 700$ to 900 K. and then the curves become nearly flat with small decrease of turbine irreversibility. It is noted from this figure that the irreversibility increase with increasing P_{rc} . This increase of irreversibility is due to the increase of heat-power ratio as the pressure increased. Also the increase of irreversibility is more rapidly for $T_{03} = 700$ and 800 K, while it is nearly flat for T_{03} higher then 900 K.

A comparison between the irreversibilities of the three components of the gas turbine cycle is shown in figure 5.20 with T_{03} at $P_{rc} = 2$ and 3. It is well noted from this figure that the irreversibility of the combustor is much than the irreversibility of the compressor and the turbine, while the irreversibility of the compressor is slightly higher than the turbine irreversibility. While most of irreversibility (exergy destruction) was found to be in the combustor and this is an indication to take care of this component in order to reduce the irreversibility loss in the gas turbine cycle and to increase its performance.

The total irreversibility for the three components were added to each other and shown in figure 5.21 with turbine inlet temperature and different P_{rc} . It is obvious from this figure that the total irreversibility is decreased with turbine inlet temperature increased, especially in the range of T_{03} from 700 to 900 K and then continue in decreasing with small rate from $T_{03} = 900$ to 1200 K. Also it is clear that the total irreversibility decreased with P_{rc} increasing for P_{rc} below 3 and then increasing for $T_{03} = 700$ to 900 K and nearly constant for $T_{03} = 1000$ to 1200 K.

5.2.2 Entropy generation

Figures 5.22 and 5.23 show the variation of entropy generation of compressor and turbine respectively with P_{rc} . It is clear from these two figures that the entropy generation increased with the increase of P_{rc} , while there is no change in entropy generation for both components with turbine inlet temperatures. Also it is noted that the compressor entropy generation is slightly higher than the turbine. It is well known that the increase in entropy generation will increase the irreversibility or exergy loss as was shown in figures 5.17 and 5.19 for compressor and turbine irreversibilities respectively.

Where the irreversibility of both components increased as P_{rc} increased such as entropy generation.

Figure 5.24 shows the variation of combustor entropy generation with turbine inlet temperature at different P_{rc} . It is clear that the combustor entropy generation increased with the increasing of turbine temperature. It is obvious from this figure that the entropy generation decreased with the increasing of P_{rc} .

The effect of ambient temperature on the combustor entropy generation is shown in figures 5.25 and 5.26. It is clear that the ambient temperature effect is very small since the curves approach each other, but it is noticed that as T_{o1} increased the combustor entropy generation decrease. Therefore, this means that increasing the air temperature at the combustor inlet can lower the combustor losses.

5.2.3 Availability change

Figure 5.27 shows the variation of availability change of the compressor with compressor pressure ratio at different turbine inlet temperature. It is noted from this figure that the compressor availability decreased with the increased of T_{o3} from about 550 kW at $T_{o3} = 700$ K to about 100 kW at $T_{o3} = 1200$ K at $P_{rc} = 5$. Also it is clear that the curves of availability change drop more steeply in the range of $T_{o3} = 700$ to 900 K and then they become nearly flat with small decrease. Also, it is obvious from this figure that the availability change increased with the increased of P_{rc} .

Figure 5.28 shows the variation of combustor availability change with compressor pressure ratio and turbine inlet temperatures. It is noted that the availability change decreased in the range of $T_{o3} = 700$ to 800 K and then it becomes nearly constant. Also it is clear that there is a large difference of availability change between the values of

$P_{rc}=2$ to 3 and then the difference is becoming more and more small between the values of $P_{rc} = 4$ and 5. It is observed that as the P_{rc} increases the combustor availability change will decrease except for $T_{o3} = 700$ K, and the drop of the curves are more rapidly in the range of $P_{rc} = 2$ to 3 and then they become nearly flat with small decrees for $P_{rc} = 3$ to 5. Also the effect of turbine inlet temperature is more noticed here, where the behavior of curves for $T_{o3} = 900$ to 1200 K are nearly the same for the whole range of P_{rc} . Also, it is clear that the availability change of the combustor decreased to reach a minimum value and then increased as the compressor pressure ratio increased. For $T_{o3} = 700$ K this minimum value occurs at $P_{rc} = 3.5$, while for other values of T_{o3} the same behavior may be obtained if the ranges of P_{rc} were extended.

The variation of turbine availability change with compressor pressure ratio at different turbine inlet temperatures is show in figure 5.29. It is clear that from this figure as the turbine inlet temperature increases the turbine availability change will decrease and this decrease is more rapidly in the range of $T_{o3} = 700$ to 900 K and then it becomes nearly flat with small decrease for $T_{o3} = 900$ to 1200 K. It is well noted that as the P_{rc} increases the turbine availability change will increase especially for $T_{o3} = 700$ to 800 K, while for the range of $T_{o3} = 900$ to 1200 K it is slightly increased.

A comparison between the availability change for the three components of the gas turbine cycle, which are the compressor, the combustor and the turbine, is shown in figure 5.30. It is clear that the availability change of the combustor is the highest of three components and the turbine is higher than the compressor.

5.2.4 Second law efficiency

Figure 5.31 shows the variation of second law efficiency with compressor pressure ratio and different turbine inlet temperature. It is clear from this figure that the second

law efficiency is less sensitive to turbine inlet temperature changes for $P_{rc} = 2$ and 3, while it is slightly increased with the increase of turbine inlet temperature for $P_{rc} = 4$ and 5. The second law efficiency is in the range of 19.1% and 35.6 for $P_{rc} = 2$ and 5 respectively. The increase in second law efficiency as T_{o3} increased is due to the decrease of irreversibility for cycle components as T_{o3} increased.

It is obviously clear that the second law efficiency increased with the increase of P_{rc} to reach a maximum value and then return to decrease, this trend is observed for $T_{o3} = 700$ and 800 K, while for other values of T_{o3} this trend may be obtained if the range of compressor pressure ratio is extended. Therefore for each turbine inlet temperature there is an optimum value for P_{rc} to have maximum second law efficiency. Also the effect of higher turbine inlet temperatures is clearly noted that the second law curves for T_{o3} 900 to 1200 K are close to each other especially for P_{rc} below 3. The increase of second law efficiency as T_{o3} or P_{rc} increased is justified by figure 5.32, which shows that the second law efficiency is increased since the total irreversibility of the gas turbine cycle, decreased as T_{o3} increased.

The effect of ambient temperature on the second law efficiency at $P_{rc} = 3$ is shown if figures 5.33 and 5.34. It is clear that as T_{o1} decreased the second law efficiency increased especially for lower values of T_{o3} such as 700 K the difference in second law efficiency is very noticeable until T_{o3} reaches 1000 K the three values are nearly the same and then the difference is nearly small.

A comparison between first law and second law efficiencies are show in figure 5.35. It is clear that for $P_{rc} = 2$ the values of first law efficiency ranged between 8.7% to 18.4% and the second law efficiency is between 19.1% to 18.5% for $T_{o3} = 700$ and 1200 K respectively. For $P_{rc}=3$ the first law efficiency is between 11.9% to 17.5% and the

second law efficiency is between 24.6% to 27.2% for $T_{03} = 700$ to 1200 K respectively. For $P_{rc} = 4$ the first law efficiency is between 12.6% to 21.1% and the second law efficiency is between 25.2% to 32.3% for $T_{03} = 700$ to 1200 K respectively. Finally for $P_{rc} = 5$ the first law efficiency is between 11.9% to 23.5% and the second law efficiency is between 32.2% to 35.6% for $T_{03} = 700$ to 1200 K respectively. It is clear that all second law efficiency curves are much higher than first law efficiency curves.

The second law analysis, which can locate and quantify the irreversibilities that cause loss of work and efficiency gives more understanding of performance than the first law analysis that makes no distinction between heat and work and thus does not quantify the quality of heat. Therefore, first law analysis does not show which system components the cycle losses should be attributed to.

5.2.5 Effectiveness of components

Figure 5.36 shows the variation of compressor second law efficiency (effectiveness) with compressor pressure ratio. It is clear that from this figure that the effectiveness is slightly increased with the increase in P_{rc} . The range of effectiveness is varied from 87.8% to 90.9% for $P_{rc} = 2$ and 5 respectively. Also there is no change of compressor effectiveness by varying turbine inlet temperatures.

Figure 5.37 shows the variation of combustor second law efficiency (effectiveness) with compressor pressure ratio at different turbine inlet temperatures. It is clear from this figure that the combustor second law efficiency is increased as compressor pressure ratio increased to reach a maximum value of $P_{rc} = 3$ and 4 for $T_{03} = 700$ and 800 K respectively and then return to decrease. This behavior is applied for other values of T_{03} as the P_{rc} range extended.

Figure 5.38 shows the variation of turbine second law efficiency (effectiveness) with turbine inlet temperature at different compressor pressure ratios. It is obvious from this figure that the turbine effectiveness increases with increasing turbine inlet temperature. The range of effectiveness is between 91.9% to 96%. It is noted that the turbine effectiveness decrease with increasing P_{rc} . Since the heat losses increased as P_{rc} increased.

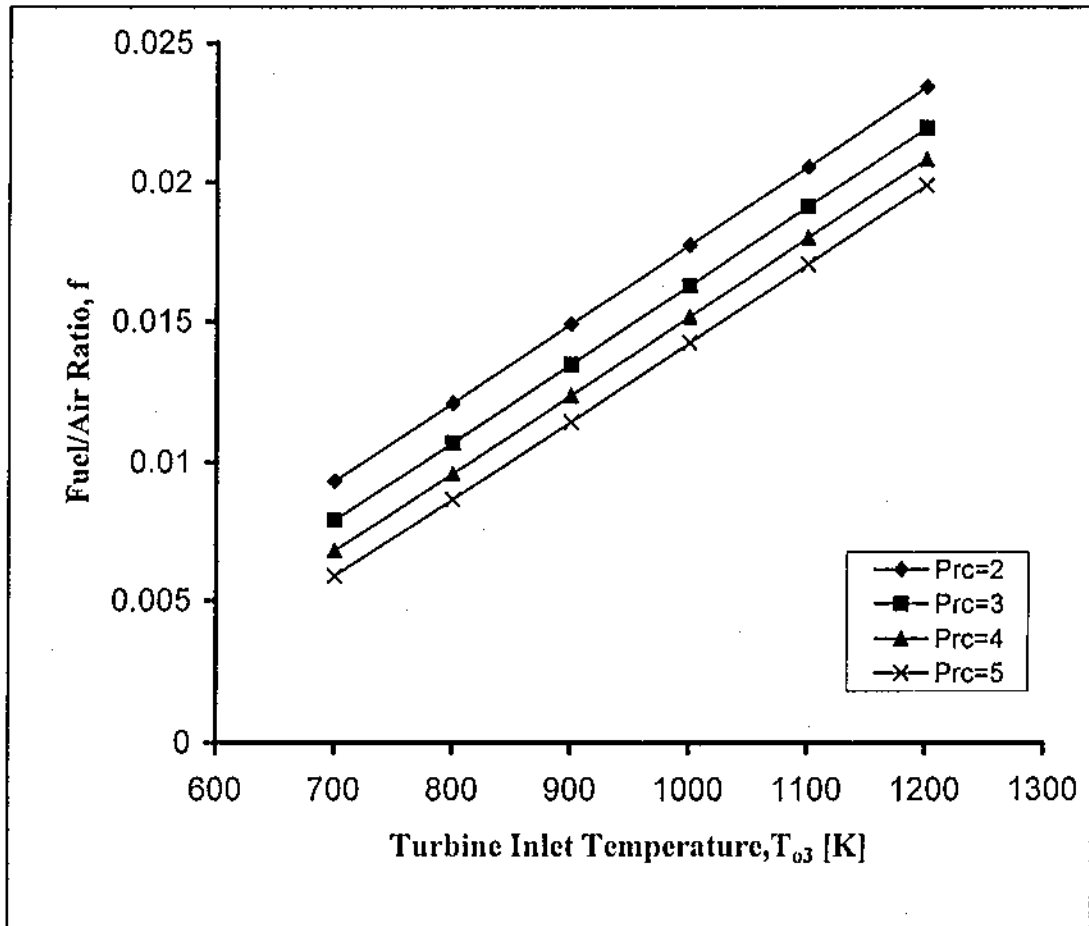


Figure 5.1: Variation of fuel/air ratio with turbine inlet temperature at 100 kW power output and different compressor pressure ratios.

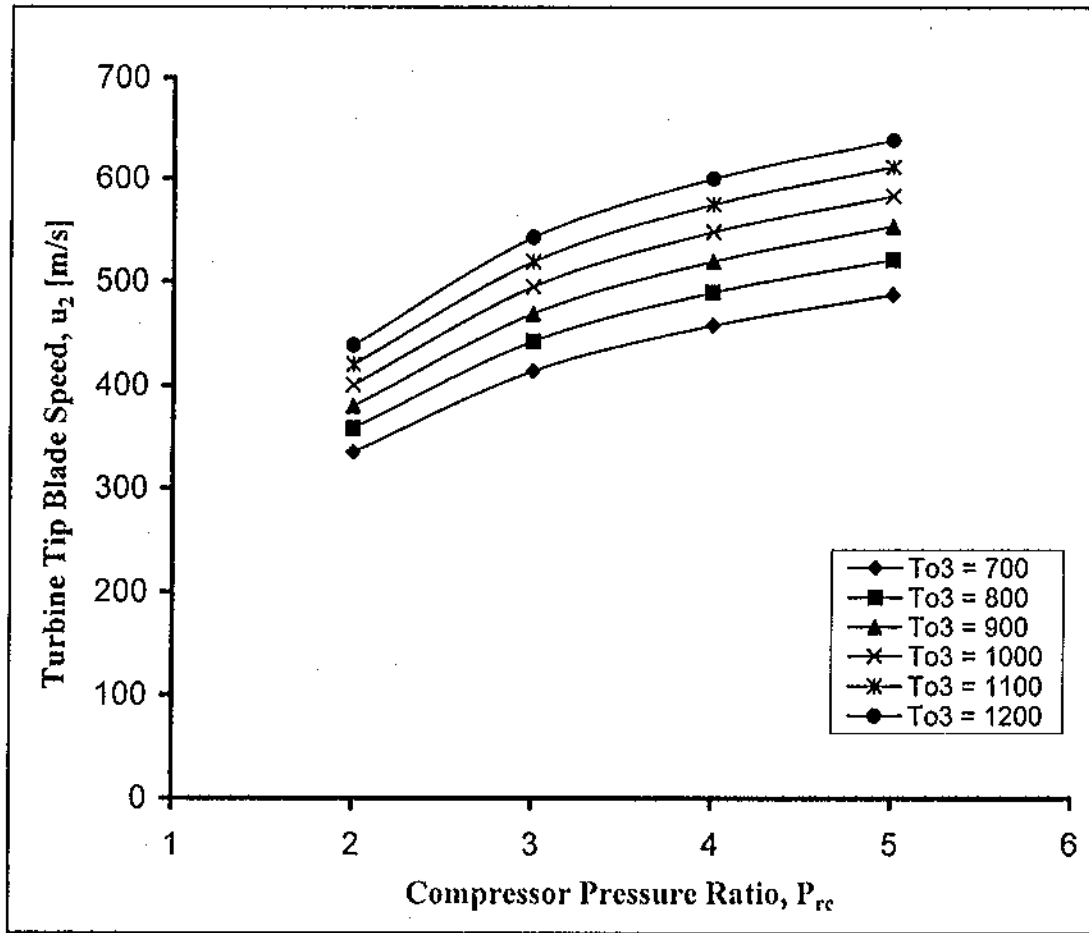


Figure 5.2: Variation of blade tip velocity at turbine rotor inlet with compressor pressure ratio at 100 kW power out put at different turbine inlet temperatures.

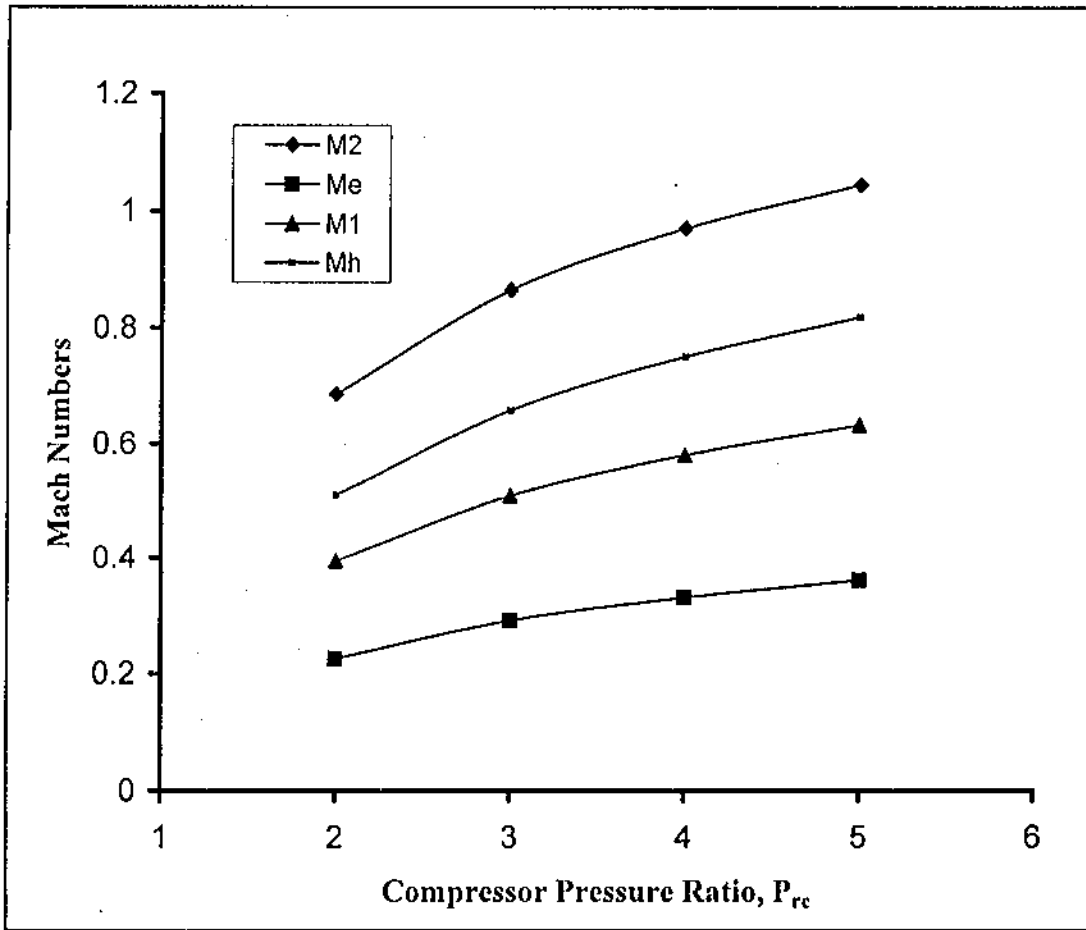


Figure 5.3: Variation of mach numbers at turbine rotor inlet, exducer, mean and hub diameters with compressor pressure ratio at 100 kW power output.

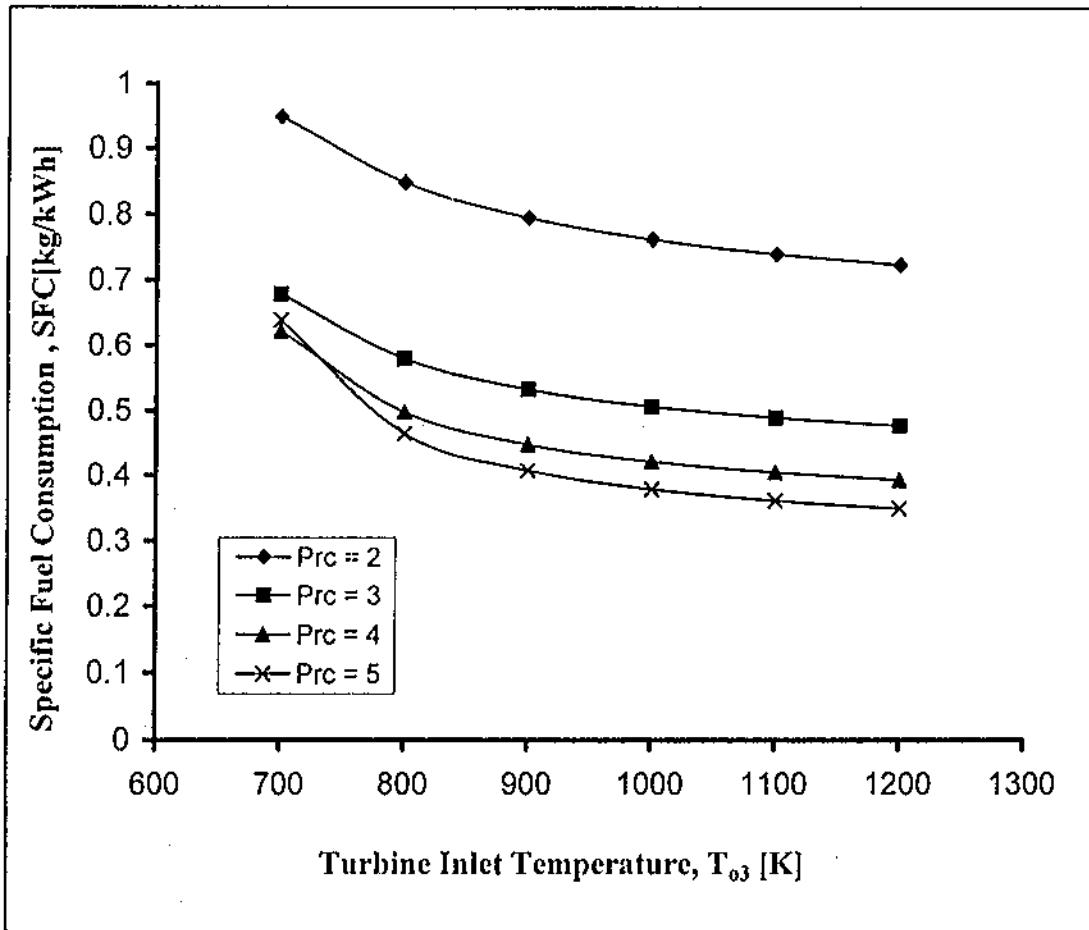


Figure 5.4: Variation of specific fuel consumption with turbine inlet temperature at 100 kW power output and different compressor pressure ratios.

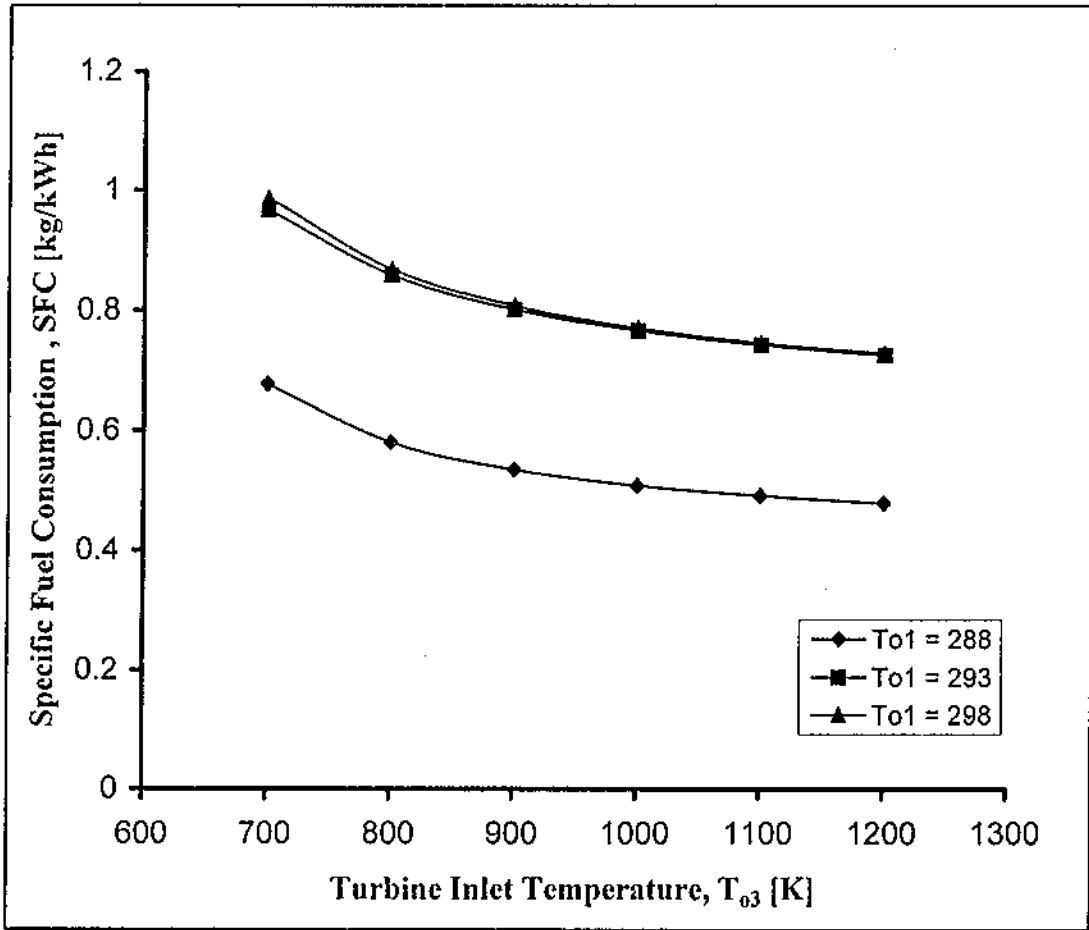


Figure 5.5: Variation of specific fuel consumption with turbine inlet temperature at 100 kW power output and different compressor inlet temperatures.

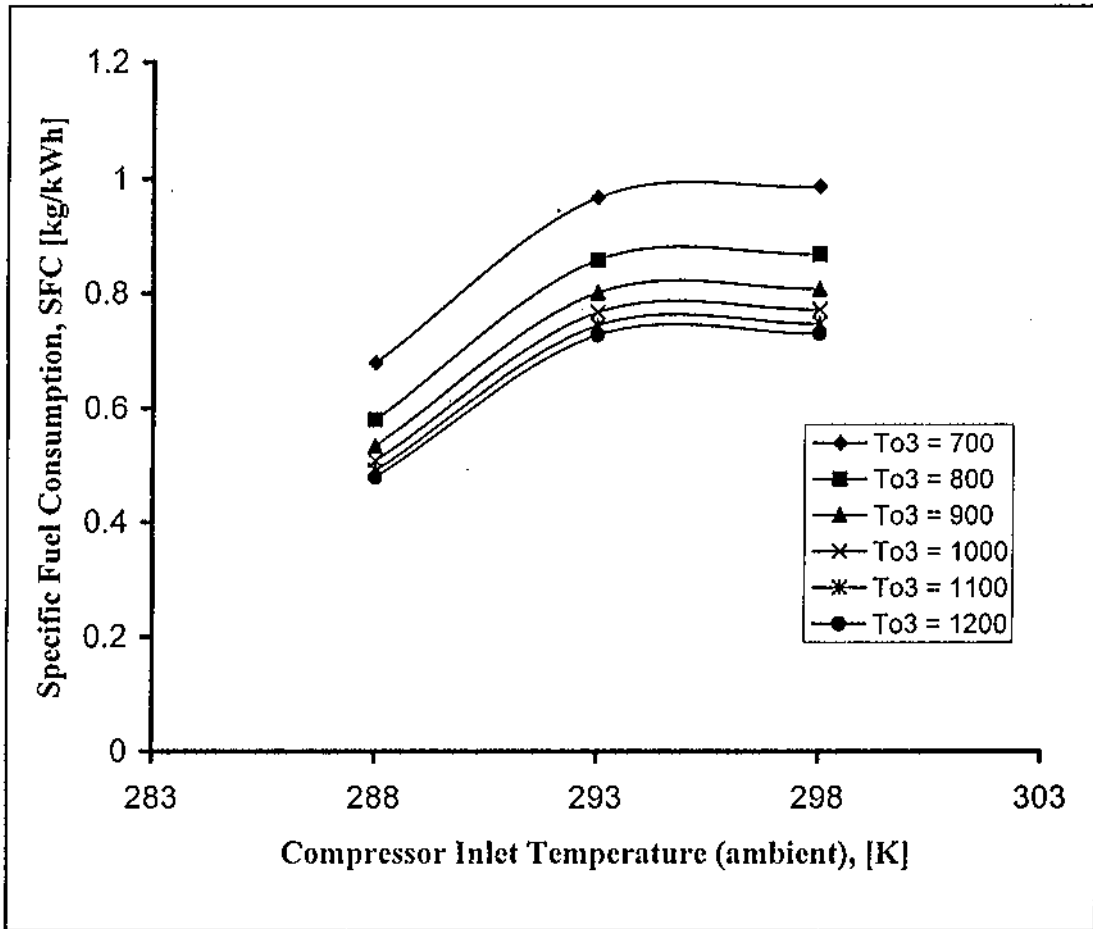


Figure 5.6: Variation of specific fuel consumption with compressor inlet temperature (ambient) and different turbine inlet temperature at 100 kW power output

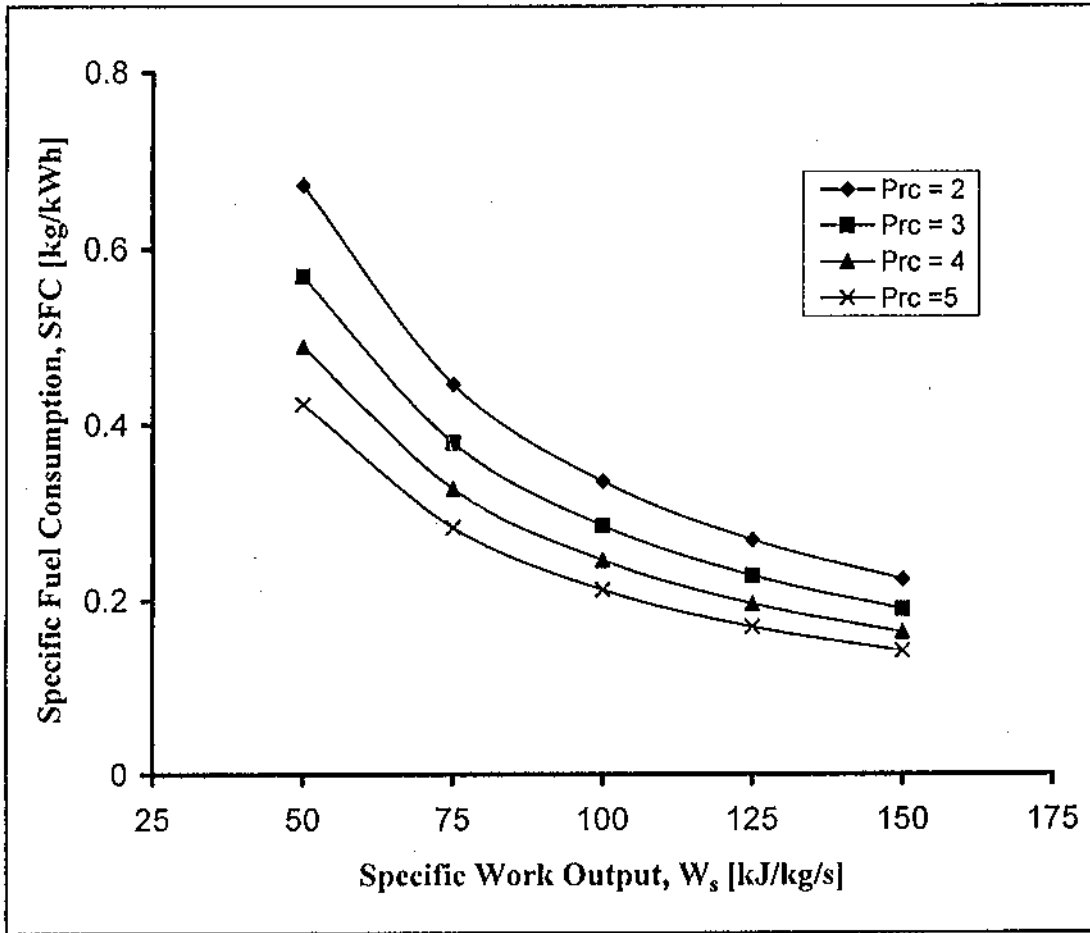


Figure 5.8: Variation of specific fuel consumption with specific work output at

$T_{03}=700$ [K] and different compressor pressure ratios.

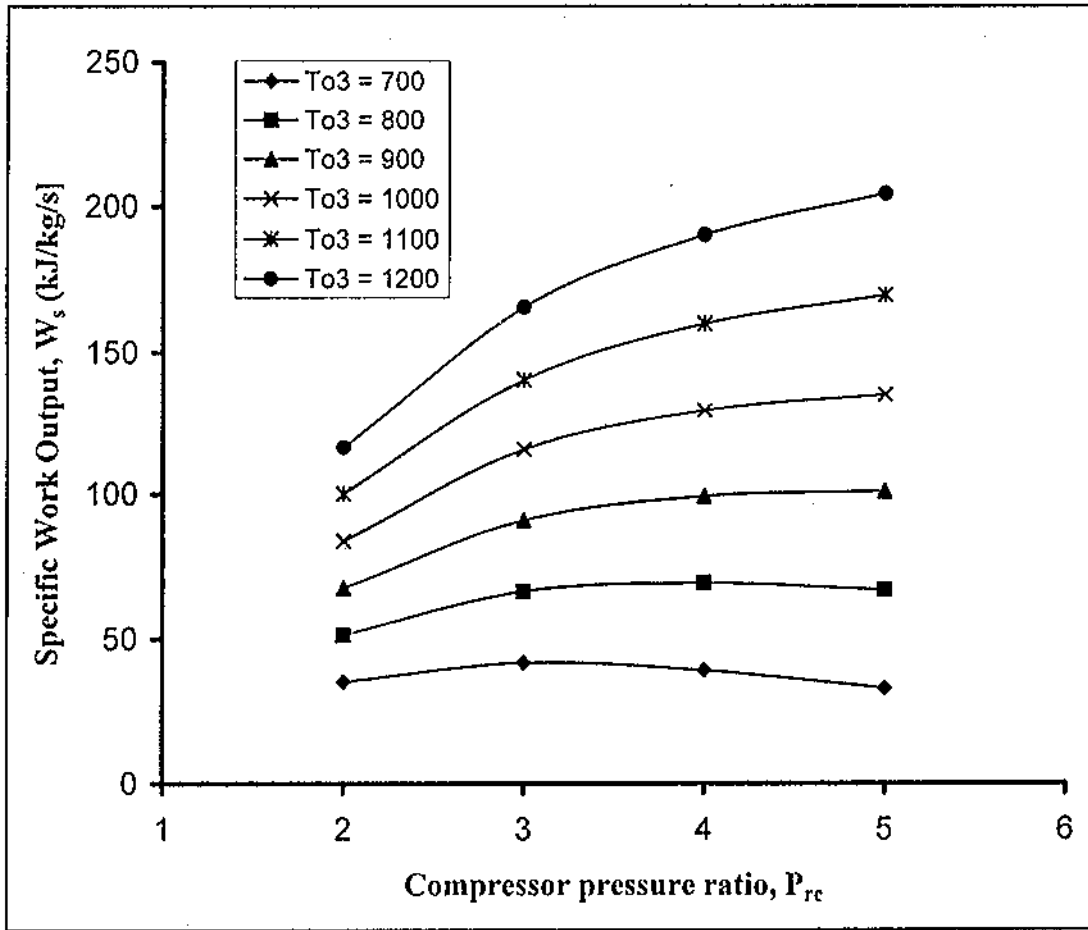


Figure 5.9: Variation of specific work output with compressor pressure ratio at 100 kW power output and different turbine inlet temperatures.

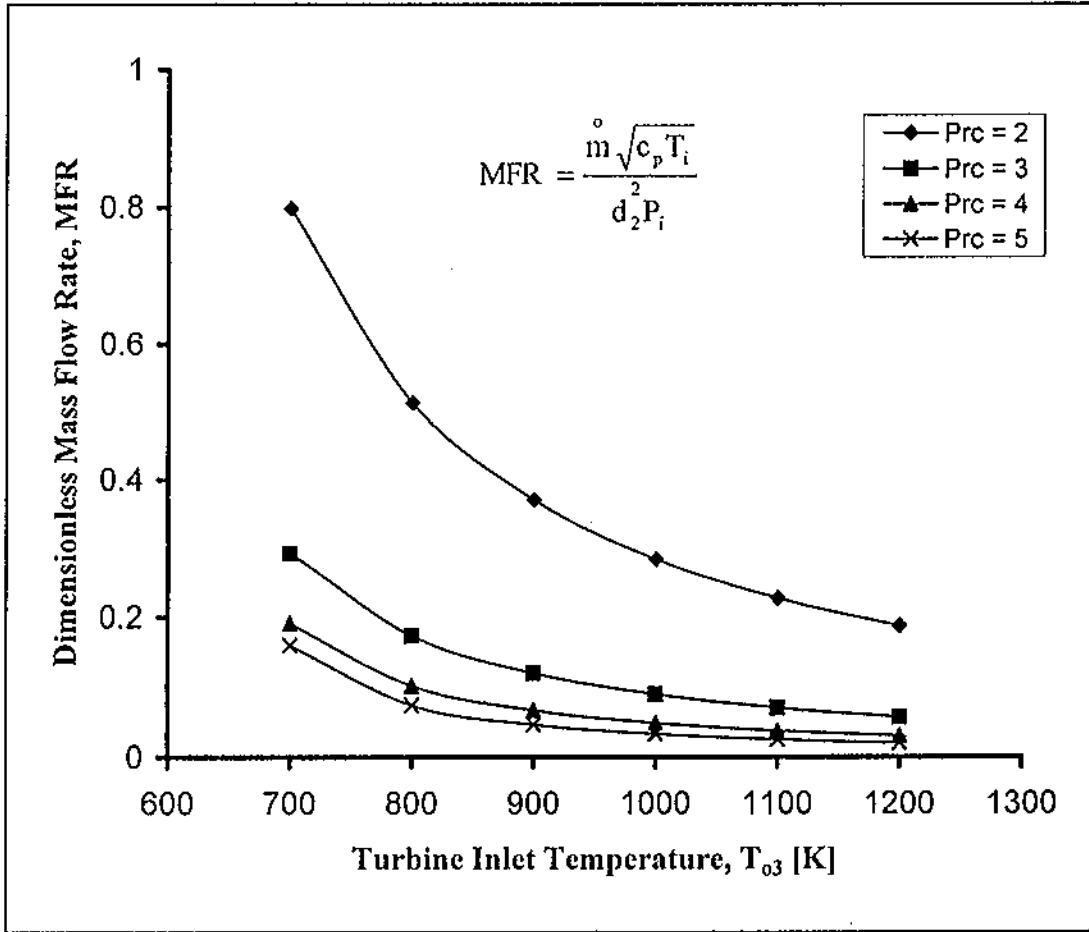


Figure 5.10: Variation of dimensionless mass flow rate with turbine inlet temperature at 100 kW power output and different compressor pressure ratios.

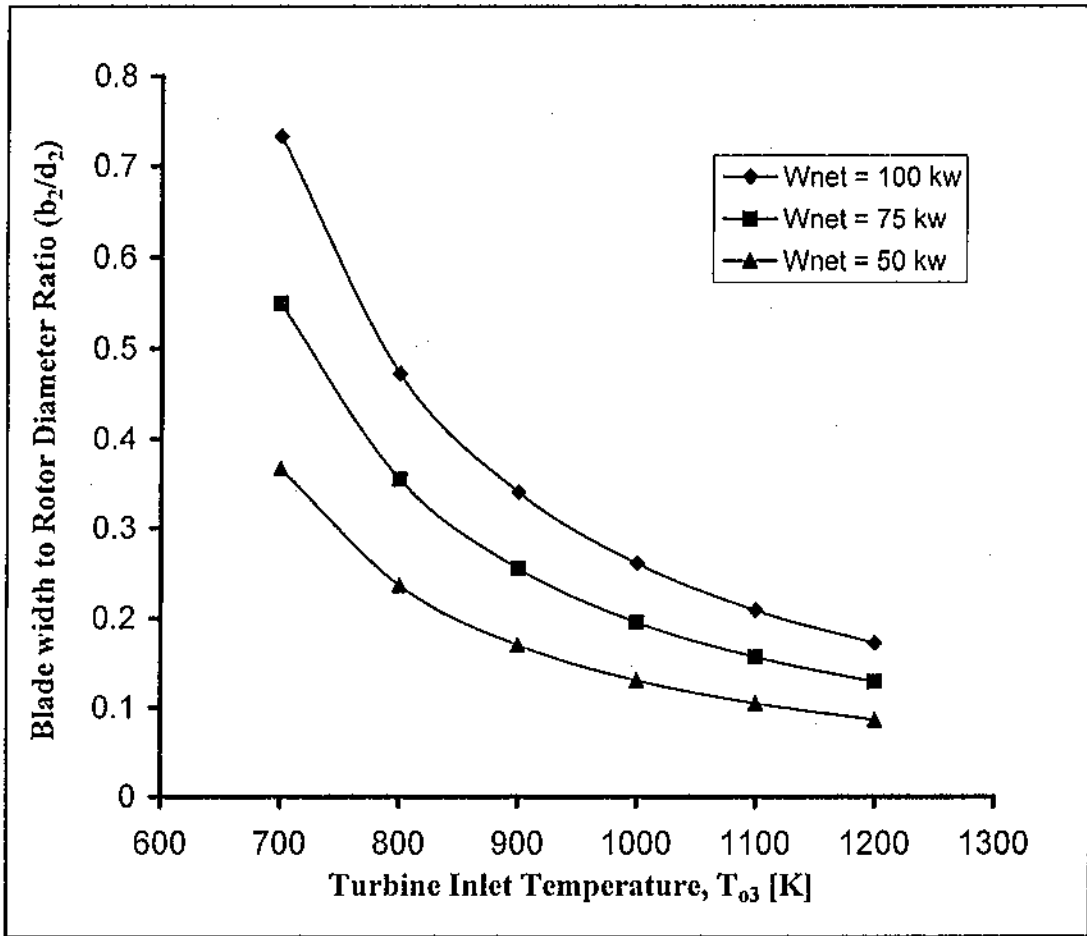


Figure 5.11: Variation of blade width to rotor tip diameter ratio (b_2/d_2) with turbine inlet temperature at $P_{re} = 2$ and different power output .

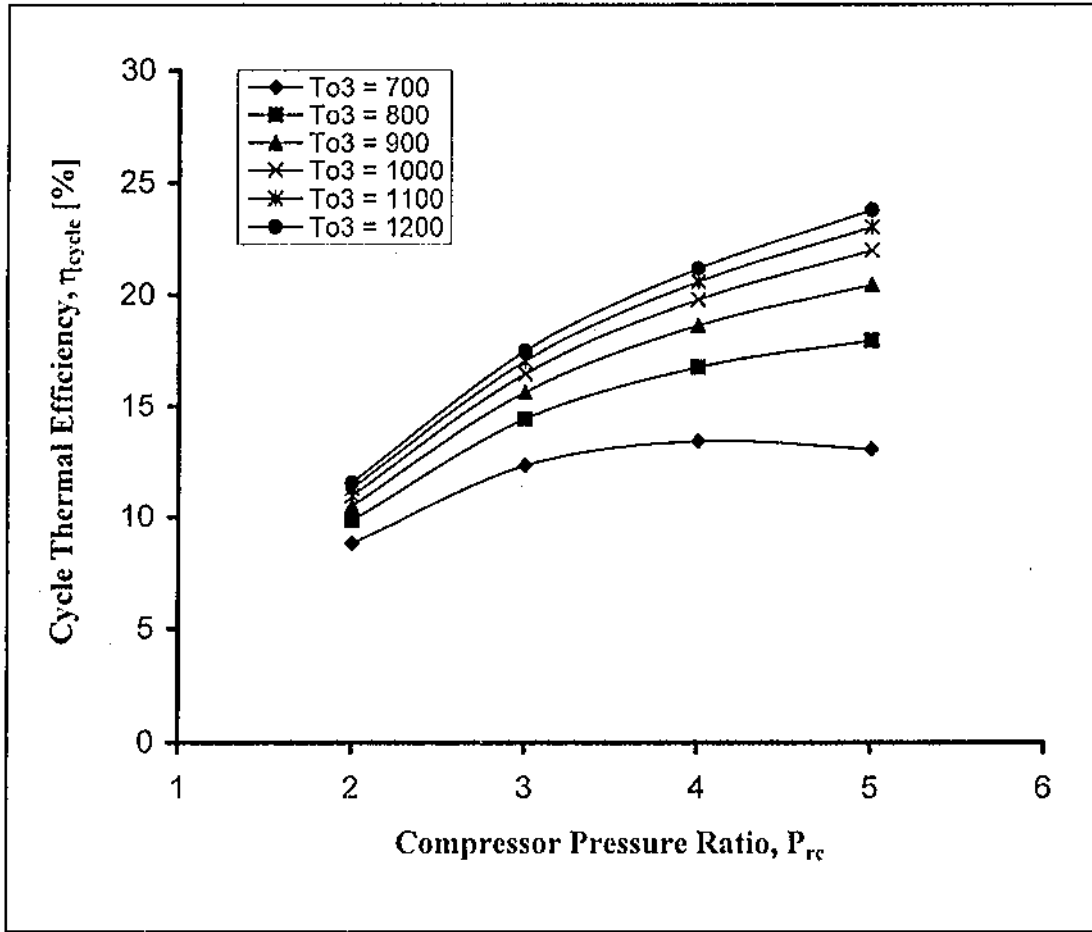


Figure 5.12: Variation of cycle thermal efficiency with compressor pressure ratio at 100 kW power output and different turbine inlet temperatures.

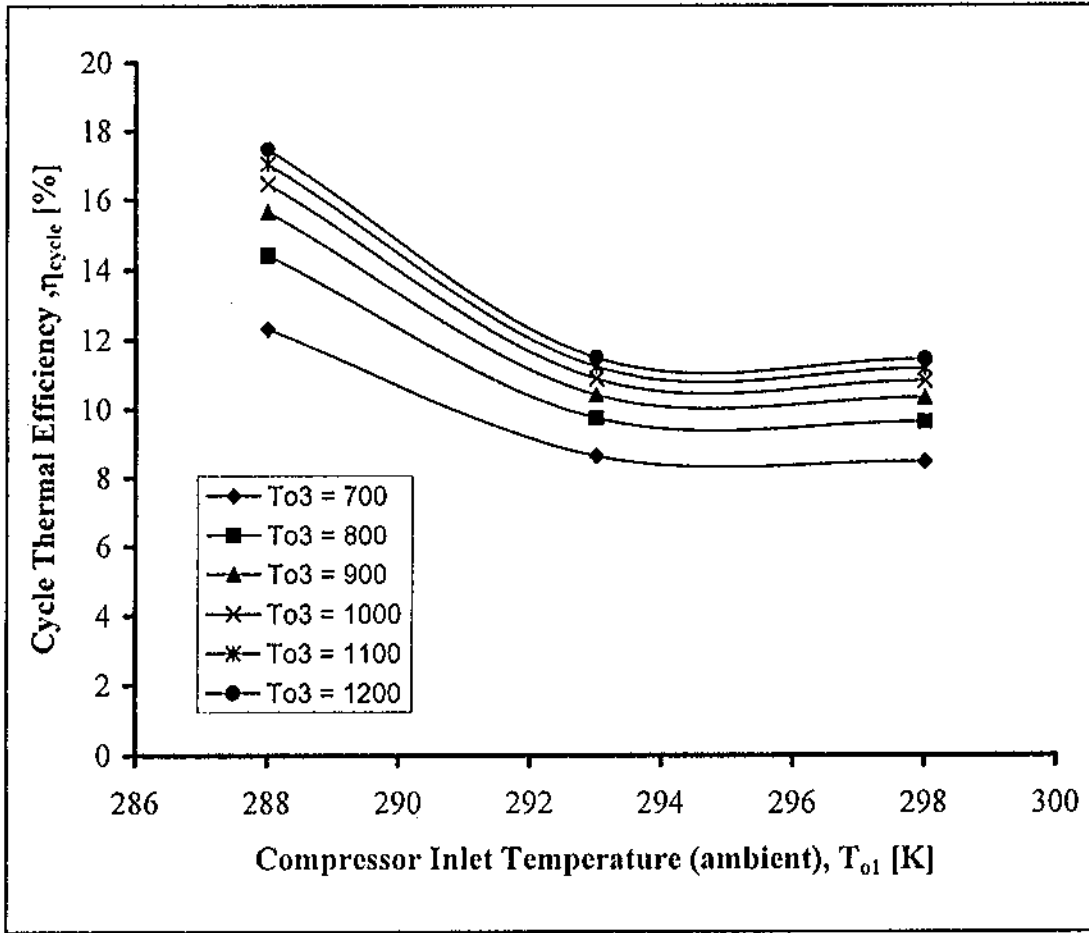


Figure 5.14: Variation of cycle thermal efficiency with compressor inlet temperature (ambient) and different turbine inlet temperature at 100 kW power output.

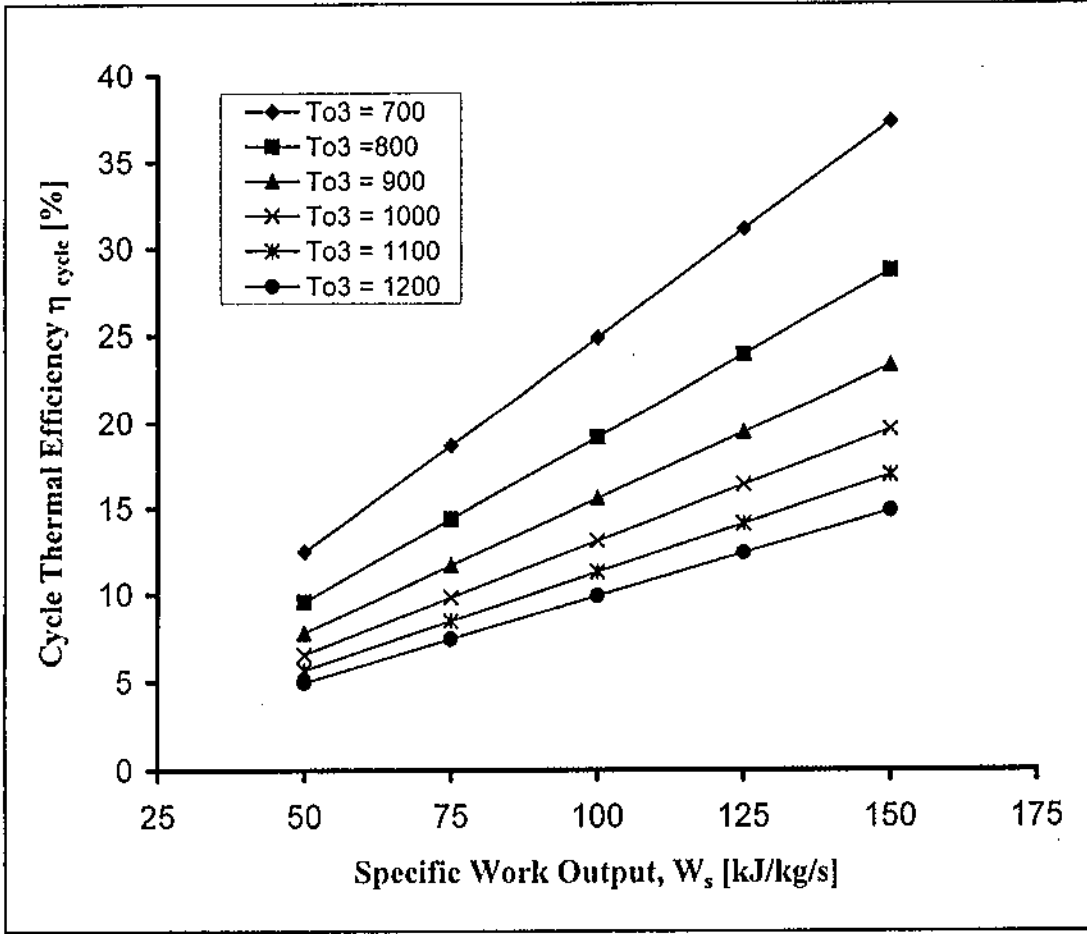


Figure 5.15: Variation of cycle thermal efficiency with specific work output at $P_{rc}=2$ and different turbine inlet temperatures.

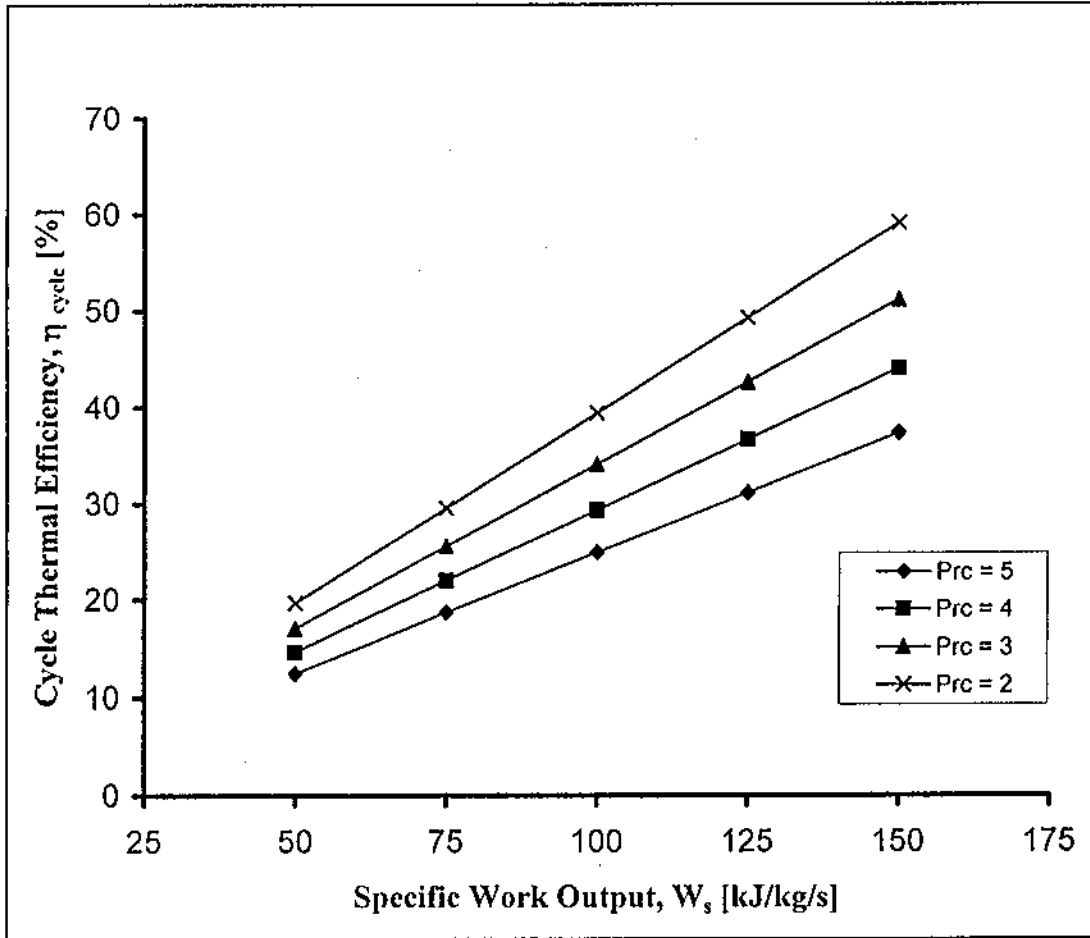


Figure 5.16: Variation of cycle thermal efficiency with specific work output at

$T_{03}=700$ [K] and different compressor pressure ratios.

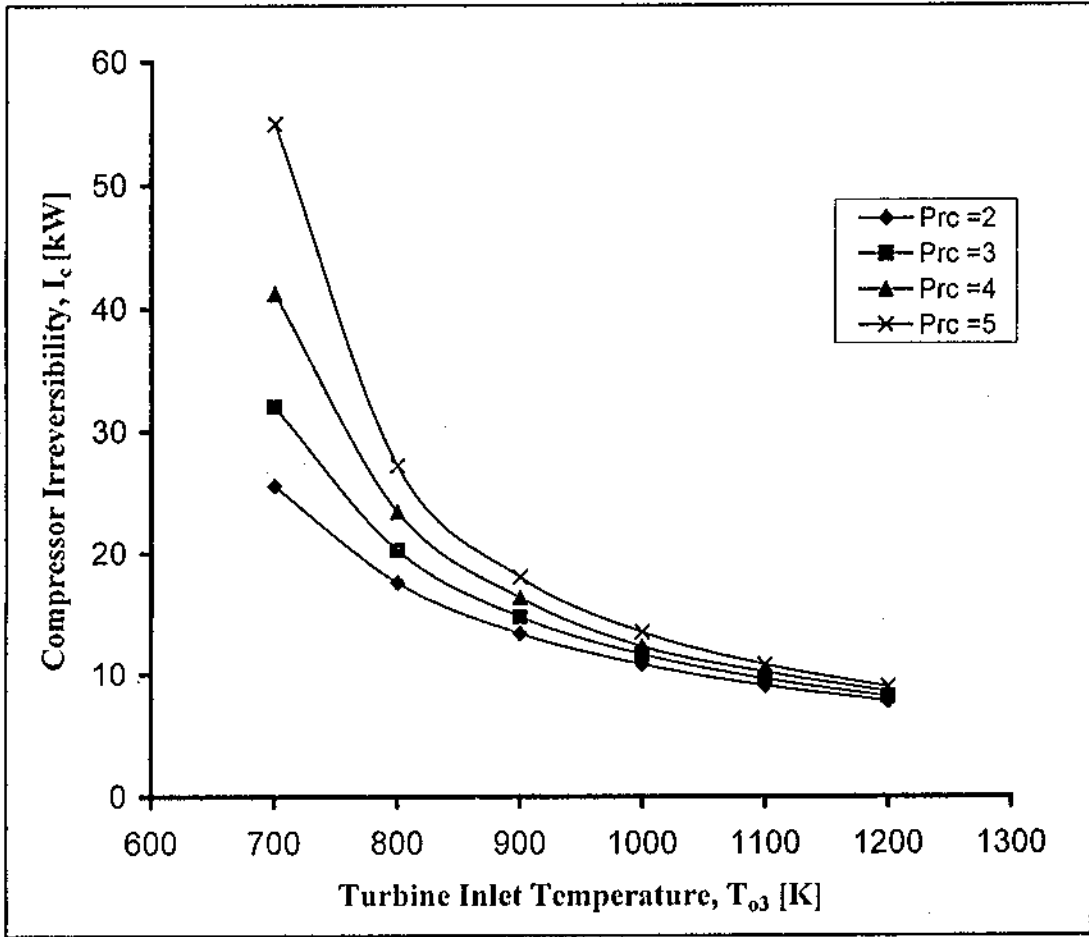


Figure 5.17: Variation of compressor irreversibility with turbine inlet temperature at different compressor pressure ratios.

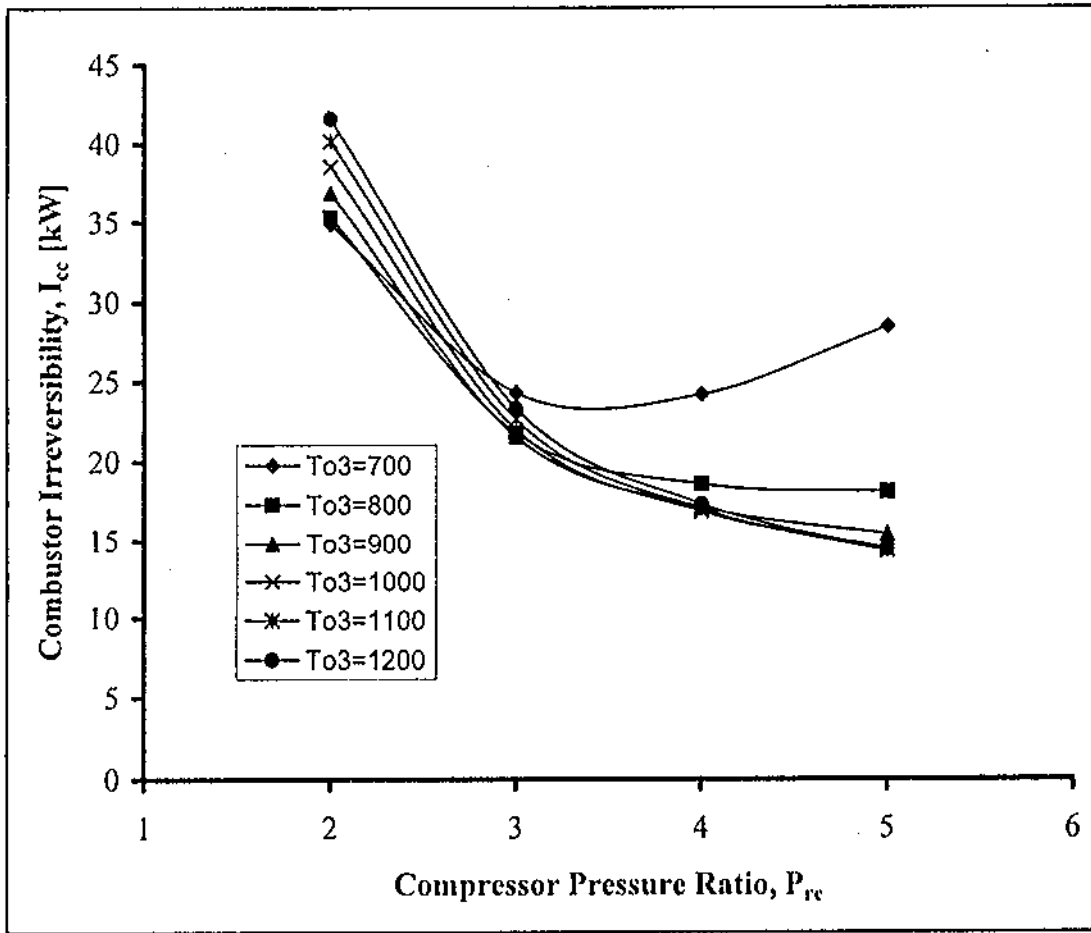


Figure 5.18: Variation of combustor irreversibility with compressor pressure ratios at different turbine inlet temperatures .

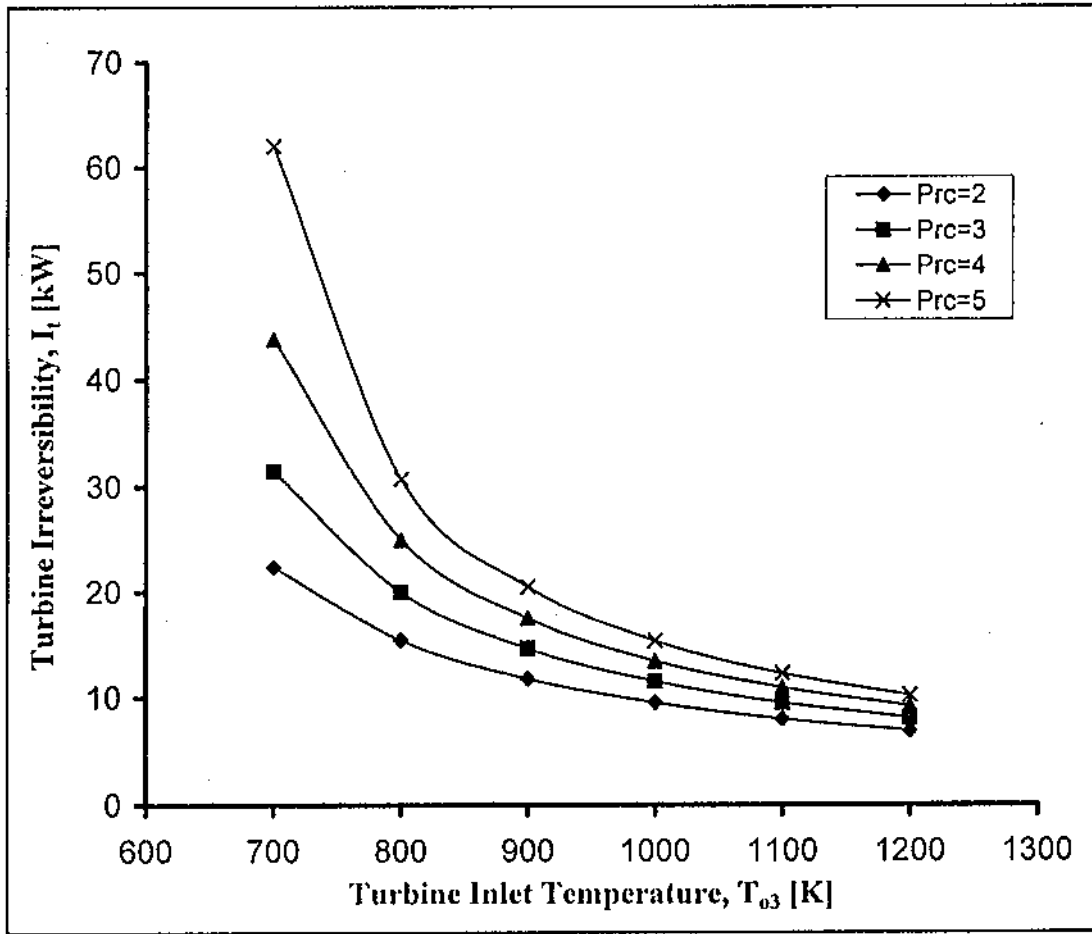


Figure 5.19: Variation of turbine irreversibility with turbine inlet temperature at different compressor pressure ratios.

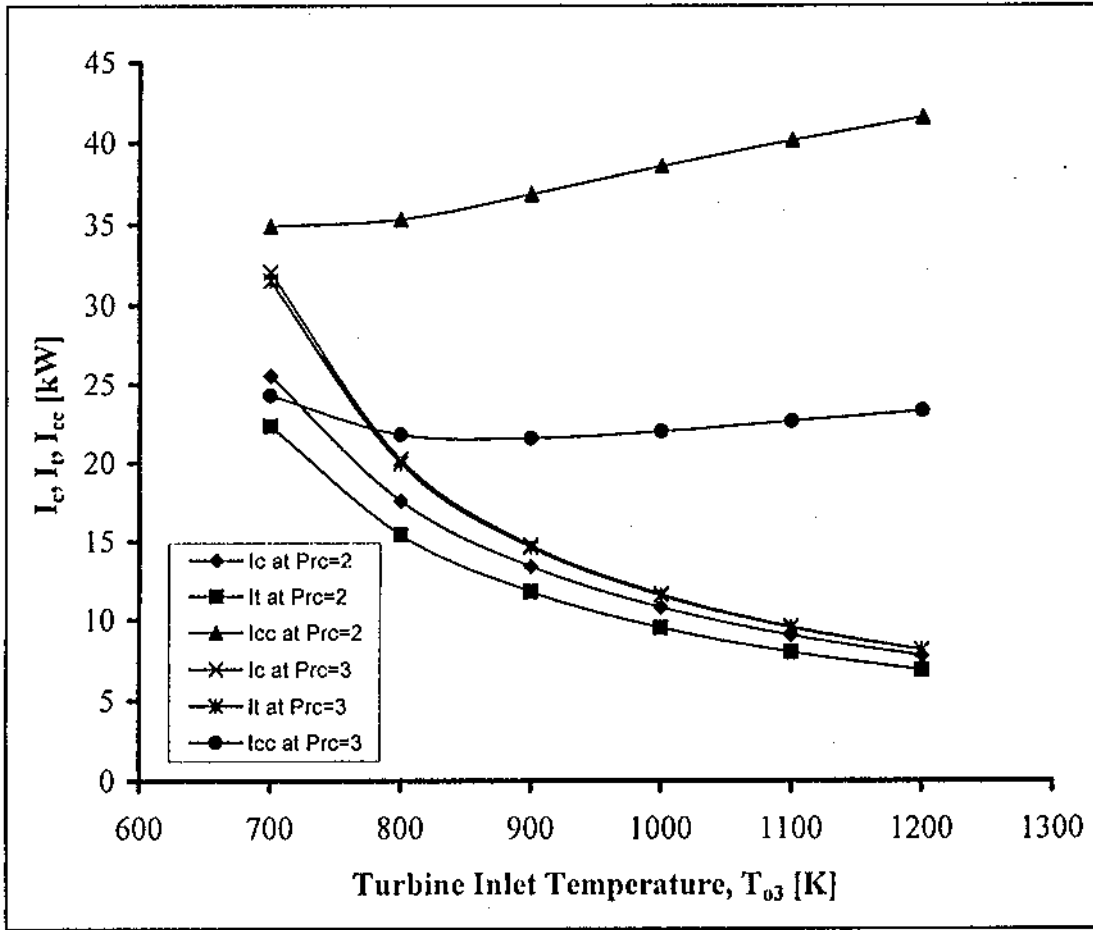


Figure 5.20: Variation of turbine, compressor and combustor irreversibilities with turbine inlet temperature at different compressor pressure ratios.

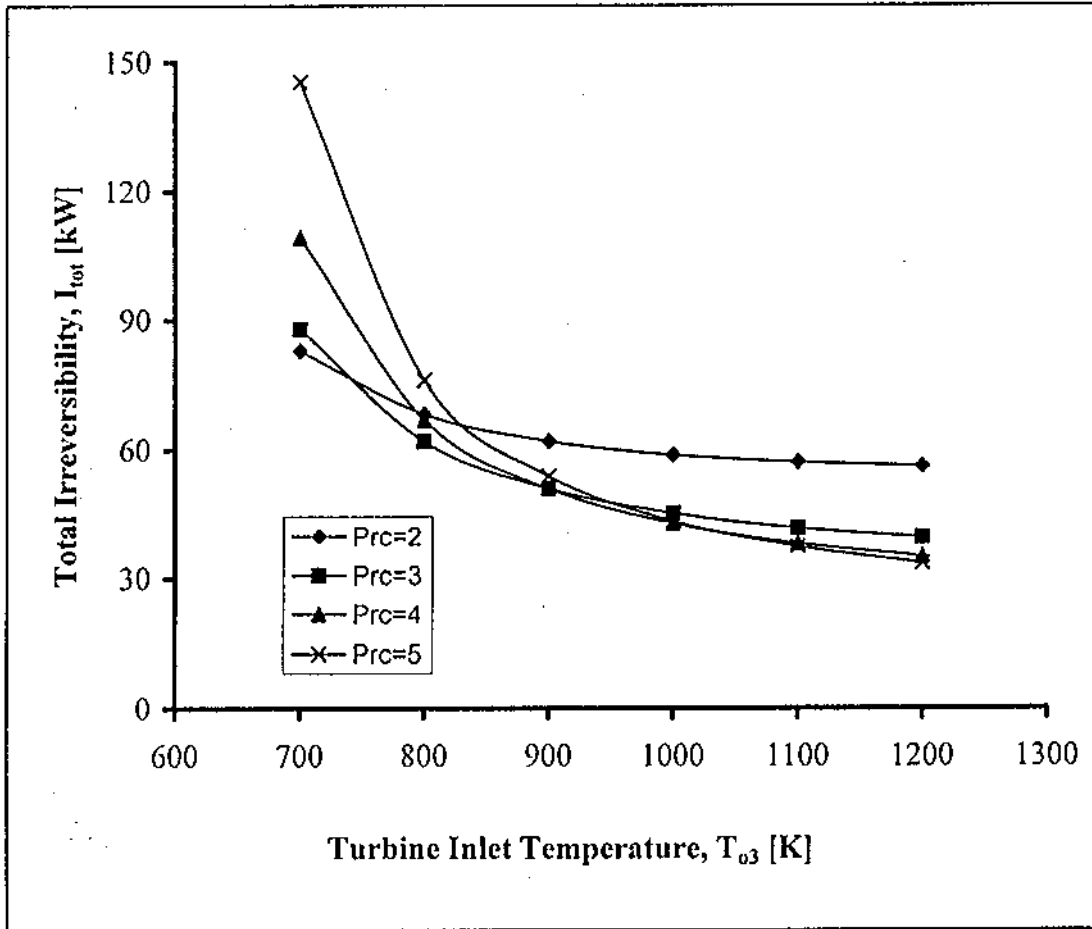


Figure 5.21: Variation of total Irreversibility with turbine inlet temperature at different compressor pressure ratios.

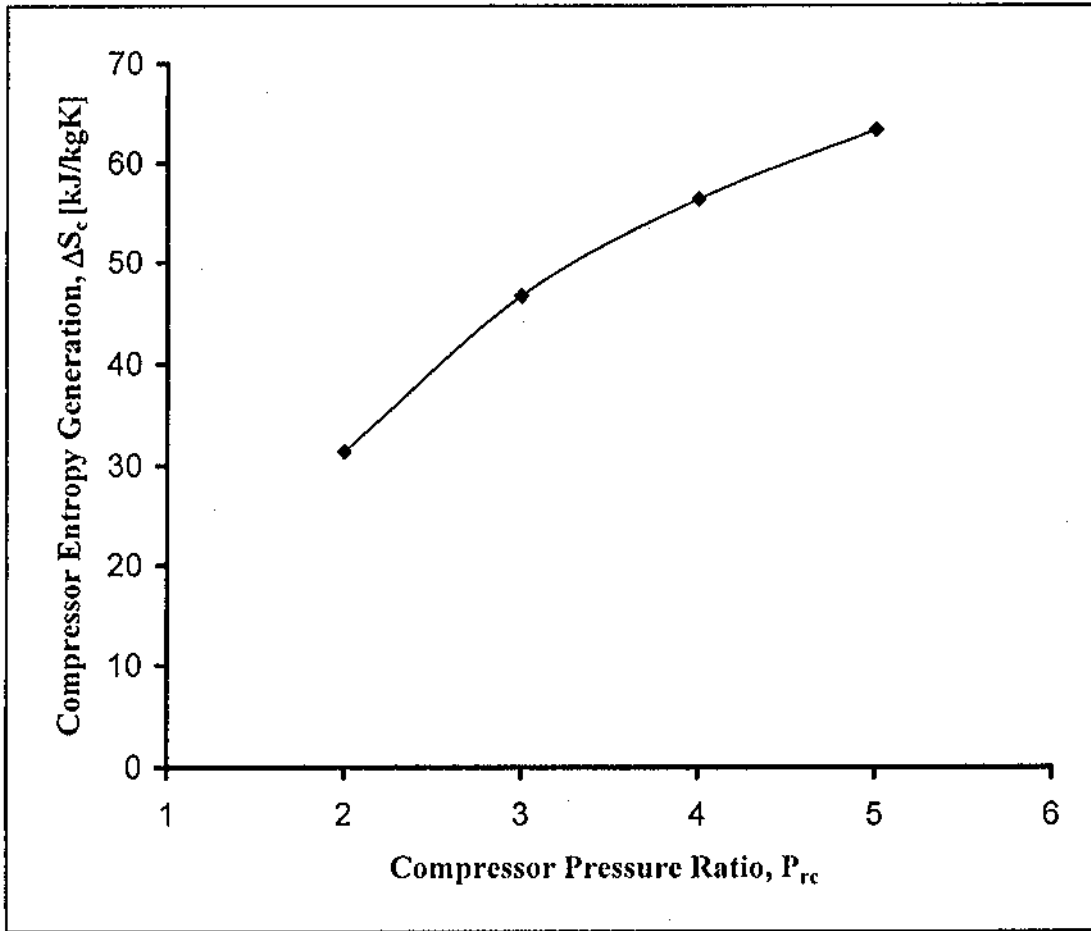


Figure 5.22: Variation of compressor entropy generation with compressor pressure ratio.

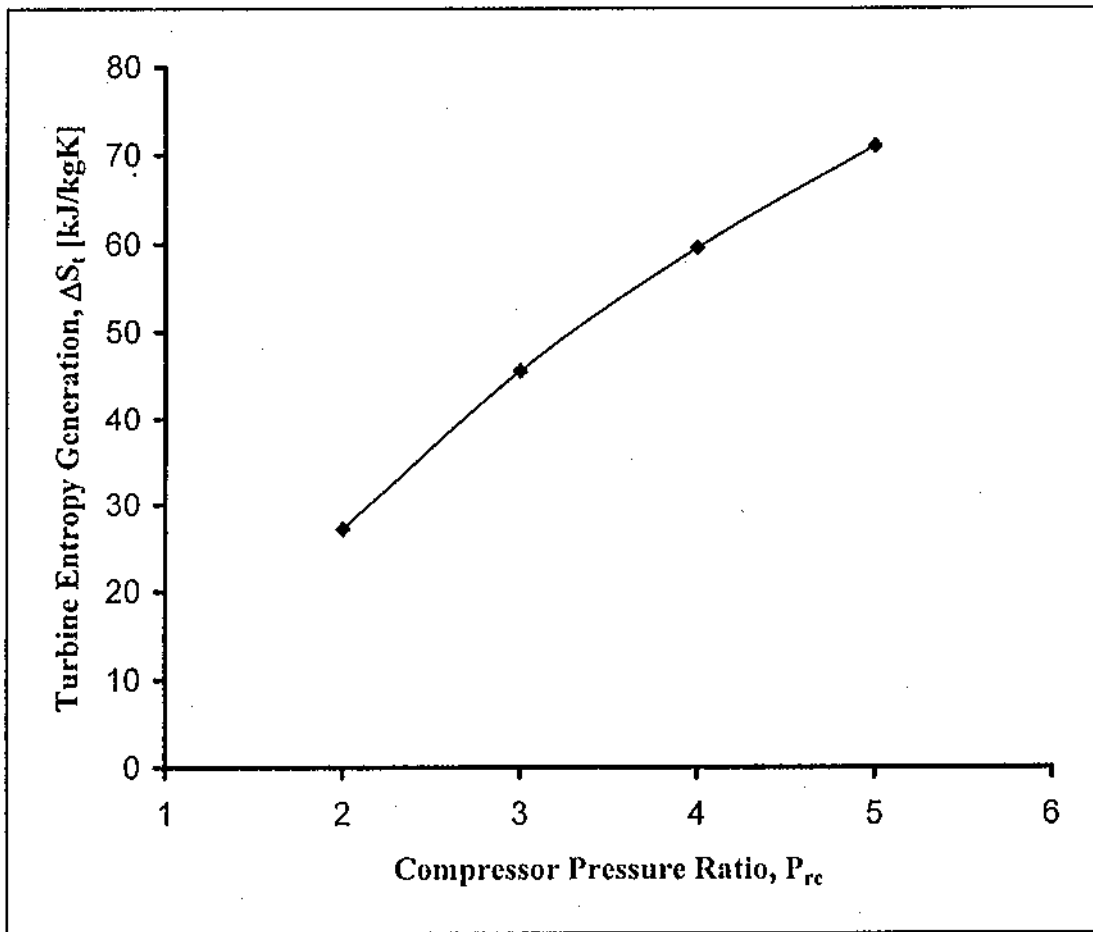


Figure 5.23: Variation of turbine entropy generation with compressor pressure ratio.

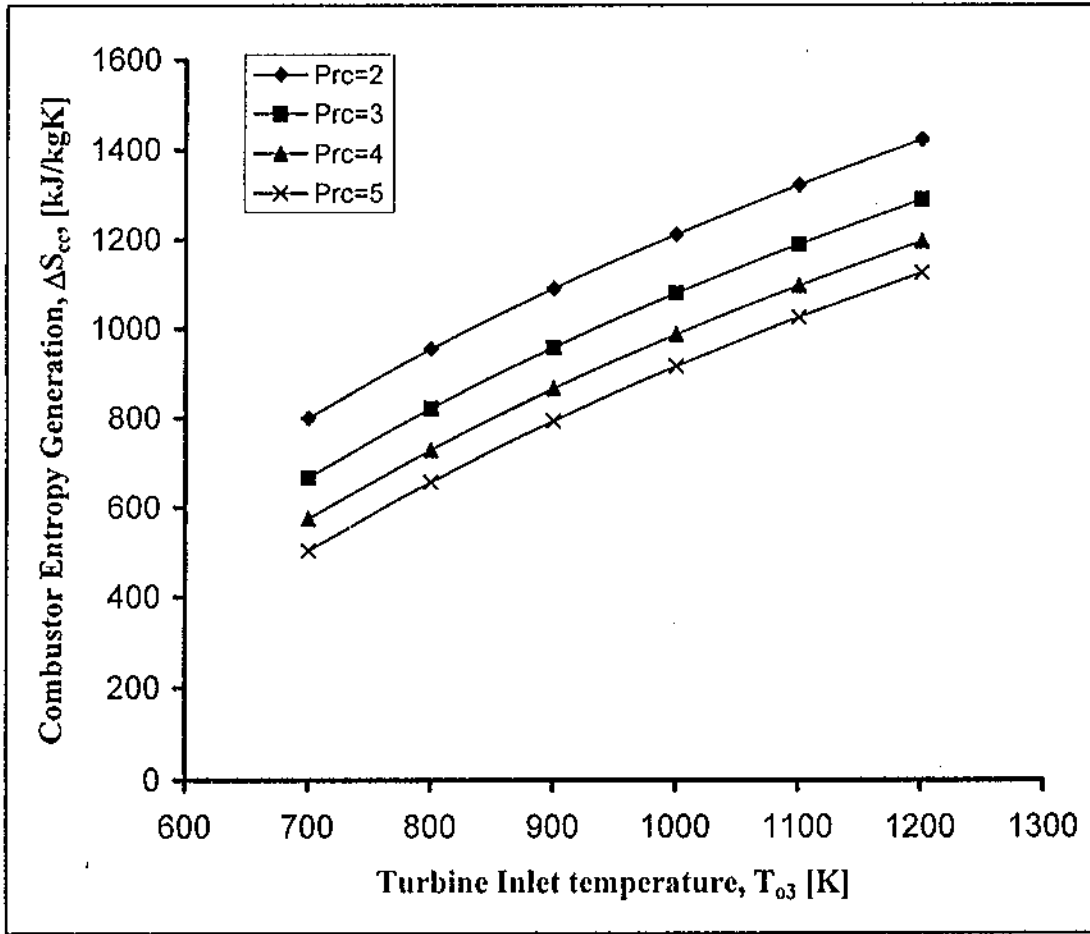


Figure 5.24: Variation of combustor entropy generation with turbine inlet temperature at different compressor pressure ratios.

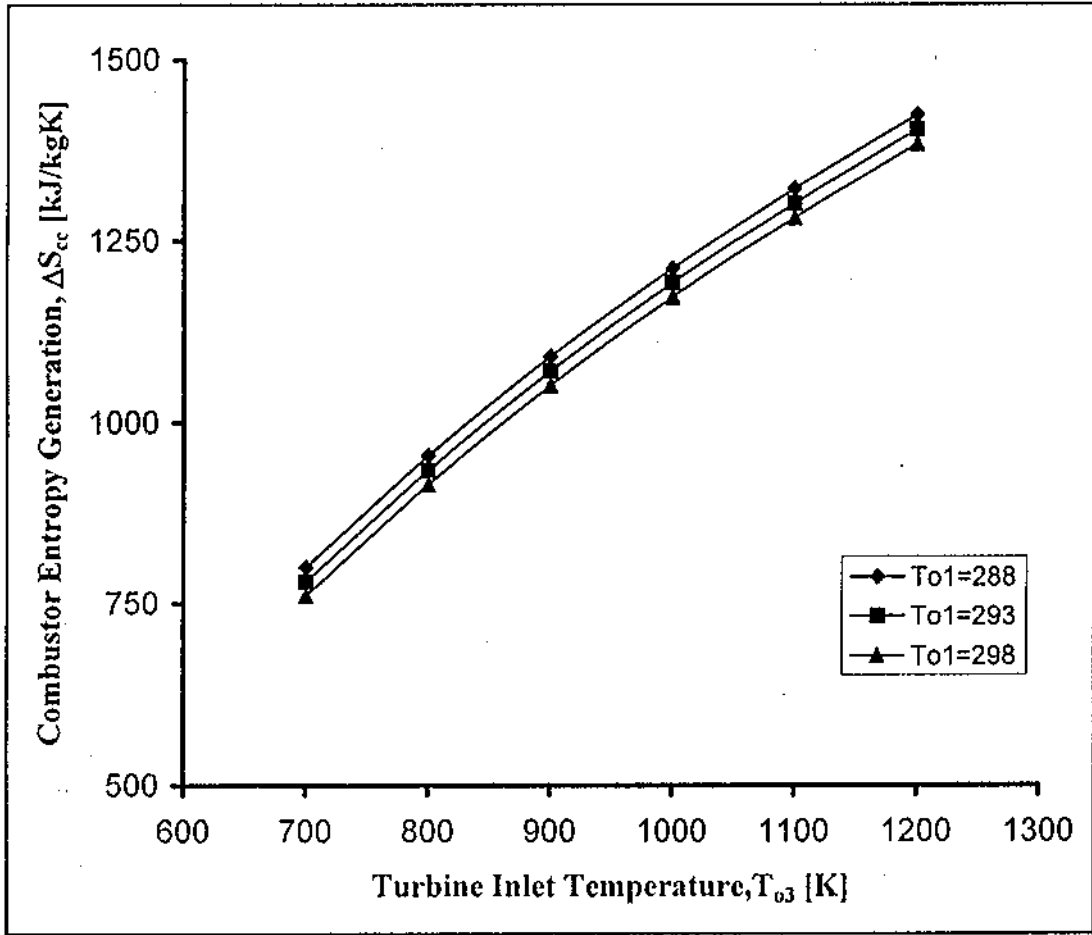


Figure 5.25: Variation of combustor entropy generation with turbine inlet temperature at different compressor inlet temperatures .

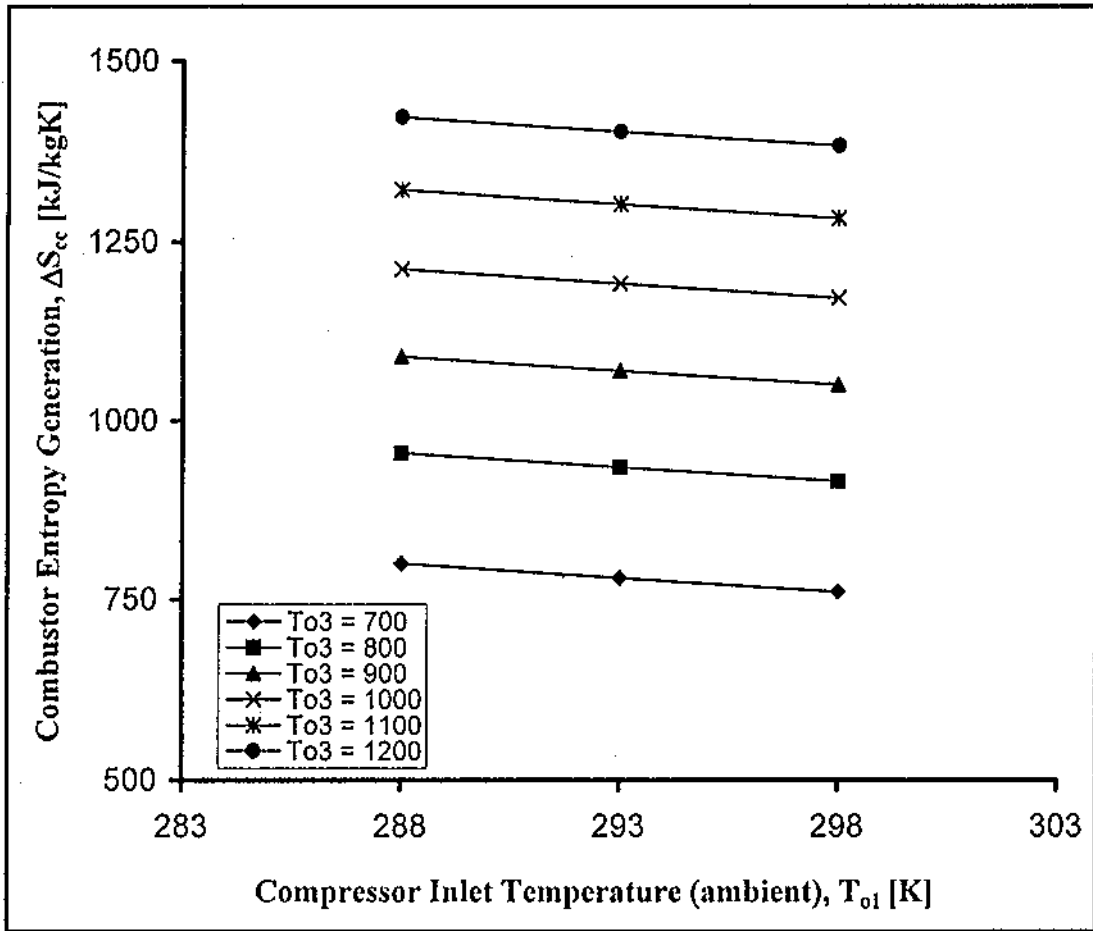


Figure 5.26: Variation of combustor entropy generation with compressor inlet temperature (ambient) at different turbine inlet temperatures.

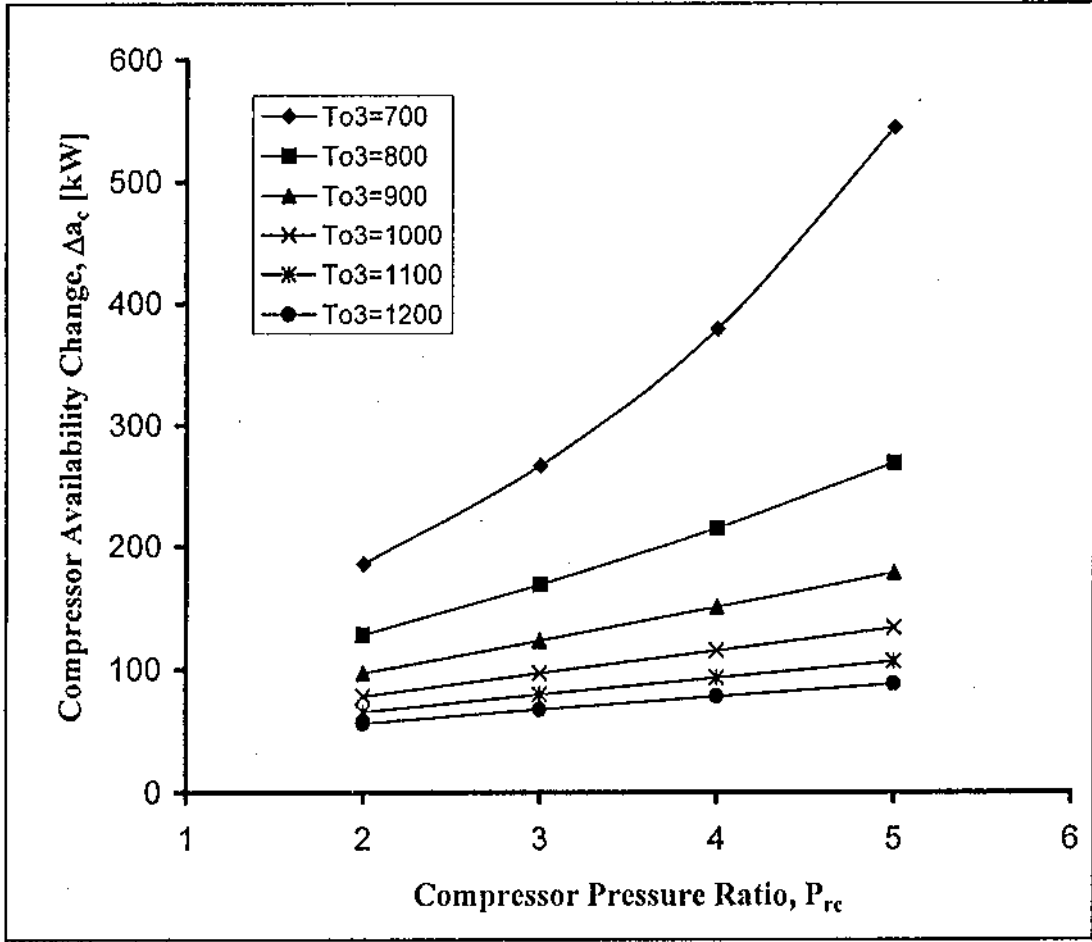


Figure 5.27: Variation of compressor availability change with compressor pressure ratio at different turbine inlet temperatures.

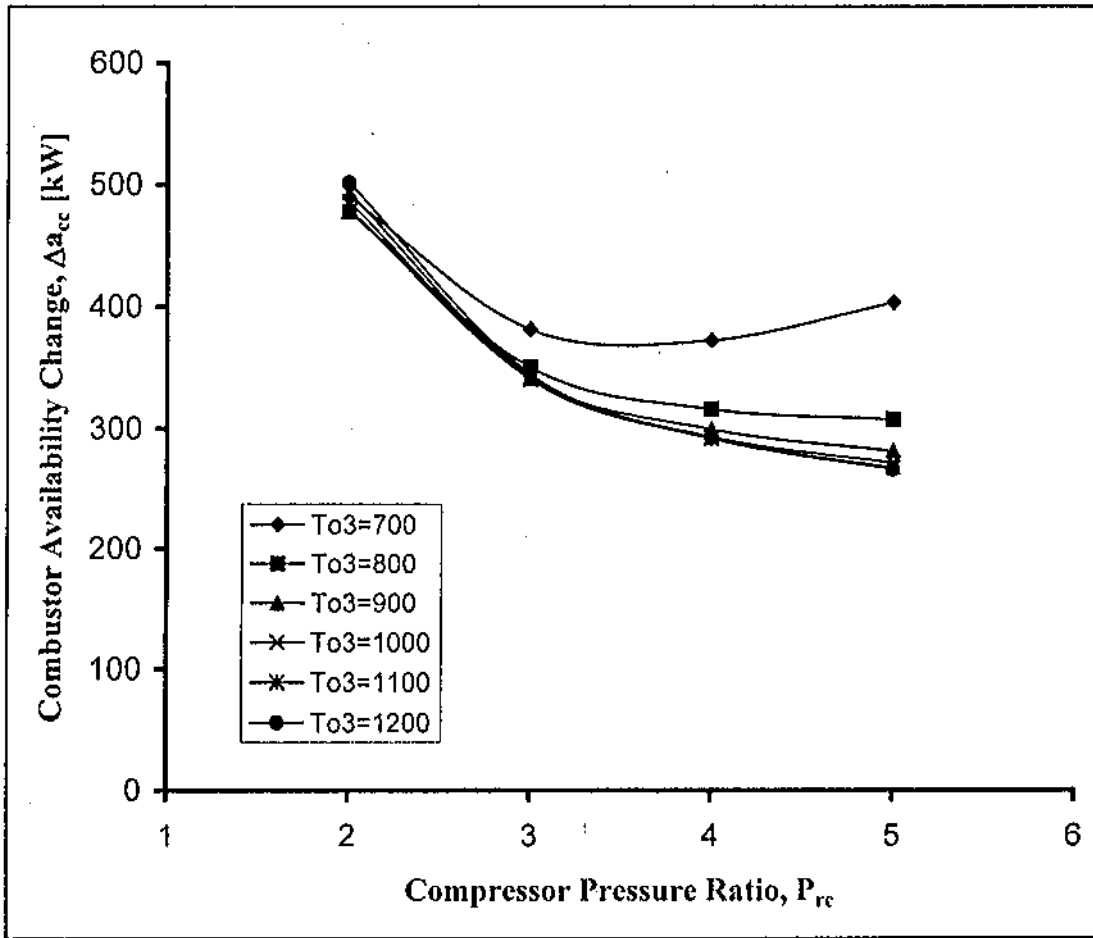


Figure 5.28: Variation of combustor availability change with compressor pressure ratio at different turbine inlet temperatures.

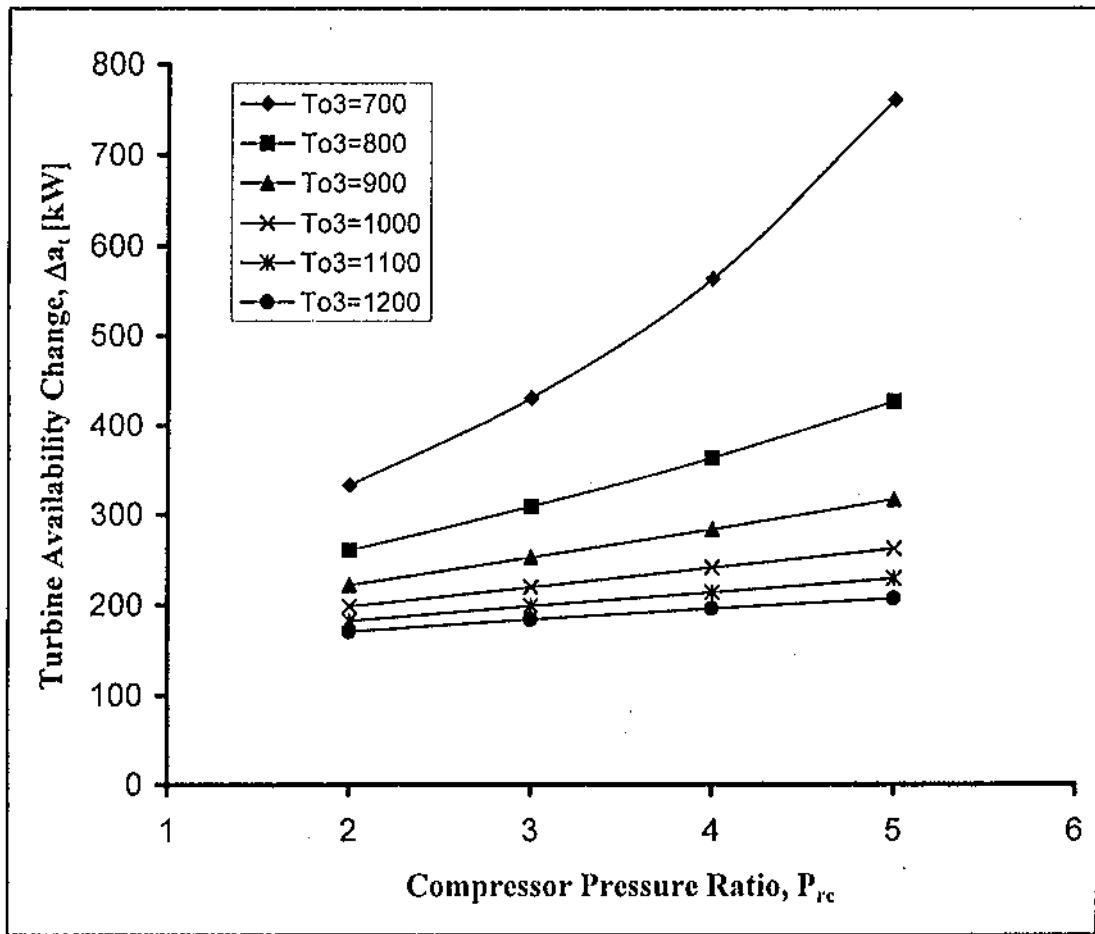


Figure 5.29: Variation of turbine availability change with compressor pressure ratio at different turbine inlet temperatures.

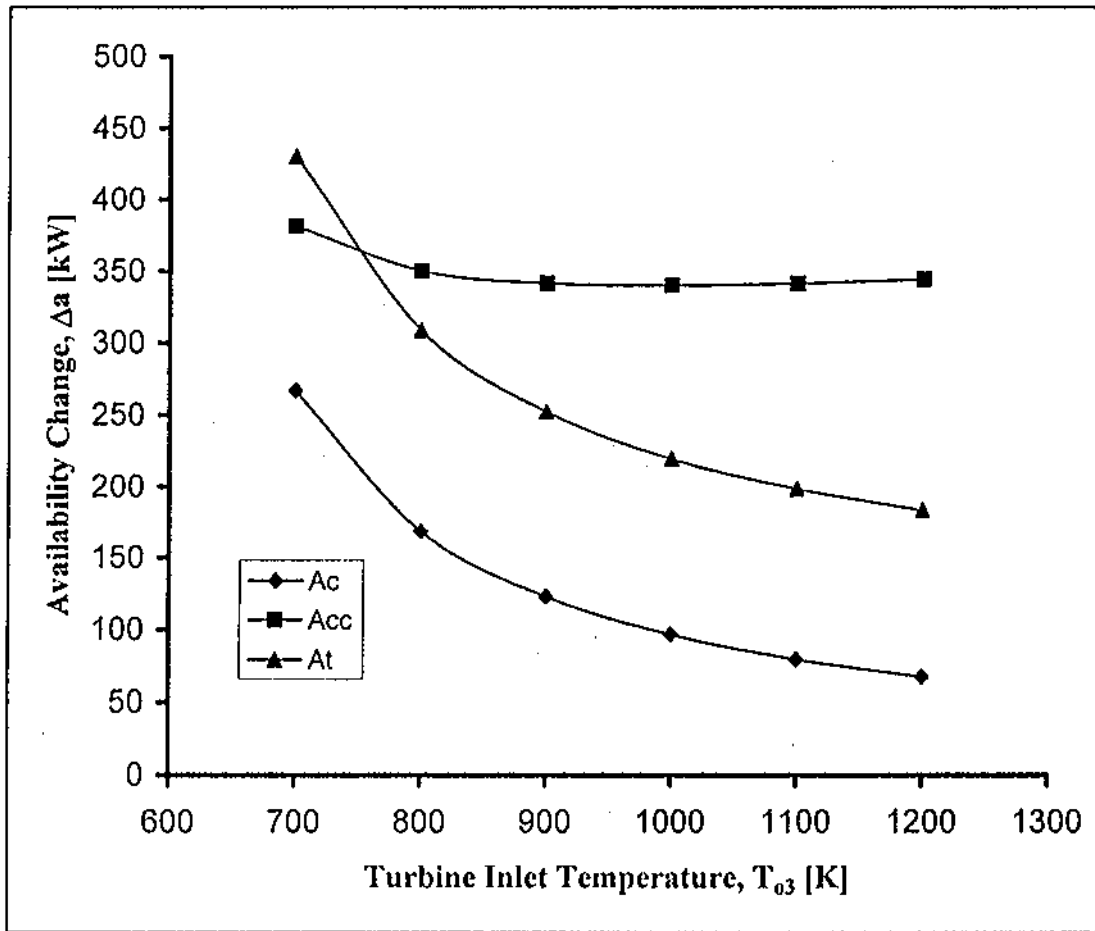


Figure 5.30: Variation of compressor, combustor and turbine availability change with turbine inlet temperature at $P_{rc} = 3$

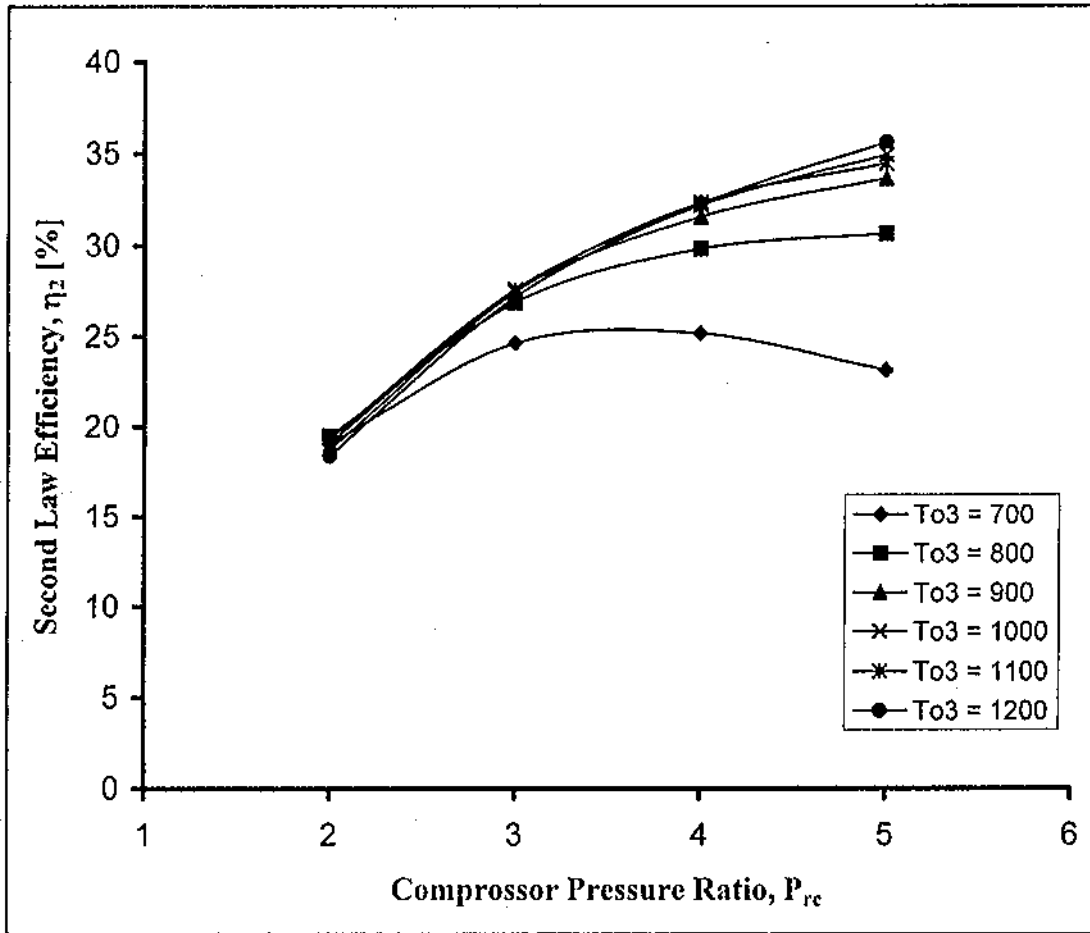


Figure 5.31: Variation of second law efficiency with compressor pressure ratio at different turbine inlet temperatures .

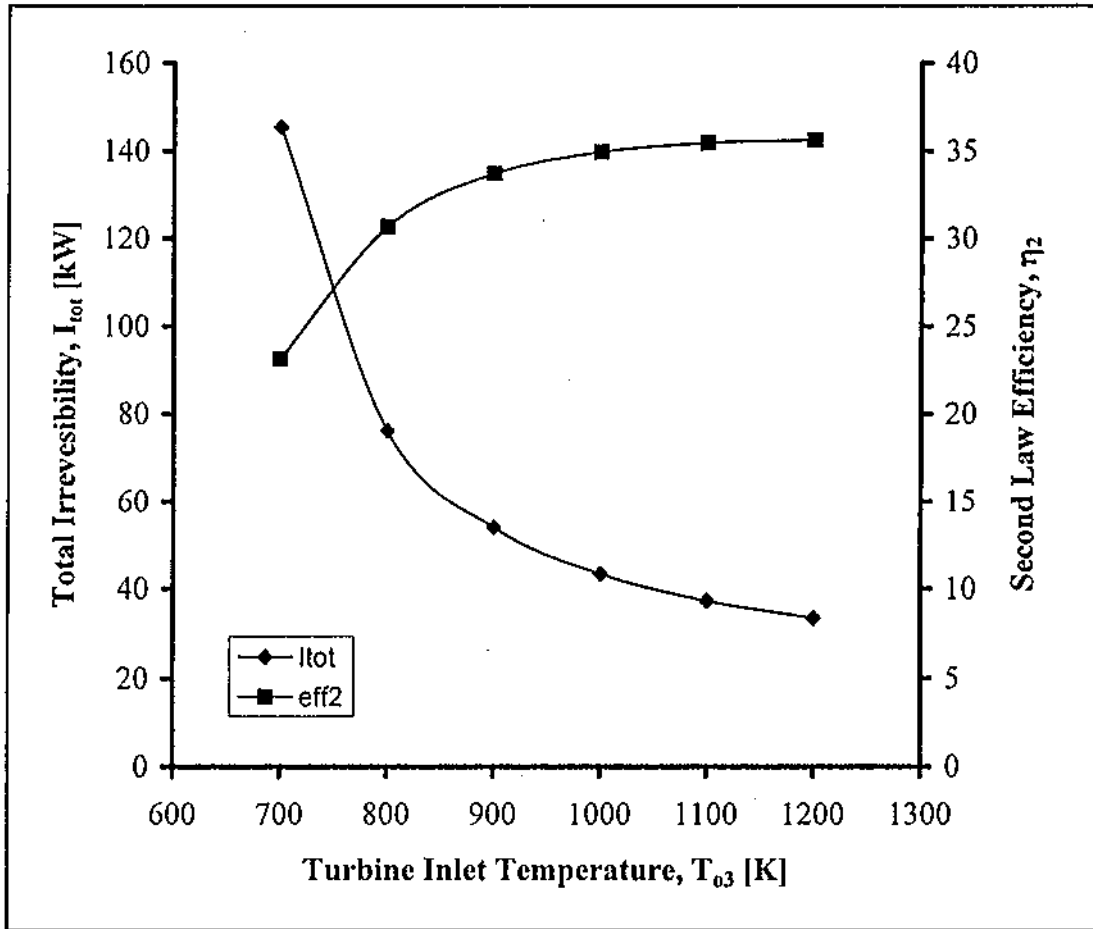


Figure 5.32: Variation of second law efficiency and total irreversibility with turbine inlet temperature at $P_{rc} = 5$.

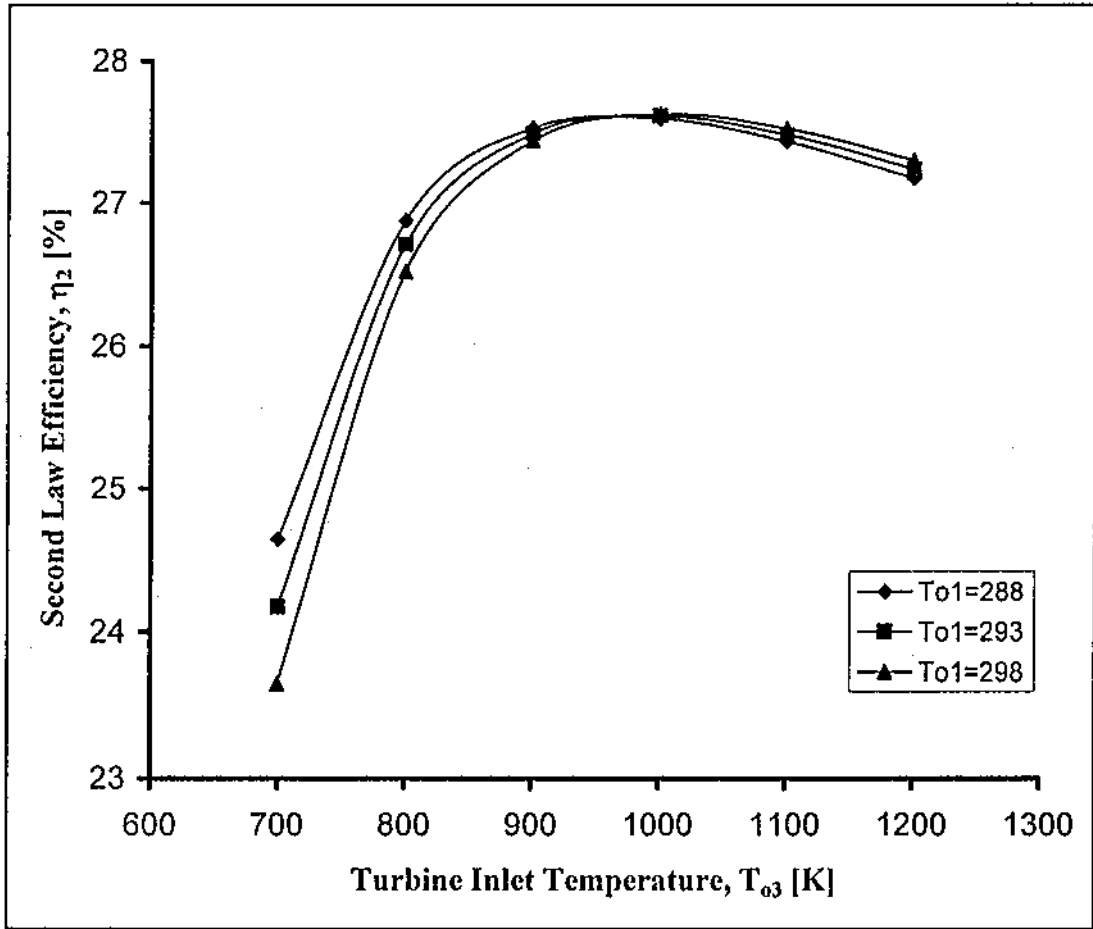


Figure 5.33: Variation of second Law efficiency with turbine inlet temperature at

$P_{rc}=3$ and different compressor inlet temperatures .

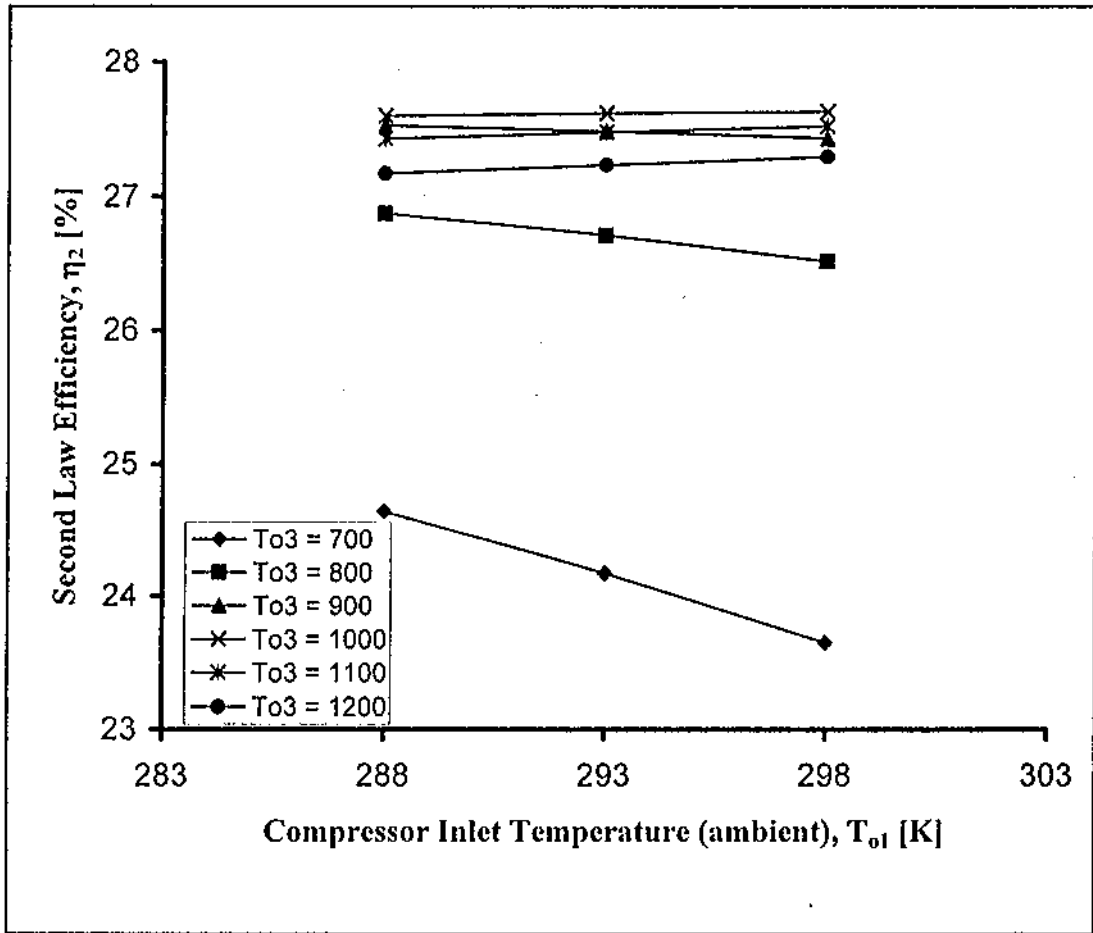
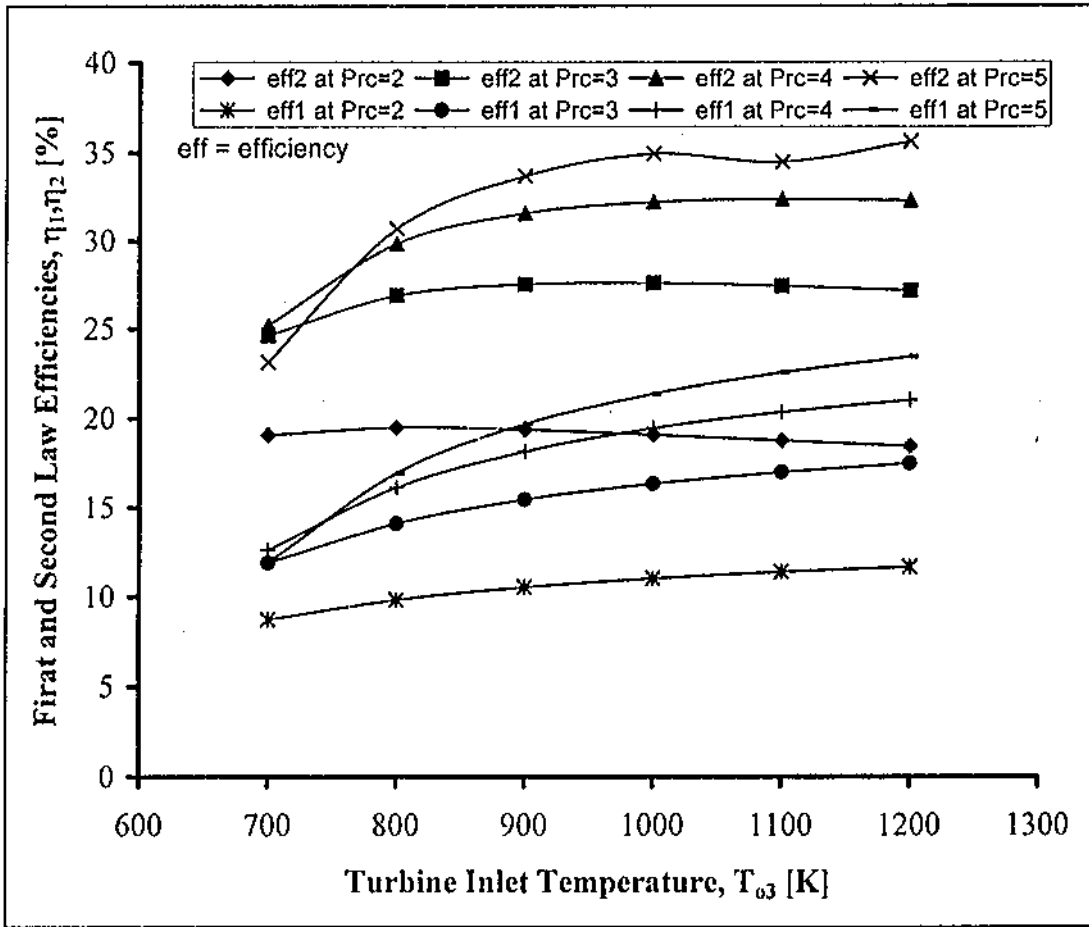


Figure 5.34: Variation of second Law efficiency with compressor inlet temperature (ambient) at different turbine inlet temperatures .



561697

Figure 5.35: Comparison of first law and second law efficiencies with turbine inlet temperature at different compressor pressure ratios.

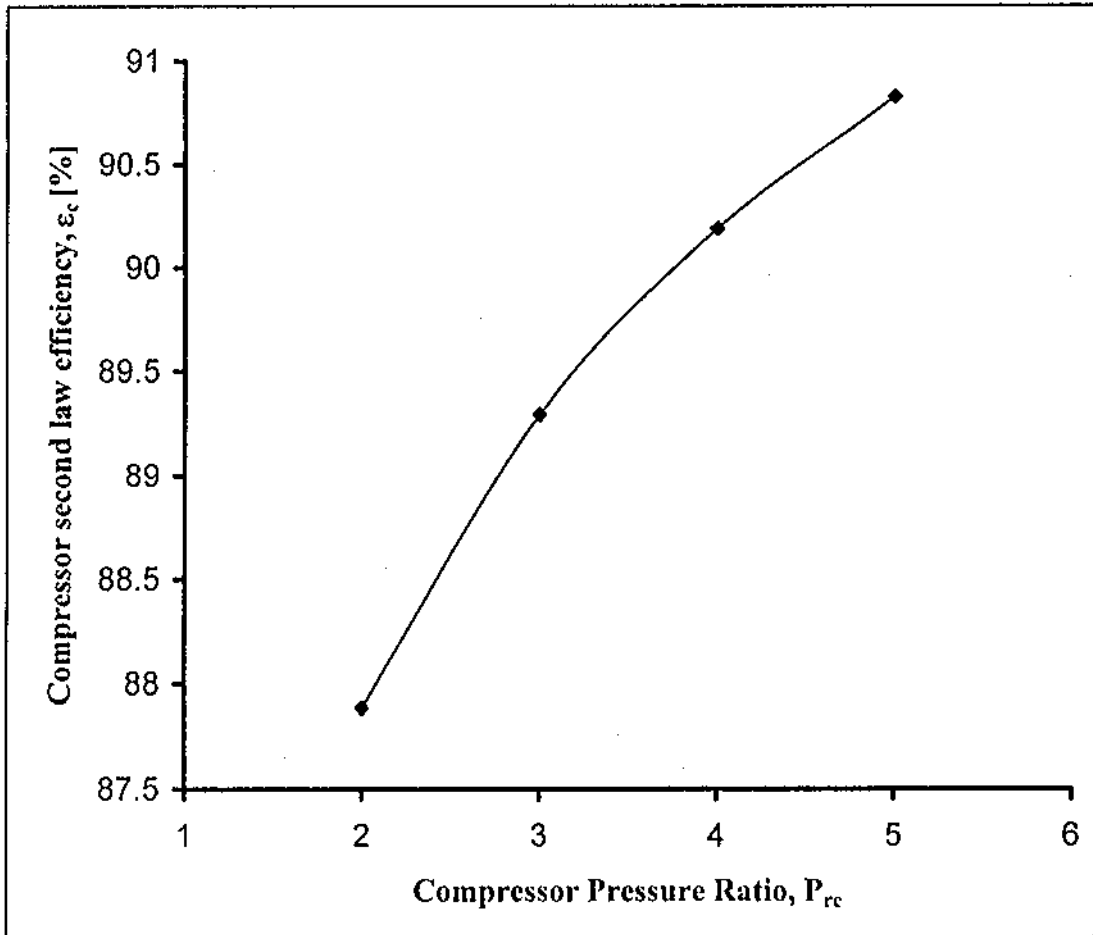


Figure 5.36: Variation of compressor second law efficiency (effectiveness) with compressor pressure ratio.

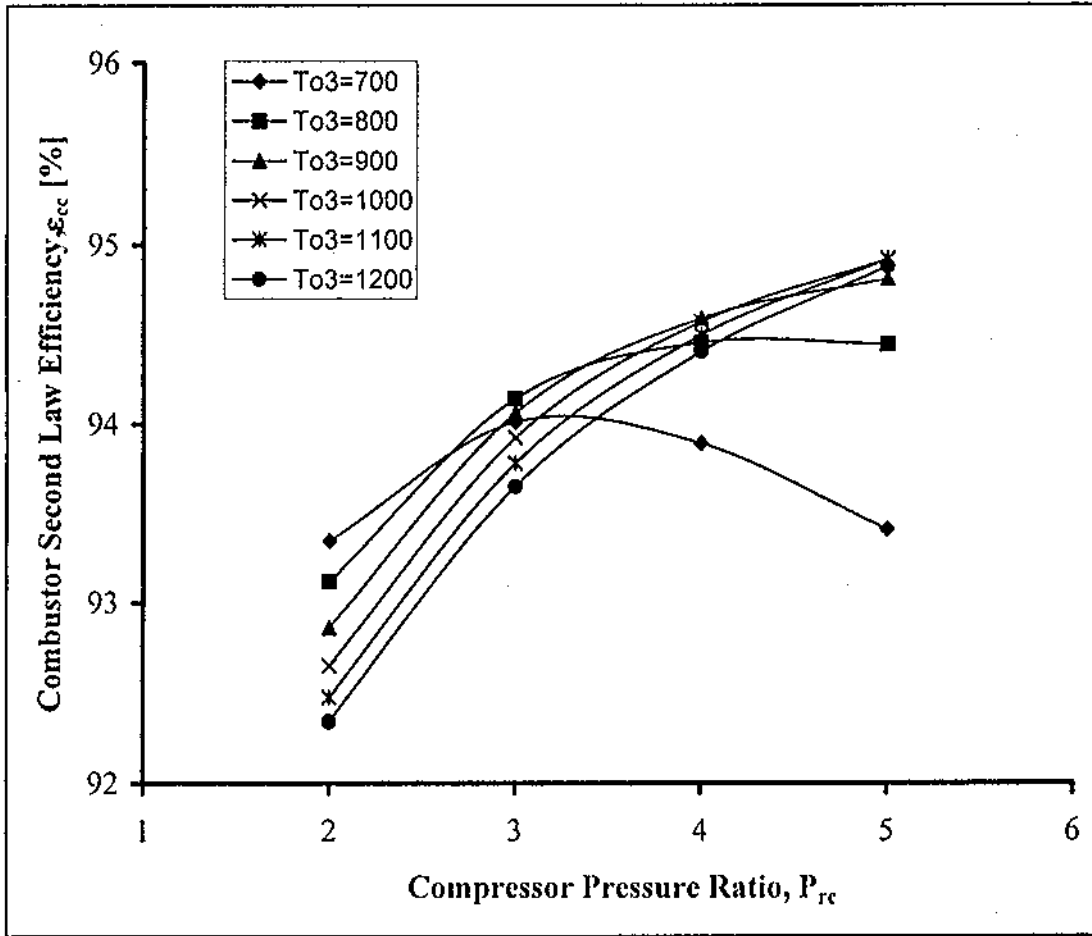


Figure 5.37: Variation of combustor second law efficiency (effectiveness) with compressor pressure ratio at different turbine inlet temperatures.

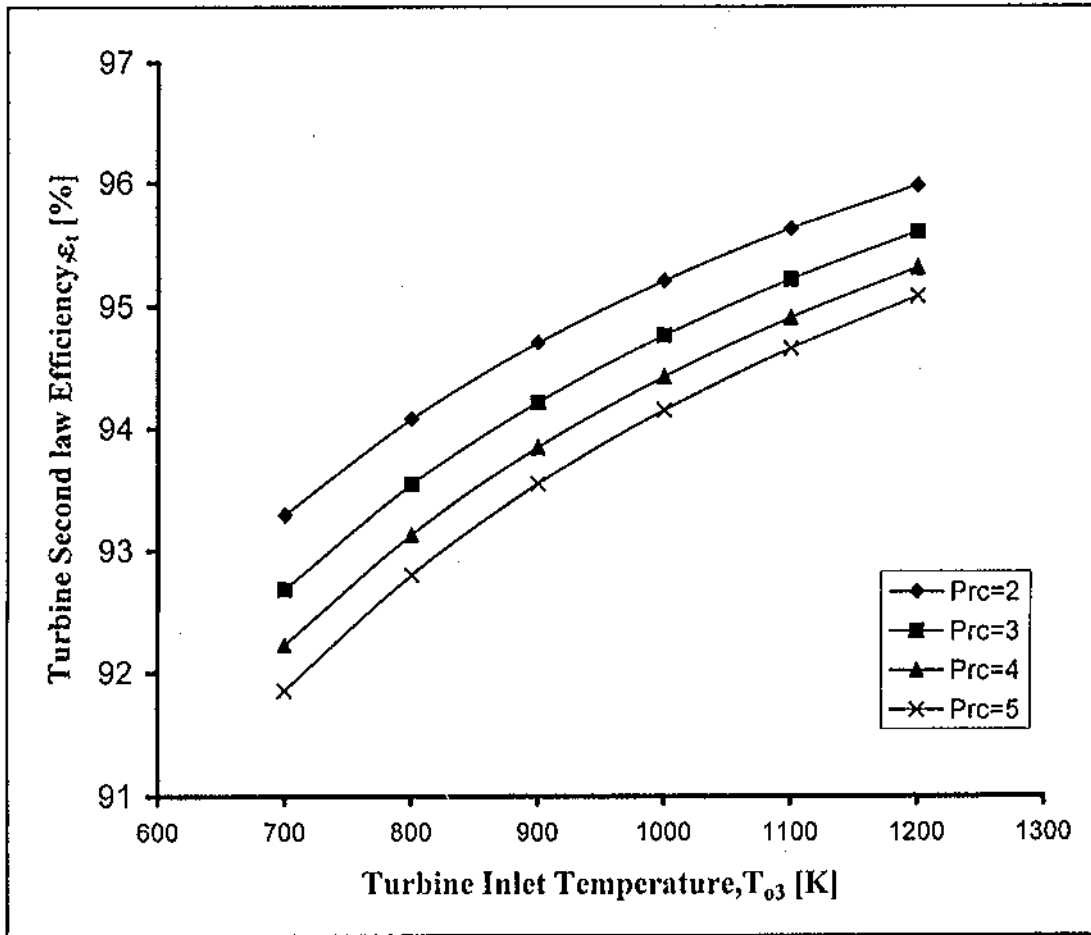


Figure 5.38: Variation of turbine second law efficiency (effectiveness) with turbine inlet temperature at different compressor pressure ratios.

6. CONCLUSIONS AND RECOMMENDATIONS

6.1 Introduction

The simple small gas turbine cycle has been investigated. The cycle was examined at various input parameters such as turbine inlet temperature, compressor pressure ratio, ambient temperature and specific work output. A detailed thermodynamic analysis based on first law of thermodynamics as well as the second law was carried out for each component of the gas turbine cycle. The availability change, entropy generation, irreversibility and second law efficiency (effectiveness) were calculated for each component of the cycle, as well as the first and second law efficiencies of the gas turbine cycle.

6.2 Conclusions

6.2.1 First law analysis

It is well known from literature that the best configuration for a small gas turbine would be a single stage centrifugal compressor, a combustor and a single stage inward flow turbine. From the analysis of first law it was found that the to air ratio f is increased by increasing T_{03} and decreased by increasing P_{rc} . The specific fuel consumption and mass flow rate are decreased either by increasing T_{03} or P_{rc} . While the increase of P_{rc} above five will not effectively improve specific fuel consumption, and most of mass flow rate decrease occurs in the range of P_{rc} from two to three.

The tip blade speed u_2 is increased either by increasing T_{03} or P_{rc} . Since there is a design limit for u_2 , therefore the selection of T_{03} or P_{rc} for radial turbine design would depend on the permissible value of u_2 taking into account the metallurgical limit of T_{03} . Also, it was found that the cycle thermal efficiency is increased by increasing T_{03} or P_{rc} or by decreasing the compressor inlet temperature T_{01} . It is clear that T_{03} and P_{rc} should be higher than 900K and three respectively to maximize the cycle efficiency.

1.2.2 Second law analysis

1. Second law analysis enables the location and magnitude of all losses to be identified.
2. Compressor and turbine irreversibilities are reduced with increasing turbine inlet temperature T_{03} and increasing P_{rc} increases them.
3. The combustor is the major source of irreversible losses for the gas turbine plant, nearly 40 – 60 % of losses occur in it.
4. The second law efficiency is increased with increasing both T_{03} and P_{rc} or decreasing compressor inlet temperature (ambient temperature).
5. The maximum second law efficiency is obtained at $T_{03} = 1200$ k and $P_{rc} = 5$, which is about 36% compared to maximum first law efficiency which is about 24%.
6. Increasing P_{rc} increases the effectiveness of compressor, while turbine effectiveness is increased by increasing T_{03} and decreased by increasing P_{rc} .

6.3 Recommendations

For better improvements or modification of the gas turbine cycle, the following are recommended:

1. The irreversibility of the combustor is the major source of losses. Thus, it is recommended to design and select a suitable combustor, taking care of the actual fraction of pressure loss across it.
2. Perform the calculations of design parameters of turbine and compressor based on second law analysis.
3. Verification of the theoretical analysis of second law by comparing the obtained results with actual experimental data.
4. The effect of using the actual specific heat capacities and air tables instead of perfect gas assumption on the gas turbine performance.

7. REFERENCES

- Allen, R.P., and Kovacic, J.M. 1984. Gas turbine cogeneration – principles and practice. *Journal of engineering for gas turbines and power*. 106: 725 – 730.
- Alvarado, S., and Gherardelli, C. 1994. Exergoeconomic optimization of a cogeneration plant. *Energy*. 19 (12): 1225 – 1233.
- Balje, O.E. 1981. *Turbomachines - a guide to design, selection, and theory*. John Wiley & sons, New York.
- Based thermodynamic analysis of Regenerative – Reheat Rankine – Cycle power Plants'. *Energy*. Vol. 17, No, PP. 295 – 301.
- Baughn, J.W., and kerwin, R.A. 1987. A comparison of the predicted and measured the rmodynamic performance of a gas turbine cogeneration system. *Transactions of the ASME*. 109: 32-38.
- Bejan, A. 1994. *Entropy generation through heat and fluid flow*. John Wiley & Sons, New York.
- Bilgen, E. 2000. Exergetic and engineering analyses of gas turbine based cogeneration systems. *Energy*. 25: 1215-1229.
- Bisio, G. 1998. A second – law analysis of the “hot blast stove / gas turbine” combination by applying the parameter “usable exergy”. *Energy convers. Mgmt*. 39 (3/4): 217-227.
- Burghardt, M.D. 1978. *Engineering Thermodynamics with applications*. Harper & Raw, New York.
- Cerqueira, S.A., and Nebra, S. A. 1999. Cost attribution methodologies in cogeneration systems. *Energy convers. Mgmt*. 40: 1587 – 1597.
- Chiesa, P. Iozza, G., Macchi, E. , and consonni, S. 1994, An assessment of the thermodynamic performance of mixed gas-steam cycles : part B: water-injected and hat cycles . *ASME*. paper No. 94-GT-424.

- Chin, W.W., and El-Masri, M.A. 1987. Exergy analysis of combined cycles: part2 – analysis and optimization of two-pressure steam bottoming cycles. *Journal of engineering for gas turbines and power*. 109: 237 – 243.
- Cohen, H., Rogers, G.F.C., and Saravanamuttoo, H.I.H. 1996. *Gas turbine theory*. Longman Group limited. 4th edition. London.
- Csanady, G.T. 1964. *Theory of turbomachines*. McGraw – Hill. New York.
- Dixon, S.L. 1978. *Fluid mechanics, thermodynamics of turbomachinery*. Butterworth-Heinemann Ltd. 3rd edition. Oxford.
- El-Masri, M.A. 1985. On thermodynamics of gas turbine cycles: part 1 – second law analysis of combined cycle. *Transactions of the ASME*. 107: 880-889.
- El – Masri, M.A. 1987. Exergy analysis of combined Cycles: Part 1 – Air – cooled Brayton – cycle gas turbines. *Transactions of the ASME*. 109 : 228-236.
- Ferrari, J. R., and Bianco, R. 1997. First and second law analysis of diesel engines and gas turbines in combines cycles: a comparative study. *Proc. AM power conf.* Illinois Inst. of technology. Chicago. II (USA). 59-2 : 847 – 852.
- Fiaschi, D. and Manfrida, G. 1998. Exergy analysis of the semi-closed gas turbine combined cycle (SCGT/CC). *Energy convers. Mgmt.* 39 (16-18): 1643 – 1652.
- Guarinello, Jr. F., Cerqueira, S.A., and Bebra, S.A. 2000. Thermodynamic evaluation of a gas turbine cogeneration system. *Energy convers. Mgmt.* 41: 1191-1200.
- Gyftopoulos, E. P. 1999. Infinite time (reversible) versus finite time (irreversible) thermodynamics: a misconceived distinction. *Energy*. 24: 1035 – 1039.
- Habib, M.A. 1992. Thermodynamic analysis of the performance of cogeneration plants. *Energy*. 17 (5): 485-491.
- Habib, M.A., and Zubair, S.M. 1992. Second-Law-Based thermodynamic analysis of regenerative-reheat Rankine-cycle power plants. *Energy*. 17 (3): 295-301.
- Habib, M.A., Said, S.A., and Al-Bagawi, J.J. 1995. Thermodynamic performance analysis of the ghazlan power plant. *Energy*. 20 (11): 1121-1130.

- Harman, R.T.C. 1981. *Gas turbine engineering – application, cycles and characteristics*. Macmillan press Ltd. London.
- Hisazumi, Y. 1999. Study on an optimized energy supply system and proposal of a new gas turbine cogeneration system based on exergy evaluation. *ASME*. 34 (2): 313 – 320.
- Huang, F.F. 1990. Performance evaluation of selected combustion gas turbine cogeneration systems based on first and second-law analysis. *Journal of engineering for gas turbines and power*. 112: 117-121.
- Kam, W. Li. 1992. Gas turbine cogeneration system study for a university campus. *IGTI. ASME. Cogen-Turbo*. 7: 139 – 147 .
- Lee, S.C., and Wagner, R.M. 1994. Second law efficiency analysis of gas – turbine engine for cogeneration. *IGTI. ASME. Cogen-Turbo*. 9 : 163 – 168.
- Moran, M. J. 1989. *Availability analysis – a guide to efficient energy use*. ASME. New York.
- Moran, M. J. 1998. On second – law analysis and the failed promise of finite-time thermodynamics. *Energy*. 23 (6): 517-519.
- Moran, M.J. and Shapiro, H.N. 1993. *Fundamental of engineering thermodynamics*. John Wiley & Sons. 2nd edition. New York. USA.
- Najjar, Y.S. 1996 Some trends and progress in gas turbine technology and research. *Energy convers. Mgmt*. 37 (12): 1713-1723.
- Rice, I.G. 1987. Thermodynamic evaluation of gas turbine cogeneration cycles: part II – complex cycle analysis. *Transactions of the ASME*. 109 : 8-15.
- Sarabchi, K. 1992. Parametric analysis of gas turbine cogeneration plant from first – and second – law viewpoints. *IGTI ASME Cogen-Turbo*. 7 : 485 – 491.
- Shepherd, D. G. 1956. *Principles of turbomachinery*. Macmillan publishing Co. New York.
- Solokolov, E. Ya. , and Martynov, V.A. 1994. The output characteristics of gas-turbine cogeneration installations. *Thermal engineering*. 41 (12): 939-944.

- Sokolov, E. Ya. , and Martynov, V.A. 1996. The output characteristics of combined-cycle cogeneration installations. *Thermal engineering*. 43 (4): 322-330.
- Tsatsaronis, G. , and Pisa, J. 1994. Exergoeconomic evaluation and optimization of energy systems- application to the CGAM problem. *Energy*. 19 (3): 287-321.
- Walsh, P.P., and Fletcher, P. 1998. *Gas turbine performance*, Blackwell Science Ltd. Oxford.
- Wilson, D.G, and Korakianitis, T. 1998. *The design of high-efficiency turbomachinery and gas turbines*. Prentice-Hall. Inc. 2nd edition. New Jersey.
- Wylen, G.J.V., and Sonntag, R.E. 1985. *Fundamental of classical thermodynamics*. John Wiley & sons, 3rd edition. New York.
- Yahya. S.M. 1993. *Turbomachines for under graduate and post graduate courses*. Tech India Publications. New Delhi.

دراسة أداء توربين غازي مولد للطاقة باستخدام

القانون الثاني للديناميكا الحرارية

إعداد

موسى أكرم محمود

المشرف

الأستاذ الدكتور محمود حماد

ملخص

عرفت التوربينات الغازية باستخداماتها الجوية ، ولكنها في هذه الأيام أصبحت تلقى عناية شديدة وذلك لأنها مولدات ذات طاقة إنتاجية عالية مقارنة بوزنها وكذلك لسهولة استخدامها في المجالات التجارية والعسكرية .

هذا البحث يركز على التحليل التيرموديناميكي الكامل للتوربينات الغازية المستخدمة لغايات توليد الطاقة. يتضمن التحليل استخدام القانونين الأول والثاني في الديناميكا الحرارية . ومن اجل تنفيذ المحاكاة الرياضية لنظام التوربين الغازي فقد تم تطوير برنامج حاسوب لإجراء الحسابات والعلاقات التيرموديناميكية اللازمة لدراسة أداء مولد الطاقة.

في هذا البحث تم دراسة تأثير عوامل التصميم على أداء التوربين الغازي. إضافة الى معدل استهلاك الوقود ، الكفاءة باستخدام القانونين الأول والثاني ، كفاءة العناصر الفردية المكونة للنظام والضيعات الناتجة عن العمليات غير المعكوسة (Irreversibility losses) عند ظروف تشغيل مختلفة. فقد تم الحصول على كفاءة أداء مقدرها ٢٤% للقانون الأول و ٣٦ % للقانون الثاني عند درجة حرارة ١٢٠٠ كلفن عند مدخل التوربين ونسبة انضغاط ٥. وكذلك وجد بان ٤٠-٦٠% من الضيعات (losses) تحدث في الحارقة .

تبعاً لما تقدم فإن التحليل باستخدام القانون الثاني يمكن أن يستخدم كموجه لتقليل المصادر التي من شأنها تقليل الكفاءة عند تصميم عناصر التوربين الغازي وكذلك فإن هذا التحليل قادر على تحديد الضيعات وأماكنها في نظام التوليد.

